4

Barite–Celestine Geochemistry and Environments of Formation

Jeffrey S. Hanor

Department of Geology and Geophysics
Louisiana State University
Baton Rouge, Louisiana 70803

INTRODUCTION

Minerals in the barite ($BaSO_4$)–celestine ($SrSO_4$) solid solution series, $(Ba,Sr)SO_4$, occur in a remarkably diverse range of sedimentary, metamorphic, and igneous geological environments which span geological time from the Early Archean (~3.5 Ga) to the present. The purpose of this chapter is to review: (1) the controls on the chemical and isotopic composition of barite and celestine and (2) the geological environments in which these minerals form. Some health risks are associated with barite, and these are discussed near the end of this chapter.

Although complete solid solution exists between $BaSO_4$ and $SrSO_4$ most representatives of the series are either distinctly Ba-rich or Sr-rich. Hence, it is convenient to use the term *barite* to refer to not only the stochiometric $BaSO_4$ endmember but also to those $(Ba,Sr)SO_4$ solid solutions dominated by Ba. Similarly, the term *celestine* will refer here not only to the stoichiometric $SrSO_4$ endmember but to solid solutions dominated by Sr. Such usage is in accord with standard mineral nomenclature. The Committee on Mineral Names and Nomenclature of the International Mineralogical Association recognizes "celestine" as the official name for $SrSO_4$. However, the name "celestite" is still commonly used in the literature.

Geological significance of barite and celestine

Most of the barite which exists in the Earth's crust has formed through the mixing of fluids, one containing Ba leached from silicate minerals, and the other an oxidized shallow fluid, such as seawater, which contains sulfate. Large deposits of barite represent areas of focused fluid flow and mineral precipitation and thus aid in the reconstruction of the hydrogeologic history of the Earth's crust. The stability of barite is redox sensitive, and the presence or absence of this mineral helps to constrain interpretation of paleoredox conditions. Pelagic barite, the precipitation of which is biologically mediated, may serve as a paleoproductivity indicator. In addition, the $^{87}Sr/^{86}Sr$, $\delta^{18}O$, and $\delta^{34}S$ isotopic composition and trace-element composition of barite help to identify sources of mineral-forming components, environments of precipitation, and secular variations in global seawater composition.

Celestine has a much more restricted geological distribution than barite, and most major occurrences appear to be the product of the reaction of hypersaline Sr-bearing fluids with gypsum and anhydrite. The presence of celestine reflects special geological environments where there has been preferential concentration of Sr over Ba.

Economic importance

Barite, because of its high density (4.48 g/cm^3), relative abundance, and ease of grinding into powder, has long been used for fillers, extenders, and weighting agents (Brobst 1994). Prior to the passage of the United States Pure Food and Drug Act of 1906, the principal use of barite in the U.S. was as an adulterant in flour and sugar. Today,

1529-6466/00/0040-0004$10.00 DOI: 10.2138/rmg.2000.40.4

barite and to a lesser degree witherite ($BaCO_3$) are the sources of barium chemicals used in glass, ceramics, ferrites and titanites, TV tubes, paint, plastics, green pyrotechnics, and photographic print paper. Kyle (1994) provides a detailed review of manufacturing processes involving barite. United States Pharmacopoeia barite is used in gastrointestinal X-ray examinations. By far the greatest use of barite, however, is as a weighting agent in drilling fluids used in the oil and gas industry. As such, annual production figures for barite closely track oil and gas exploration and development. Of the 2.18×10^6 metric tons (or 2.18 megatons, Mt) of barite used in the United States in 1997, the most recent year for which detailed figures were available at the time of this writing (1999), 2.08 Mt were used in drilling fluids (Searls 1997). Much of this barite was imported from China, the world's largest 1997 producer at 3.5 Mt, and was processed in Louisiana for use in petroleum exploration and development in the Gulf of Mexico sedimentary basin. Total world production was 6.93 Mt at an estimated total value in United States currency of $173,000,000 or $25/t. Nearly 50 countries currently produce barite. The top producers in 1997 were China, United States, Morocco, Kazakhstan, and India.

Celestine is the principal source of strontium chemicals used in ceramics, glass, red pyrotechnics, and metallurgy (Ober 1997). In 1997, more than 75% of the strontium consumed in the United States was used in color-television face plates, which are required by law to contain strontium to block X-ray emissions. Faceplate glass contains approximately 8 wt % SrO. World production of celestine in 1997 was estimated at 0.306 Mt, with a value of $72/t. Seven countries currently mine celestine: the principal producers are Mexico, Spain, Turkey, and Iran. There have been no active celestine mines in the United States since 1959.

Some conventions and terms used in this chapter

Concentration units. A variety of units are used to describe the concentrations of dissolved species in aqueous solutions. Marine chemists and geochemists routinely use mass of solute per kg of seawater. Units of mass per L of solution are typically used in studies of groundwater and basinal waters. Molality, *m*, moles of solute per kg H_2O, is the concentration unit used in thermodynamic work. Precise conversion between these three types of units requires knowledge of fluid density and total dissolved solutes for each analysis. This information is not always readily available, and no attempt has been made to convert units here. Concentrations are reported in the units given in the original paper cited. It should be noted, however, that units such as mg/L and mg/kg of solution or ppm are generally numerically comparable to two significant figures, i.e. 21 mg/L ≈ 21 mg/kg solution.

Bedded barite. Barite disseminated as individual grains and nodules in a layered sediment matrix conformable to bedding. Can include detrital barite, syngenetic barite, and diagenetic nodules. Equivalent in meaning to stratiform barite.

Deep-sea barite. Barite found in deep-sea sediments located away from continental margins.

Diagenetic. Precipitated within the host sediment from autochthonous sources of Ba and sulfate. Examples are barite nodules formed by the local dissolution, mobilization, and reprecipitation of syngenetic barite.

Epigenetic. Precipitated within a previously deposited host sediment from allochthonous sources of Ba and/or sulfate. An example is carbonate-hosted Mississippi Valley type barite. There is considerable overlap in usage between the terms syngenetic and diagenetic and between diagenetic and epigenetic among various workers.

Hydrothermal Deposited from allochthonous waters of sedimentary, igneous, or metamorphic origin, warmer than the initial temperature of the host rock or sediment.

MOR. Mid-ocean rise or ridge.

Pelagic barite and celestine. Barite and celestine formed in the upper part of the open-ocean water column by any process.

Sedex deposits. Sedimentary-exhalative mineral deposits. Mineral deposits formed by fluids venting into a marine environment where there is no obvious magmatic source of heat.

Syngenetic or synsedimentary. Formed penecontemporaneously with the host sediment, usually by mixing of Ba-rich fluids with marine waters, or by the incorporation of pelagic barite.

VHM deposits . Volcanic-hosted mineral deposits in which magmatic activity drives convective circulation of fluids. Includes volcanic-hosted massive sulfide (VMS or VHMS) deposits.

PHYSICAL CHEMISTRY

Crystal chemistry and solid-phase relations

Crystallography. The barite ($BaSO_4$) structure is orthorhombic, dipyramidal, and has the space group *Pnma*. Celestine ($SrSO_4$) is isostructural with barite. The sulfur and two oxygen atoms of each SO_4 tetrahedron in the $BaSO_4$ structure lie on a mirror plane (Gaines et al. 1997). The other two oxygens are equidistant above and below the plane. The Ba ions lie on the same mirror plane and are in 12-fold coordination with oxygens belonging to seven different sulfate groups.

Barite and celestine sometimes occur as a replacement of the mineral anhydrite ($CaSO_4$). Solid solution between $BaSO_4$ and $SrSO_4$ is complete, but that with $CaSO_4$ is incomplete. The anhydrite ($CaSO_4$) structure is also orthorhombic, but of the space group *Cmcm*. Unlike the barite structure, S and Ca atoms lie on lines of intersection of two sets of mirror planes, and planes containing evenly spaced Ca and SO_4 ions lie parallel to (100) and (010). In contrast to the larger barium ion, which is in 12-fold coordination in the barite structure, Ca is in 8-fold coordination with oxygens belonging to six different sulfate groups. According to Gaines et al. (1997), the anhydrite structure is similar to that of zircon.

A more detailed description of the crystal chemistry of these sulfate minerals is given by Hawthorne et al. (this volume).

Table 1. Ionic radii (6-fold coordination) of selected cations.

Cation	Ionic radius, angstroms	Cation	Ionic radius, angstroms
K^{+}	1.33	Pb^{2+}	1.18
Mg^{2+}	0.72	La^{3+}	1.05
Ca^{2+}	1.00	Ce^{3+}	1.01
Sr^{2+}	1.16	Lu^{3+}	0.85
Ba^{2+}	1.36	Eu^{2+}	1.17
Ra^{2+}	1.43		

Source: Huheey (1972)

Solid solutions . The substitution of cations other than Ba^{2+} and Sr^{2+} into barite and celestine is controlled by their degree of similarity in charge, ionic radius, and electronegativity to Ba^{2+} and Sr^{2+}. Table 1 shows the ionic radii (Huheey 1972) for key cations which will be discussed further in this chapter. Values are given for 6-fold coordination. Ionic radii generally increase with increasing coordination number, but the proportional differences in ionic radii between cations are similar with increasing coordination number.

Despite the fairly significant difference in ionic radii between Ba^{2+} and Sr^{2+}, 1.34 Å and 1.18 Å respectively, there is complete solid solution between $BaSO_4$ and $SrSO_4$ at room temperature, at least metastably, as first established by Grahmann (1920). Additional evidence for complete solid solution between barite and celestine has been obtained through X-ray diffraction by Sabine and Young (1954), Boström et al. (1967), and Burkhard (1973, 1978). Boström et al. (1967) further established the existence of complete solid solution between $BaSO_4$, $SrSO_4$, and $PbSO_4$ at 375°C. Takano et al. (1970), however, document a structure gap in the $BaSO_4$-$PbSO_4$ series.

There is more restricted solid solution between $CaSO_4$ and barite and celestine, reflecting the greater differences in ionic radii between Ca^{2+} and Ba^{2+} and the significant differences in crystal structure between barite and anhydrite noted above. Grahmann (1920) showed that at room temperature only approximately 6 mol % $CaSO_4$ can enter the $BaSO_4$ structure, slightly more $CaSO_4$ in strontian barite, and 8 mol % $BaSO_4$ in anhydrite. Grahmann also established that 12 mol % $CaSO_4$ can substitute in celestine and much as 42 mol % $SrSO_4$ in anhydrite. Substitution of K^+, Ra^{2+}, and rare-earth elements (REE) for Ba^{2+} and Sr^{2+} also occurs (e.g. Church 1979, Guichard et al. 1979, Morgan and Wandles 1980, Jebrak et al. 1985). The temperature dependence of the degree of substitution of other cations for Ba^{2+} and Sr^{2+} has not been established.

Chang et al. (1996) have summarized previous analytical work reporting minor substitution of Ba in barite by Fe, Cu, Zn, Ag, Ni, Ra, Hg and V. The minerals and compounds $BaSeO_4$, $PbSeO_4$, $SrSeO_4$, $BaCrO_4$, $KMnO_4$, $KClO_4$, and $(K,Cs)BF_4$ are isostructural with barite, and the anionic groups $[MnO_4]$, $[SeO_4]$, and $[CrO_4]$ have been substituted for sulfate in synthetic material (Chang et al. 1996). Some Archean barites contain Xe produced by cosmic ray bombardment of Ba (Srinivasin 1976).

Thermal stability. Barite undergoes a transition at 1148°C to a monoclinic structure that melts at 1580°C (Weast 1974). $SrSO_4$ melts at 1605°C (Weast 1974). An increase in pressure probably increases these melting temperatures. Hence, it is safe to assume that barite and celestine are intrinsically stable over the entire P-T range of the Earth's crust in the absence of other, reactive components.

Solubility of barite and celestine in aqueous solutions

Both Ba^{2+} and Sr^{2+} have high ionic potentials (the ratio of charge to ionic radius) and can be readily accommodated in aqueous solution as hydrated divalent cations, without the need for exotic aqueous complexing. The solubilities of barium chloride and strontium chloride, for example, are 375 g/L at 26°C and 538 g/L at 20°C, respectively (Weast 1974). The sulfate anionic complex is also readily accommodated in aqueous solution as a hydrated anionic species. For example, the solubility of $Na_2SO_4 \cdot 10H_2O$ is 927 g/L at 30°C (Weast 1974). The reaction between dissolved Ba, Sr, and sulfate, however, produces solids of such low solubility that natural waters can exist which have significant concentrations of either dissolved barium and strontium or of sulfate, but not both.

P-T conditions of natural waters that precipitate barite and celestine. Barite and, to a much lesser extent, celestine have formed over a wide range of tempera-tures and pressures in many different geological settings. As we shall see, most barite has formed by precipitation from aqueous solution. It is thus of interest to examine the aqueous solubility of barite and celestine over a wide range of pressure and temperature conditions. Figure 1 shows typical temperature and pressure ranges for fluids in seawater, sedimentary basins, seafloor vents, and volcanic areas, all environments in which barite has been found. Much of the *P-T* space between 0 and 400°C and 1 to 2000 bars represents potential conditions under which barite can precipitate. Barite has also been found in metamorphic and igneous rocks, although it is not common, and the *P-T* conditions could be extended

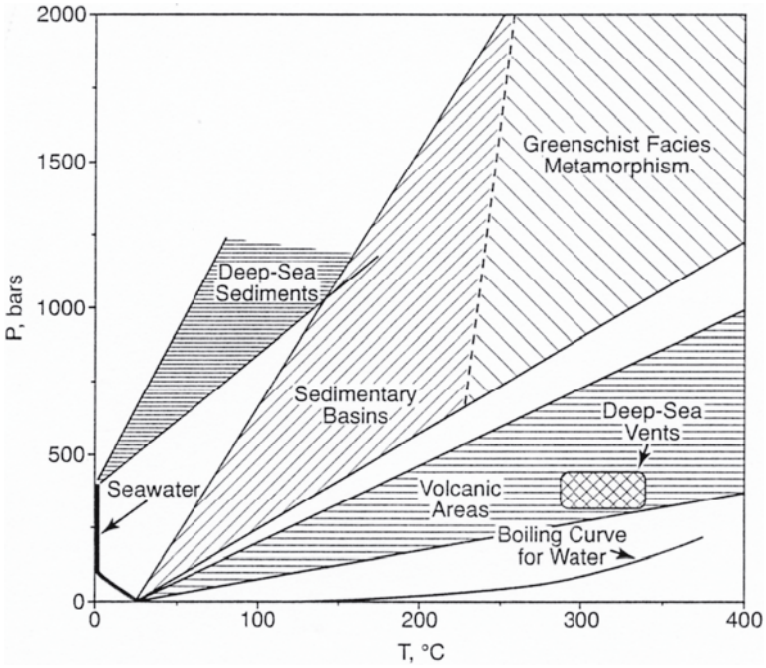

Figure 1. Pressure-temperature conditions for shallow crustal and marine environments.

beyond those shown in Figure 1.

Hydrolysis reactions involving pure endmembers. The mass-action relations for pure barite and celestine and an aqueous phase can be written as

$$BaSO_{4(s)} = Ba^{2+}_{(aq)} + SO_4^{2-}{}_{(aq)} \quad (1)$$

$$SrSO_{4(s)} + Sr^{2+}_{(aq)} + SO_4^{2-}{}_{(aq)} \quad (2)$$

For each of these reactions we can define an equilibrium constant, K

$$K_{BaSO_4} = (a_{Ba^{2+}})(a_{SO_4^{2-}})/(a_{BaSO_4}) \quad (3)$$

$$K_{SrSO_4} = (a_{Sr^{2+}})(a_{SO_4^{2-}})/(a_{SrSO_4}) \quad (4)$$

where a_i is the activity of component or species i. If we define standard state conditions such that the activities of pure $BaSO_4$ and pure $SrSO_4$ are unity at any given P and T, then

$$K_{BaSO_4} = (a_{Ba^{2+}})(a_{SO_4^{2-}}) \quad (5)$$

$$K_{SrSO_4} = (a_{Sr^{2+}})(a_{SO4^{2-}}) \quad (6)$$

Based on the calculated values of these equilibrium constants by Bowers et al. (1984), there is a several order-of-magnitude range in K_{BaSO_4} and K_{SrSO_4} over the P-T range of Table 2**.** At any fixed temperature, there is an increase in K_{BaSO_4}, and thus aqueous solubility, with increasing pressure, reflecting the reduction in volume accompanying the release of ions into solution. At a fixed pressure, there is an increase in K_{BaSO_4} of nearly an order of magnitude from 0 to 100°C, then a progressive decrease with increasing temperature. Celestine, in contrast, has retrograde solubility with increasing temperature over the entire temperature range. The lowest values of K for both phases are at high-T, low-P conditions. The saturation state for pure barite or celestine can be defined by Q/K or log(Q/K), where Q is the measured value of the activity product in Equation (5) or (6). At equilibrium, Q = K and thus Q/K = 1 and log(Q/K) = 0.

Table 2. Log hydrolysis constants for barite and celestine and barite-celestine equilibria at selected temperatures and pressures. Data from Bowers et al. (1984).

lg K(barite)

P, kbar \ T, °C	0	25	50	100	150	200	250	300	350	400
2.0	-9.12	-8.72	-8.50	-8.36	-8.47	-8.74	-9.11	-9.57	-10.11	-10.79
1.5	-9.30	-8.94	-8.72	-8.58	-8.70	-9.00	-9.14	-9.92	-10.57	-11.41
1.0	-9.56	-9.21	-8.98	-8.84	-8.97	-9.29	-9.76	-10.39	-11.25	-12.48
0.5									-15.73	-15.43
sat.*	-10.49	-9.96	-9.68	-9.51	-9.69	-10.16	-10.96	-12.35		

lg K(celestine)

P, kbar \ T, °C	0	25	50	100	150	200	250	300	350	400
2.0	-5.09	-5.13	-5.28	-5.72	-6.26	-6.85	-7.47	-8.12	-8.82	-9.63
1.5	-5.29	-5.38	-5.53	-5.97	-6.51	-7.13	-7.79	-8.49	-9.30	-10.28
1.0	-5.61	-5.67	-5.81	-6.24	-6.80	-7.44	-8.16	-8.99	-10.01	-11.39
0.5									-14.65	-14.46
sat.*	-6.51	-6.43	-6.53	-6.95	-7.56	-8.35	-9.41	-11.03		

lg [K(barite)/K(celestine)]

P, kbar \ T, °C	0	25	50	100	150	200	250	300	350	400
2.0	-4.03	-3.59	-3.22	-2.64	-2.21	-1.89	-1.64	-1.45	-1.29	-1.16
1.5	-4.01	-3.56	-3.19	-2.61	-2.19	-1.87	-1.35	-1.43	-1.27	-1.13
1.0	-3.95	-3.54	-3.17	-2.60	-2.17	-1.85	-1.60	-1.40	-1.24	-1.09
0.5									-1.08	-0.97
sat.*	-3.98	-3.53	-3.15	-2.56	-2.13	-1.81	-1.55	-1.32		

*sat. = saturation vapor pressure

Solubility in non-ideal aqueous solutions. The complex electrostatic inter-actions that occur in aqueous solutions, particularly in saline waters of high ionic strength, give rise to considerable departures between analytically-determined molal concentrations, m_i, of solute species and their thermodynamic activity, a_i (Nordstrom and Munoz 1994). The non-ideal behavior of sulfate, in particular, is pronounced even at moderate ionic strengths. These deviations can be accounted for by use of conventional free-ion activity coefficients, γ_i

$$a_{Ba^{2+}} = (\gamma_{Ba^{2+}})(m_{Ba^{2+}}) \quad (7)$$

or stoichiometric activity coefficients, γ^*_i

$$a_{Ba^{2+}} = (\gamma^*_{Ba^{2+}})(m_{Ba\ tot}) \quad (8)$$

where $m_{Ba\ tot}$ is the molality of total dissolved Ba.

There is an extensive body of experimental work on the solubility of end-member barite (e.g. Strübel 1967, Gundlach et al. 1972, Blount 1977) and celestine (e.g. Strübel 1966, Reardon and Armstrong 1987) in a variety of electrolyte solutions at different temperatures. The information derived both from theoretical considerations and experimental studies has been useful in deriving more generalized equations of state,

such as those of Pitzer (1987) which can be used to establish activity–concentration relations for dissolved Ba, Sr, and sulfate over a wide range of fluid compositions (e.g. Monnin and Galinier 1988, Monnin 1999, Ptacek and Blowes, this volume).

We examine briefly here some of the experimental work by Blount (1977) to assess the magnitude of the effects of increasing salinity on barite solubility. Many subsurface saline waters are dominated by Na and Cl as the principal solutes (Hanor 1994). Figure 2 shows the solubility of barite in NaCl solutions of varying NaCl concentration, as plotted from Blount's (1977) data. There is a significant increase in the solubility of barite by over an order of magnitude with increasing concentration of NaCl from 0 to 6 *m*, reflecting in large part the strongly non-ideal behavior of the sulfate ion in concentrated electrolyte solutions. The solubility curves are convex up relative to the NaCl axis, and mixing of two barite-saturated solutions of differing NaCl concentration would produce an intermediate water which is undersaturated with respect to barite.

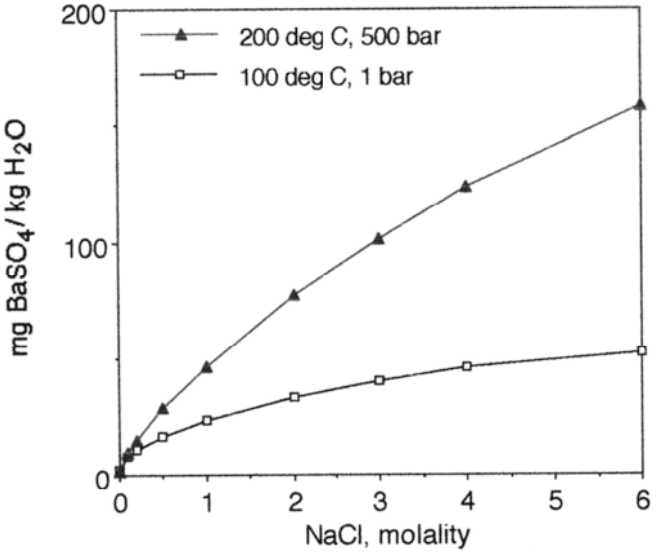

Figure 2. Variation in the solubility of barite in NaCl solutions as a function of the molality of NaCl at two selected *P-T* conditions. Plotted from data of Blount (1977). Mixing of two barite-saturated solutions of differ-ing salinity at a fixed temperature and pressure produces an intermediate solution which is undersaturated.

Aqeas sltinsld-sltin eqilb. A detailed account of solubility and thermodynamic properties of sulfate solid solutions is given by Glynn (this volume), and only a very brief overview is presented here. The problem of determining the stability of barite and celestine in natural waters is made complex by the fact that they rarely exist in nature as pure end-member phases, unlike the solids used in much experimental work, but rather as solid solutions. The activities of the components in the solid solution are given by

$$a_{BaSO_4} = (\lambda_{BaSO_4})(X_{BaSO_4}) \quad (9)$$

$$a_{SrSO_4} = (\lambda_{SrSO_4})\,(X_{SrSO_4}) \quad (10)$$

where λ_i is the activity coefficient and X_i is the mole fraction of the end-member component. In an ideal solid solution, λ_i is unity and $a_i = X_i$ for all components.

In theory, in a aqueous system in equilibrium with respect to both components, $BaSO_4$ and $SrSO_4$, must meet both conditions (9) and (10). In a strictly binary solid solution, these two equations are coupled through the relation.

$$X_{BaSO_4} + X_{SrSO_4} = 1 \quad (11)$$

A variety of graphical and computational techniques have been developed to portray or evaluate equilibrium involving aqueous solutions and binary solid solutions (see Glynn and Reardon 1990, Glynn et al. 1990, Felmy et al. 1993, Glynn this volume). One simple

method for predicting the composition of solid solutions that should be formed during precipitation is through the use of partition coefficients in which the activity of sulfate is eliminated as a variable. Subtracting mass-action Equation (2) from Equation (1) we have:

$$BaSO_{4(ss)} + Sr^{2+}_{(aq)} = SrSO_{4(ss)} + Ba^{2+}_{(aq)} \quad (12)$$

The equilibrium constant for this new mass-action relation is

$$K_{Sr\text{-}Ba} = (a_{SrSO_4})(a_{Ba^{2+}})/(a_{BaSO_4})(a_{Sr^{2+}}) \quad (13)$$

where

$$K_{Sr\text{-}Ba} = K_{BaSO_4}/K_{SrSO_4} \quad (14)$$

At equilibrium we can rewrite Equation (13) as

$$(a_{SrSO_4})/(a_{BaSO_4}) = K_{Sr\text{-}Ba}\,(a_{Sr^{2+}})/(a_{Ba^{2+}}) \quad (15)$$

Thermodynamic partition coefficients for ideal solid solutions. Assuming initially that the barite-celestine solid-solution series behaves ideally and that deviations from ideality of Sr^{2+} and Ba^{2+} are similar, Equation (15) can be used to estimate the ($SrSO_4/BaSO_4$) activity ratio of a solid that should precipitate out of a solution of a given (Sr/Ba) ratio under equilibrium conditions. Table 2 shows the variation in $K_{Sr\text{-}Ba} = (K_{BaSO_4}/K_{SrSO_4})$ over the *P-T* range of Figure 1. There is a very slight decrease in $K_{Sr\text{-}Ba}$ with increasing pressure at a fixed temperature, but there is a nearly three order-of-magnitude increase in $K_{Sr\text{-}Ba}$ with increasing temperature, from values of approximately 10^{-4} at 0°C to values approaching 10^{-1} at temperatures of 400°C. These extremely small values of $K_{Sr\text{-}Ba}$, particularly at low temperatures, result in the strong preferential partitioning of Ba into the solid phase and Sr into the aqueous phase.

Partition coefficients from precipitation experiments. A number of laboratory studies have been made of the partitioning of Ba and Sr between coexisting aqueous solutions and crystalline sulfate phases. Here, partitioning is expressed not as a thermodynamic constant, but rather a proportionality term, $D_{Sr\text{-}Ba}$, whose magnitude may reflect non-ideal behavior of the aqueous and/or solid solution, kinetics of precipitation, back reaction or re-equilibration after precipitation, and compositional zoning of the precipitate:

$$(Sr)/(Ba)_{solid} = D_{Sr\text{-}Ba}\,[(Sr^{2+})/(Ba^{2+})]_{aqueous} \quad (16)$$

Experimental studies of Ba-Sr partitioning during the precipitation of $(Ba,Sr)SO_4$ from aqueous solution include those of Goldschmidt (1938) at 18°C, Gordon et al. (1954) at 83°C, Starke (1964) at various temperatures between 20°C and 250°C, Church (1970) at temperatures of between 3 and 55°C, and Blount (1977) at 95°C. Experimental procedures and aqueous media varied widely among these workers. In general, experimentally derived partition coefficients, $D_{Sr\text{-}Ba}$, from most of the above precipitation experiments are one or more orders of magnitude *greater* than thermodynamic exchange constants at the same temperature. For reference, the thermodynamic $K_{Sr\text{-}Ba}$ at 25°C and 1 bar is $10^{-3.53}$. Starke (1964) reported a $D_{Sr\text{-}Ba}$ of approximately $10^{-1.5}$ at 20°C, Goldschmidt a value of approximately $10^{-2.5}$ at 18°C, and Blount, $D_{Sr\text{-}Ba}$ values of between 0.015 and 0.03 at 95°C. Starke's values for $D_{Sr\text{-}Ba}$ progressively increase with increasing temperature to values of 0.6 at 250°C.

In his experiments to determine partition coefficients for barite in seawater, Church (1970) mixed dilute sulfate-free seawater containing low concentrations of Ba with large volumes of seawater and observed that slower reaction rates produced lower concentrations of Sr, Ca, and K in the solids precipitated. Church's values of approximately $10^{-4.0}$ for $D_{Sr\text{-}Ba}$ and $10^{-6.0}$ for $D_{Ca\text{-}Ba}$ at 25°C are closer to thermodynamically predicted values that those of other workers.

Precipitation experiments involving $(Ba,Sr)SO_4$ are complicated because the preferential partitioning of Ba into the precipitate results in a continuing increase in the Sr/Ba ratio of the aqueous solution and hence in the Sr/Ba ratios of solids sequentially precipitated from solution. If earlier-formed solids do not back-react with the fluid, then the progressive change in fluid composition as a result of partitioning can be described by the Doerner-Hoskins relation, originally developed to describe the coprecipitation of Ra with Ba (Gordon and Rowley 1957):

$$\ln (Sr_i/Sr_f) = \lambda_{Sr\text{-}Ba} \ln (Ba_i/Ba_f) \quad (17)$$

where $\lambda_{Sr\text{-}Ba}$ is the logarithmic distribution coefficient, which is usually of the same magnitude as $D_{Sr\text{-}Ba}$, and the subscripts i and f refer to initial and final aqueous solution concentrations. Prieto et al. (1993) provide an in-depth review and discussion.

Partition coefficients from re-equilibration experiments. A second technique for determining equilibrium relations between aqueous and solid solution is to attempt to re-equilibrate a previously formed solid precipitate with an aqueous fluid. This is one of the approaches followed by Church (1970), who attempted to re-equilibrate pure barite and an artificial barite enriched in Sr, Ca, and K with surface seawater at 3°C for 17 months. Church observed a progressive loss with time of Sr, Ca, and K from the artificial barite.

In their re-equilibration experiments involving a wide range of solid compositions over a time span of nearly three years, Felmy et al. (1993) found evidence that small quantities of a phase close in composition to pure barite controlled aqueous Ba concentrations, and that substitution of Sr occurred in a second solid-solution phase in which the Ba component did not attain equilibrium with the aqueous phase.

Evidence for non-ideal behavior of the $BaSO_4$-$SrSO_4$ solid solution. The thermodynamic properties of the $BaSO_4$-$SrSO_4$ solid solution have not yet been rigorously established, but there is evidence for non-ideal behavior. This is not surprising in view of the large difference in ionic radii between Ba^{2+} and Sr^{2+} (Malinin and Urusov 1983). Goldish (1989) found that cell dimensions deviate from strictly linear relations as a function of composition. Burkhard (1973) demonstrated nonlinear variations in barite-celestine refractive indices. Brower and Renault (1971), however, concluded that the solid solution was ideal on the basis of their experimentally determined enthalpy values. See Hanor (1973) for a critical review of their experimental techniques.

Hanor (1966) noted that $D_{Sr\text{-}Ba}$ in Starke's (1964) precipitation experiments varied as a function of solid composition at fixed temperature, and attempted from Starke's precipitation data to derive values for B in the following equation relating activity coefficients and solid-solution compositions

$$RT \ln \lambda_1 = B (X_2)^2 \quad (18)$$

where B is comparable to the term W_G in a symmetrical Margules model solid solution (cf., Nordstrom and Munoz 1994). The results, not surprisingly, show increasing departure from ideal behavior with decreasing temperature. Church (1970) calculated the free energy of non-ideal mixing for K^+, Sr^{2+}, and Ca^{2+} in synthetic marine barite from long-term precipitation-equilibration experiments. He found that K behaved nearly ideally, but that Sr is non-ideal and Ca more strongly non-ideal, consistent with the progressive differences in ionic radii with Ba^{2+} (Table 1). Not discussed by Church (1970) is the fact that the K^+ substitution must in some way be coupled to preserve charge balance. Felmy et al. (1993) reviewed more recent work and some of the experimental problems that make determination of the thermodynamic properties of this solid solution difficult in re-equilibration experiments, including the apparent formation of two solid phases, one nearly pure barite, the other a $(Ba,Sr)SO_4$ solid solution, as noted above.

Kinetics of precipitation and dissolution. The kinetics of precipitation and dissolution of barite and celestine are dealt with in detail by Hina and Nancollas (this volume). Some recent studies include those of Bosbach et al. (1998), Christy and Putnis (1993), Denis and Michard (1983), Fernandez-Diaz et al. (1990), Kornicker et al. (1991), Mohazzabi and Searcy (1976), Prieto et al. (1990), and Putnis et al. (1992, 1995).

As discussed in this chapter, the precipitation of barite occurs in geologic settings which range from the rapid mixing of 350°C Ba-bearing hydrothermal fluids with 2°C deep seawater to the replacement of solid gypsum and anhydrite in probably nearly isothermal settings over extended periods of time. Barite thus exists in a wide range of crystal sizes, morphologies, and textures which in part reflect the kinetics and conditions of its crystallization. Barite, because of its low solubility, resists wholesale aqueous dissolution. Barite can be effectively dissolved, however, in highly reducing systems. Here the rates of dissolution may ultimately be dependent on the kinetics of biologically mediated redox reactions.

Practical problems involving the kinetics of barite and celestine precipitation and dissolution include the formation of barite scale in hydrocarbon wells (Weinritt and Cowan 1967) and the destruction of particles of pelagic barite and celestine that are produced in near-surface seawater and subsequently settle down through undersaturated marine waters (Dehairs et al. 1980).

Stability ranges in multicomponent systems

The thermodynamic stability of barite and celestine depends not only on their solubility in aqueous solution at various P-T and salinity conditions, but also on the presence or absence of other reactive components that can combine with Ba, Sr, and sulfate. Some of these other stability constraints are briefly reviewed.

Redox stability. Both barite and celestine can be destroyed through the inorganic and the biologically mediated reduction of sulfate, as in the following reactions at intermediate pHs, where $SO_4^{2-}{}_{(aq)}$, $HS^-{}_{(aq)}$, and $HCO_3^-{}_{(aq)}$ are predominant species:

$$BaSO_{4(s)} \rightarrow Ba^{2+}{}_{(aq)} + SO_4^{2-}{}_{(aq)} \quad (19)$$

$$SO_4^{2-}{}_{(aq)} + H^+{}_{(aq)} \rightarrow HS^-{}_{(aq)} + 2O_{2(aq\ or\ g)} \quad (20)$$

In low temperature marine environments, organic carbon, here represented by CH_2O, is a common reductant of sulfate:

$$SO_4^{2-}{}_{(aq)} + CH_2O_{(s)} \rightarrow HCO_3^-{}_{(aq)} + HS^-{}_{(aq)} + O_{2(aq\ or\ g)} \quad (21)$$

The reduction of barite and celestine is thus favored by low f_{O_2} and high H^+ (low pH) conditions. The low solubility of barite extends the stability field of $BaSO_4$ well into conditions where reduced sulfur, not sulfate, is the predominant aqueous sulfur species, and it is common to find stable coexisting mineral assemblages consisting of barite with pyrite, galena, and sphalerite (Fig. 3). BaS has been found in some anthropogenic reducing environments (Baldi et al. 1996) and is often used in constructing phase diagrams to denote the lower practical limit of barite stability. With progressively decreasing f_{O_2}, $CaSO_4$ will be reduced first because of it is more soluble, followed by $SrSO_4$, and then $BaSO_4$.

Potential reducing agents for barite at elevated *P-T* conditions include CH_4, H_2, CO, NH_3, and solid carbon. Theoretical calculations by Kritsotakis and von Platen (1980) show that reduction is favored by temperatures in excess of 200°C, low pH, and high gas fugacities. Despite the results of these theoretical calculations, there is abundant field

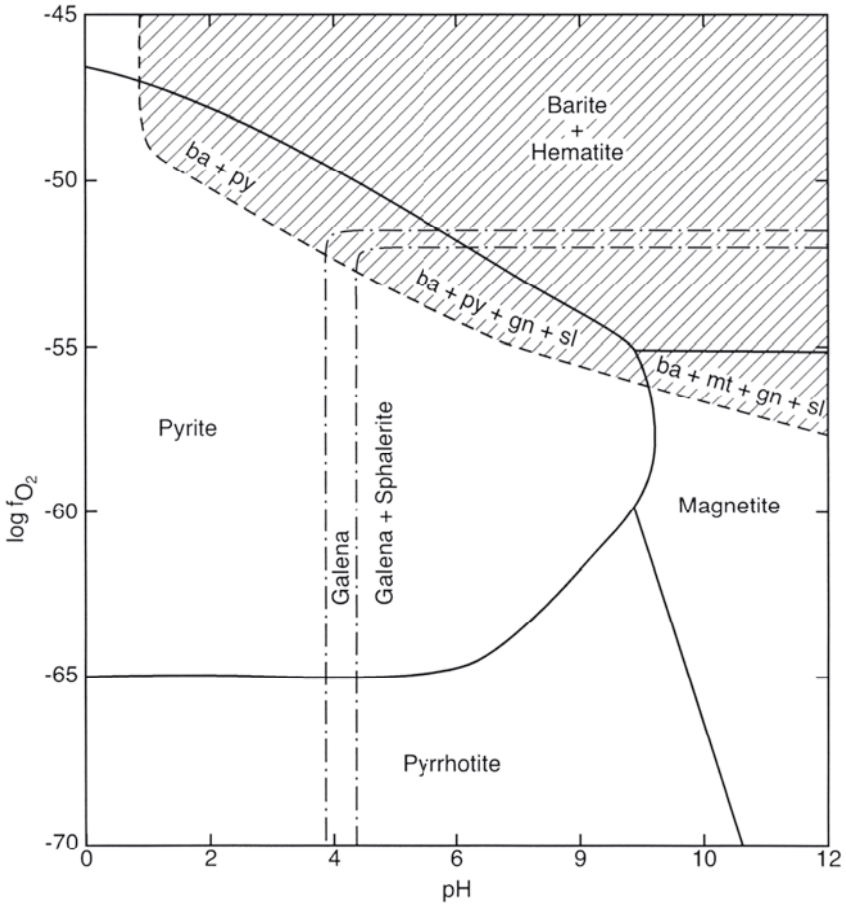

Figure 3. Log f_{O_2}–pH diagram showing the stability fields for barite (shaded), Fe oxides and sulfides, galena, and sphalerite at 100°C and a salinity of 20 wt % in seawater proportions. Total sulfur = 5.5×10^{-4} *m*. Galena and sphalerite fields drawn for 1 ppm each of Pb and Zn. Barite field drawn for 100 ppm Ba. Modified from Cooke et al. (1998). Note overlap of stability fields for barite and pyrite, galena, and sphalerite.

evidence of the remarkable stability of barite during metamorphism in the presence of reducing agents, as discussed later in this chapter.

Stability in presence of calcium sulfates. Both barite and celestine occur as replacements of gypsum or anhydrite as the result of reaction of Ba- and Sr-bearing fluids with calcium sulfate. Neglecting solid solution, these stability relations can be described by the following reactions:

$$BaSO_{4(s)} + Ca^{2+}_{(aq)} = CaSO_{4(s)} + Ba^{2+}_{(aq)} \quad (22)$$

$$SrSO_{4(s)} + Ca^{2+}_{(aq)} = CaSO_{4(s)} + Sr^{2+}_{(aq)} \quad (23)$$

The corresponding ion activity ratios at equilibrium are given by:

$$a_{Ba^{2+}}/a_{Ca^{2+}} = \log (K_{BaSO_4}/K_{CaSO_4}) \quad (24)$$

$$a_{Sr^{2+}}/a_{Ca^{2+}} = \log (K_{SrSO_4}/K_{CaSO_4}) \quad (25)$$

For example, based on data of Bowers et al. (1984) at 25°C and 1 bar (Table 3), anhydrite is unstable relative to barite in waters having log activity ratios of Ba^{2+}/Ca^{2+} greater than -5.69 and could be replaced by celestine where waters have Sr^{2+}/Ca^{2+} log activity ratios greater than -2.16. We will pursue this theme further when we discuss replacement of calcium sulfate minerals by barite and celestine.

Table 3. Log hydrolysis constants for barite-anhydrite and celestine-anhydrite equilibria at selected temperatures and pressures.
Calculated from data in Bowers et al. (1984).

lg [K(barite)/K(anhydrite)]

P, kbar \ T, °C	0	25	50	100	150	200	250	300	350	400
2.0	-6.43	-5.78	-5.19	-4.27	-3.59	-3.07	-2.66	-2.34	-2.06	-1.83
1.5	-6.41	-5.74	-5.16	-4.24	-3.55	-3.04	-2.36	-2.30	-2.03	-1.78
1.0	-6.36	-5.71	-5.13	-4.21	-3.53	-3.01	-2.60	-2.26	-1.98	-1.71
0.5									-1.71	-1.52
sat.*	-6.42	-5.69	-5.10	-4.17	-3.47	-2.95	-2.52	-2.13		

lg [K(celestine)/K(anhydrite)]

P, kbar \ T, °C	0	25	50	100	150	200	250	300	350	400
2.0	-2.40	-2.19	-1.97	-1.63	-1.38	-1.18	-1.02	-0.89	-0.77	-0.67
1.5	-2.40	-2.18	-1.97	-1.63	-1.36	-1.17	-1.01	-0.87	-0.76	-0.65
1.0	-2.41	-2.17	-1.96	-1.61	-1.36	-1.16	-1.00	-0.86	-0.74	-0.62
0.5									-0.63	-0.55
sat.*	-2.44	-2.16	-1.95	-1.61	-1.34	-1.14	-0.97	-0.81		

*sat. = saturation vapor pressure

Carbonate-sulfate equilibria. Witherite, $BaCO_3$, occurs in low-temperature deposits, and its formation is generally described as the replacement of barite (Chang et al. 1996). Witherite may react with sulfuric acid produced by the oxidation of sulfide ores to form barite (Fitch 1931). Strontianite, $SrCO_3$, also is generally formed from alteration of celestine and/or in association with celestine. In the presence of Ca, witherite requires high activities of barium and low activities of sulfate (Fig. 4) to be stable. Such conditions can exist where barite is being dissolved through sulfate reduction.

There are, in addition to witherite, other barium carbonates whose origin may include replacement of barite. These include alstonite, paralstonite, and barytocalcite, all

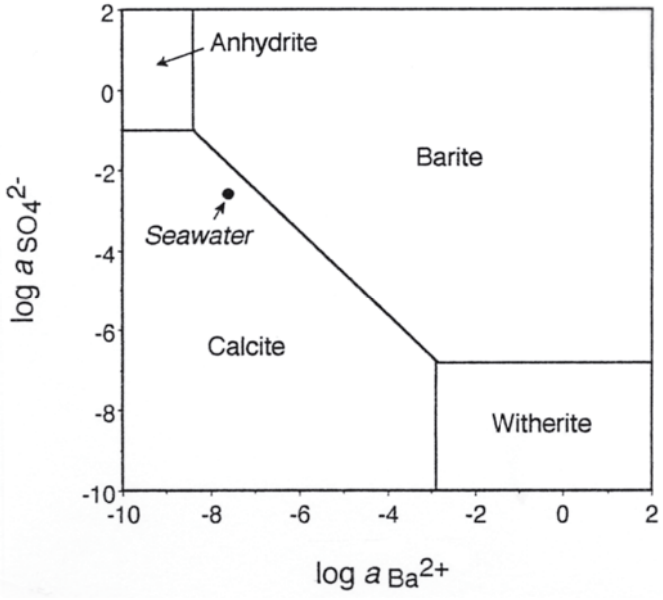

Figure 4. Stability fields for Ba-Ca sulfates and carbonates in aqueous solution at 25°C and 1 atm in aqueous solutions of modern seawater composition. Modified from Maynard and Okita (1991).

polymorphs having the formula $BaCa(CO_3)_2$, and norsethite, $MgBa(CO_3)_2$ (Chang et al. 1996). Benstonite, $(Ba,Sr)_6(Ca,Mn)_6Mg(CO_3)_{13}$, occurs in the Chamberlain Creek sedimentary-exhalative (sedex) bedded barite deposit in Arkansas (Lippman 1962).

Sulfate-silicate equilibria. Several Ba-bearing silicates coexist with barite in some metamorphosed barite deposits and are potential sinks for Ba during metamorphism. These minerals include the zeolite harmotome, $(Ba_{0.5}Ca_{0.5},K,Na)_5Al_5Si_{11}O_{32}\cdot 12H_2O$, and the feldspars celsian, $BaAl_2Si_2O_8$, and hyalophane, $(K_{1-x}Ba_x)Al(Si_{3-x}Al_x)O_8$, where x = 0.25 to 0.40, and cymrite, $BaAl_2Si_2(O,OH)_8\cdot H_2O$. The thermodynamic properties of the Ba aluminosilicates have not been well established, so their stability ranges are not well known. However, barite is remarkably refractory during metamorphism in silicate-bearing rocks in the absence of a sink for sulfate, as is described in the section in this chapter on behavior of barite during metamorphism.

Naerh and Bohrmann (1999) described Ba-rich authigenic clinoptilolite in sediments from the Japan sea, which they propose as a sink for dissolved Ba. Removal of Ba in silicate phases may be occuring inhydrothermal systems on the flank of the Juan de Fuca ridge (Bautier et al. in press).

Ba, Sr, AND S IN CRUSTAL ROCKS AND NATURAL WATERS

Most barite and celestine has been precipitated from aqueous fluids which contain Ba and Sr derived from the alteration of silicate, carbonate, and sulfate minerals in sedimentary, metamorphic, and igneous rocks. It is thus useful in understanding the controls on the distribution and composition of barite and celestine to examine briefly the crustal distribution of Ba, Sr, and sulfate both in terms of bulk-rock and bulk-fluid compositions. More extensive reviews on the general geochemistry of Ba and Sr are given by Puchelt (1967, 1972) and Faure (1972).

Crustal abundance and controls on the distribution of Ba and Sr

Barium, Sr, and S are relatively abundant and widely distributed elements in the rocks of the Earth's crust. Estimates of average crustal abundance vary, but Faure (1998) gives the following subequal values: Ba, 250 ppm; Sr, 260 ppm; and S, 310 ppm. The crustal geochemistry of Ba^{2+} and Sr^{2+} is dominated by their similarity in ionic radius and electronegativity to the major rock-forming cations, K^+ and Ca^{2+}, respectively. Most Ba in the Earth's crust exists in solid solution for K in K-bearing minerals, such as K-feldspars and K-micas, including biotite. A lesser amount substitutes for Ca in Ca-silicates. In marked contrast, most strontium exists as a proxy for Ca in Ca minerals such as anorthite, calcite, gypsum, and anhydrite.

Barium and Sr are present in most major igneous and siliciclastic rock types in subequal amounts at concentrations of between 200 and 900 ppm (Table 4, in the section entitled *Barite of Continental-Igneous and Igneous-Hydrothermal Origin,* below). Exceptions are tholeiite mid-ocean-ridge basalts, which have very low concentrations of both Ba and Sr, and carbonatites, which have exceptionally high concentrations. The abundance of Ba and Sr in igneous rocks increases with increasing Si, and hence, K and Ca, concentrations. The Sr/Ba weight ratio of most major rock types varies within the fairly narrow range of between 5 and 0.5, with the important exception of evaporites and carbonates, which can have Sr/Ba ratios in excess of 1000. This significant fractionation of Sr over Ba into Ca-carbonate and Ca-sulfate sediments plays a key role in the formation of celestine deposits, as is discussed later in this chapter. The general lack of celestine deposits of Precambrian age may well reflect the paucity of carbonate and Ca-sulfate sediments of this age and hence the absence of a mechanism for concentrating Sr.

Sulfate geochemistry

Sulfur exists primarily as sulfide, S^{2-}, sulfate, SO_4^{2-}, and as native sulfur, S°, although other valence states are known. The geochemistry of sulfur in the Earth's crust is controlled largely by redox state. Under reducing conditions sulfur may exist primarily as H_2S and metal sulfides, and in highly oxidizing conditions it exists mainly as dissolved sulfate and the alkaline earth sulfates gypsum, anhydrite, celestine, and barite.

The geochemical cycling of sulfur has evolved significantly over time in Earth history. The Earth's earliest atmosphere was most likely reducing and dominated by CO_2, N_2, and perhaps CH_4, with small amounts of reduced gases such as H_2, CO, and reduced S species (Kasting 1993, Des Marais 1994). The appearance of small amounts of free oxygen in the atmosphere and in surface ocean waters probably did not occur until the Proterozoic during a transition period marked by the appearance of redbeds at 2.3 Ga (Grotzinger and Kasting 1993). By 2.0 Ga, the Earth entered an aerobic stage in which free oxygen pervaded the entire ocean-atmosphere system (Eriksson et al. 1998).

Although minor occurrences of evaporitic gypsum are reported in the Archean (Buick and Dunlop 1990) they seem to reflect local sources of sulfate, perhaps ultimately magmatic in origin. The first extensive sedimentary sulfates known were deposited in the MacArthur basin, Australia from 1.7 to 1.6 Ga (e.g. Warren 1997, Cooke et al. 1998). Halite was commonly deposited immediately above carbonates in Early Proterozoic sediments, without intervening Ca-sulfates. According to Eriksson et al. (1998) the scarcity of Ca-sulfate evaporites may reflect either low concentrations of sulfate in seawater or a bicarbonate/Ca ratio that was sufficiently high to remove Ca by carbonate precipitation before the gypsum stability field was reached (Grotzinger and Kasting 1993). Most gypsum and anhydrite deposits are of Phanerozoic age.

Waters in sedimentary basins

As a result of an extensive body of analyses of waters coproduced with crude oil and natural gas, much is known about the composition of aqueous fluids in deep sedimentary basins. The behavior of Ba, Sr, and S in these waters provides clues as to the probable behavior in aqueous fluids in other shallow crustal rock types as well.

As discussed by Hanor (1979, 1994), the salinity of pore fluids in sedimentary basins varies by nearly five orders of magnitude, from <100 mg/L in shallow meteoric groundwater systems to hypersaline brines containing >400,000 mg/L. Barium and strontium show a similarly wide range in concentrations, from 0.1 to >1000 mg/L each.

In contrast to the anionic composition of saline waters, which is dominated almost entirely by chloride, there is a progressive, systematic change in the cationic makeup of formation waters with increasing salinity (Fig. 5), reflecting rock-buffering of fluid compositions (Hanor 1988). Where the composition of a fluid is rock-buffered by a specific silicate-carbonate mineral assemblage, the activity ratios of individual major cations to hydrogen ion, e.g. Na^+/H^+, $Ca^{2+}/(H^+)^2$, are nearly constant at a fixed *P* and *T* and vary only slightly as a result of variations in the activity of H_2O induced by changes in salinity (Hanor 1994). Hanor (1996a) showed that fixed cation-activity ratios and charge-balance constraints in such systems require that the activities of monovalent cations such as H^+, Na^+ and K^+ increase in 1:1 proportion to increases in total anionic charge or salinity, but that activities of Mg^{2+}, Ca^{2+}, and Sr^{2+} increase by a factor of 10:1. These relations for Ca^{2+} and Sr^{2+} versus TDS are reflected in 2:1 slopes on log-log scatter plots for basinal fluids world-wide (Fig. 5). Rather than a single unique phase assemblage responsible for controlling fluid compositions, various assemblages made up of common sedimentary silicate and carbonate minerals impose broadly similar constraints on fluid composition.

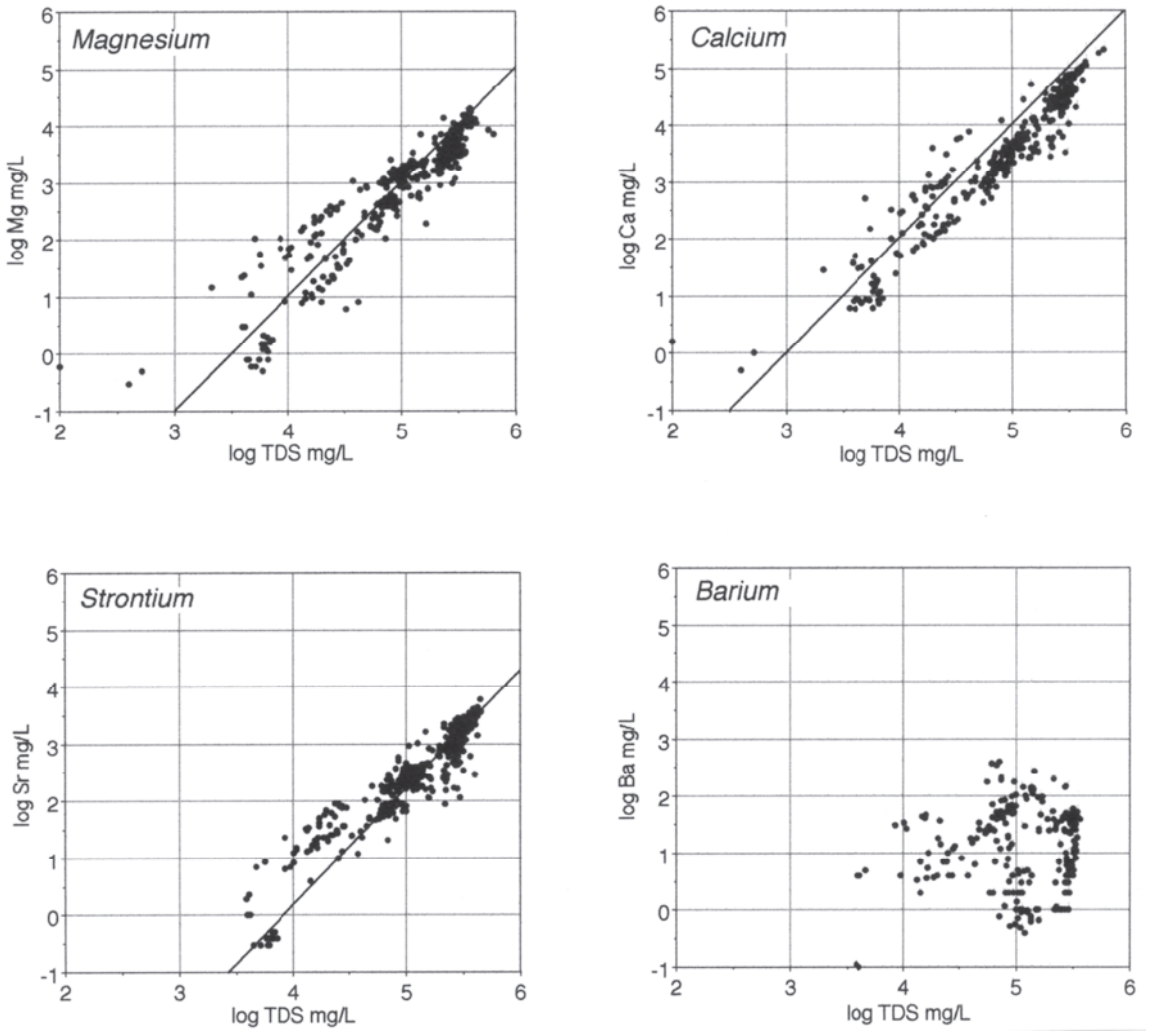

Figure 5. Variations in concentration of Mg, Ca, Sr, and Ba as a function of salinity in basinal waters worldwide. Solid lines for Mg, Ca, and Sr represent a 2:1 log-log slope. Data: Hanor (1994).

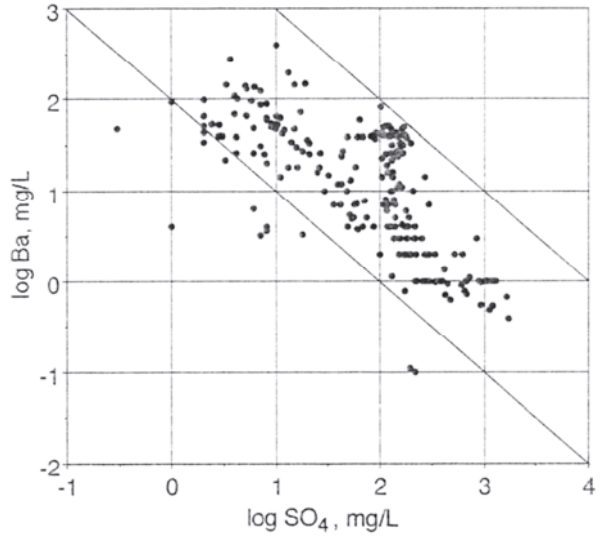

Figure 6. Dissolved Ba as a function of dissolved sulfate in basinal waters world-wide. Solid lines represent a -1:1 log-log slope. Data from Hanor (1994).

Of significance in the discussion of barite and celestine deposits is the dissimilarity of the behavior of Sr and Ba in basinal waters. In contrast to Ca^{2+} and Sr^{2+}, which each show a 10:1 increase in concentration with increasing salinity (Fig. 5), Ba shows a high degree of scatter. There is, how-ever, a rough inverse correlation with a slope of minus 1 between log Ba and log sulfate (Fig. 6), which is consistent with the hypothesis that equilibrium with respect to barite ($BaSO_4$) may be one factor controlling Ba concentrations (see also Macpherson 1989). Calculations by Fisher (1995, 1998) for similar subsurface brines in Texas

show the fluids to be close to saturation with respect to barite. The master variable controlling Ba concentrations in many basinal waters thus seems to be sulfate, whose own concentration is controlled by rate-dependent processes of dissolution of gypsum and anhydrite, dispersive fluid mixing, and reduction to sulfide. Not surprisingly, the waters highest in Ba are low in sulfate. Based on presently available data, fluids that would have the potential for transporting >10 mg/L Ba to a site of ore-mineral precipitation would typically have sulfate concentrations of <200 mg/L but could have salinities ranging from 10,000 to 300,000 mg/L.

Meteoric groundwaters

Buffering by barite is an important control on the concentration of barium in some shallow meteoric groundwater systems (Fig. 7). Where there has been bacterial reduction of sulfate, dissolved Ba can exceed the U.S. Environmental Protection Agency drinking water standard of a maximum of 2 mg/L (Gilkeson et al. 1981), even in waters of very low salinity.

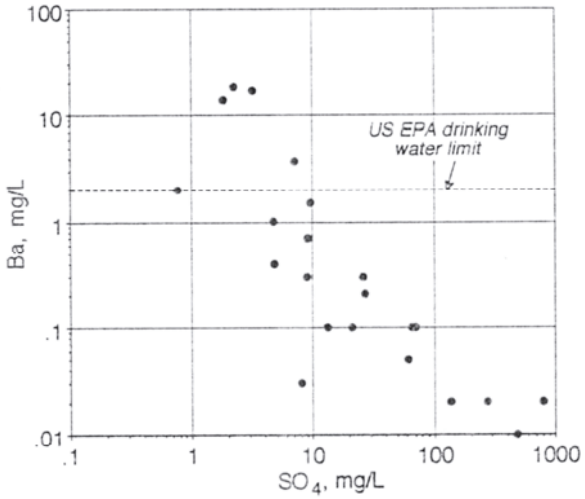

Figure 7. Dissolved Ba as a function of dissolved sulfate in portions of fresh and brackish water aquifers in northeastern Illinois. The waters are close to equilibrium with respect to barite. Plotted from data of Gilkeson et al. (1981).

Seawater

The approximate residence time of Ba in open seawater is a relatively short 5×10^4 y (Chester 1990), which, in the presence of sources and sinks for Ba within the water column, gives rise to significant spatial variations in dissolved Ba. The concentration of Ba in seawater typically varies from approximately 5 to 20 μg/kg of seawater (~5 to 20 μg/L) in open ocean water. The lowest values occur in the surface North Atlantic, the highest are in deep North Pacific waters (Chan et al. 1977, Ostlund et al. 1987, Rhein et al. 1987, Rhein and Schlitzer 1988, Jeandel et al. 1996). Much higher Ba concentrations, up to 60 μg/kg, are found in marine anoxic basins, such as the deep Black Sea (Falkner et al. 1993) and the anoxic hypersaline brines of the Tyro and Bannock basins, eastern Mediterranean (de Lange et al. 1990a,b).

Interest in the use of dissolved Ba as a potential stable proxy for radium led Chow and Goldberg (1960) to make the first studies of the concentration of dissolved Ba in seawater. These authors established that the depth distribution of dissolved Ba is similar to that of Ra (Koczy 1958), namely low in surface waters and higher at depth (Fig. 8). They concluded that Ba is extracted from surface waters by some process and is then released into deeper water. Chow and Goldberg (1960) also made the first calculations of saturation state of barite in seawater, taking into account pressure and temperature, and concluded that surface seawater is undersaturated with respect to barite but that saturation may be reached at greater depths.

The establishment of the GEOSECS program in the early 1970s brought with it large

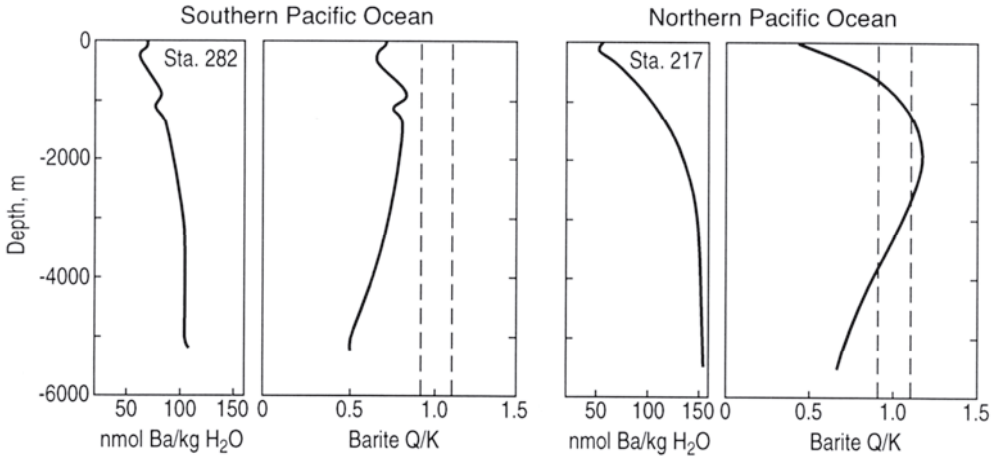

Figure 8. Concentration of dissolved Ba in nmol/kg H_2O and calculated saturation state, Q/K, for pure barite for seawater samples from two GEOSECS stations in the Pacific Ocean. A value of Q/K = 1 represents saturation. Modified from Monnin et al. (1999).

numbers of high-precision analyses of dissolved Ba (Church and Wolgemuth 1972; Chan et al. 1977; Chan and Edmund 1987). Church and Wolgemuth (1972) calculated the concentration of Ba in seawater saturated with respect to pure barite as a function of depth, taking into account the concentration of sulfate in seawater and the decreases in temperature and increases in pressure with depth. They compared their calculated values with the then recently measured Ba concentrations from the GEOSECS program and from Ba concentrations in pore waters in deep sea sediments and demonstrated that waters of the eastern Pacific were undersaturated from the surface to the seafloor, but that pore waters in deep-sea sediments were approximately saturated. The high-precision barium analyses of seawater of Chan et al. (1977) and Chan and Edmund (1987) have been utilized in a more recent study by Monnin et al. (1999) to calculate the saturation state of the oceans with respect to pure barite (Fig. 8). The results of these calculations show that while the oceans are generally undersaturated with respect to barite, equilibrium is reached in cold surface waters of the Southern Ocean, intermediate waters of the Pacific and deep waters of the Bay of Bengal. Slight supersaturation occurs in surface waters of the Waddell Gyre. Waters of the Atlantic are undersaturated. The calculated saturation state (Q/K) for pure barite ocean-wide ranges from approximately 0.15 to nearly 1.5.

Strontium is much more abundant in seawater than Ba. Strontium concentrations range from approximately 7.7 to 8.1 mg/kg of seawater, and its residence time is approximately 4×10^6 y (Chester 1990). The residence time of Sr is several orders of magnitude larger than oceanic mixing times of 1500 years, and hence the isotopic composition of marine Sr is uniform at any given time, although it shows long-term secular variations. There are only minor variations in Sr/salinity ratios in the open ocean. Bernstein et al. (1992) estimated the saturation index of celestine in surface ocean water to be approximately 0.16.

Sulfate is the second most abundant anion in modern seawater at an average concentration of 2712 mg/kg of seawater, and is surpassed in abundance only by chloride (Chester 1990). The long residence time of sulfate, 8.7×10^6 y, results in uniform sulfate/salinity ratios in the open ocean. In anoxic basins, however, sulfate can be reduced to sulfide. Like Sr, the isotopic composition of marine S is uniform at any given time in open ocean conditions, although it shows long-term secular variations.

Seawater today is sulfate-rich and Ba-poor. Although the oceans are generally slightly undersaturated with respect to pure $BaSO_4$ and biological activity is effective in maintaining this undersaturation, the principal reason the oceans are Ba-poor is the

presence of high levels of dissolved sulfate. Is it possible that during the Archean, when there was little free oxygen and sulfate, that the oceans were barium-enriched.

River and estuarine waters

The concentration of Ba in surface ocean water is significantly less than that of average river water. Hanor and Chan (1977) for example, found that dissolved Ba in the lower Mississippi River at the time of their study of the Mississippi River Estuary was 60 μg/L, whereas the Gulf of Mexico had Ba values of only 11 μg/L (~11 μg/kg seawater). Hanor and Chan (1977) also found that the behavior of dissolved Ba in the Mississippi River Estuary is strongly non-conservative, with excess Ba introduced into solution during mixing as a result of Na displacing adsorbed Ba on suspended clays. Waters of intermediate salinity are actually approximately two times supersaturated with respect to barite. Approximately half of the flux of dissolved Ba into the Gulf of Mexico from the Mississippi River was derived by desorption occurring near the mouth of the river. Shaw et al. (1998) have recently documented a diffuse flux of dissolved Ba from groundwaters discharging into the ocean along the U.S. Atlantic coast. Additional information on Ba in river and estuarine systems is given by Edmond et al. (1978), Carroll et al. (1993), Coffey et al. (1997), and Stecher and Kogut (1999).

Waters in crystalline rocks

Data on Ba in pore waters in crystalline rocks of the upper crust are limited. Most of the major cations, however, show trends with salinity and chlorinity similar to those documented for sedimentary basins, and it is probable that minor dissolved species such as Ba and Sr may show trends similar to those observed in sedimentary basins.

Continental rifts

Analyses of waters from the Salton Sea continental rift, California (McKibben and Hardie 1997) provide clues as to the behavior of Ba and Sr in areas of high heat flow and continental hydrothermal activity. Temperatures of waters which have been analyzed range from 200 to >300°C. Most dissolved sulfate values are <100 mg/kg fluid. Under these conditions of high temperature and low sulfate, concentrations of Ba are not buffered by barite. Barium instead shows a roughly 2:1 increase with increasing salinity on a log-log plot, similar to the behavior of Ca and Sr for these same waters (Fig. 9).

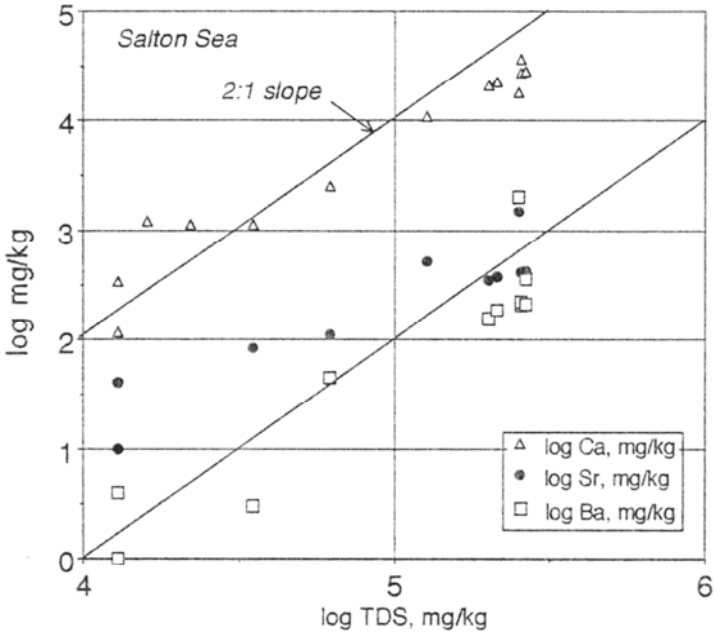

Figure 9. Variation in dissolved Ca, Sr, and Ba in waters from the Salton Sea continental rift. Solid lines show 2:1 slopes on the log-log plot. Compare Ba to Figure 5. Plotted from data of McKibben and Hardie (1997).

Seafloor hydrothermal vents

Hydrothermal vents are a significant source of Ba to the ocean. Edmond et al. (1979) and Von Damm (1995) estimated that the hydrothermal input of Ba is about 1/3 its total input into the ocean. Scott (1997) summarized Ba, Sr, and chlorinity values for modern seafloor hydrothermal vents and noted that Ba values represent minima because of the rapid removal of Ba by precipitation as barite. Barium values range from 0.01 to 0.06 mmol/L, or roughly two orders of magnitude higher than seawater levels of Ba. Strontium ranges from from 0.04 to 0.27 mmol/L, or from approximately half to three times seawater levels. Chlorinities range from slightly less to nearly twice that of seawater.

Review of controls on Sr/Ba ratios in natural waters

The Sr concentration of many crustal waters appears to be controlled largely by buffering by multi-phase silicate-carbonate mineral assemblages, whereas the concentration of Ba in many crustal waters is controlled instead by buffering with respect to barite. This decoupling of the geochemical behavior of Sr and Ba has given rise to a wide range of Sr/Ba ratios in crustal fluids. It is this diverse range of fluid Sr/Ba ratios that is partly responsible for the observed range of Sr/Ba ratios in naturally occurring barite and celestine. Because of the strong preferential partitioning of Ba into the solid sulfate phase during precipitation, only waters of extremely high Sr/Ba ratios are capable of precipitating celestine. The highest Sr/Ba waters today are those of high salinity (Fig. 10) and low Ba/SO_4 ratio (Fig. 11), i.e. highly saline waters with significant concentrations of dissolved sulfate.

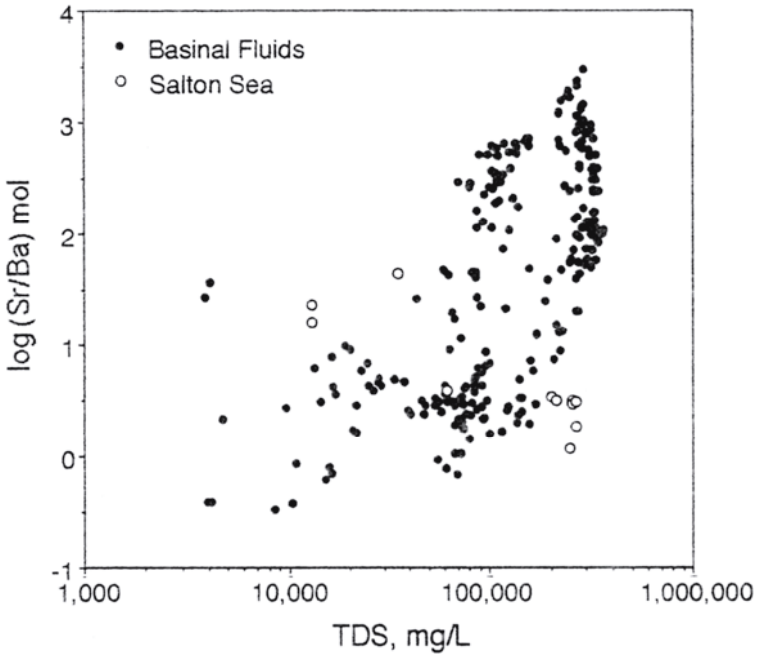

Figure 10. Relation between Sr/Ba ratio and salinity of basinal waters and the Salton Sea rift. Data from Hanor (1994) and McKibben and Hardie (1997).

ENVIRONMENTS OF FORMATION OF BARITE AND CELESTINE: AN OVERVIEW

This section reviews some of the recurring themes discussed in the remainder of this chapter. These include general mechanisms for forming barite and celestine and the global relations between the occurrence of barite and celestine and regional tectonics, hydrogeology, and the secular evolution of the composition of seawater and sedimentary rocks.

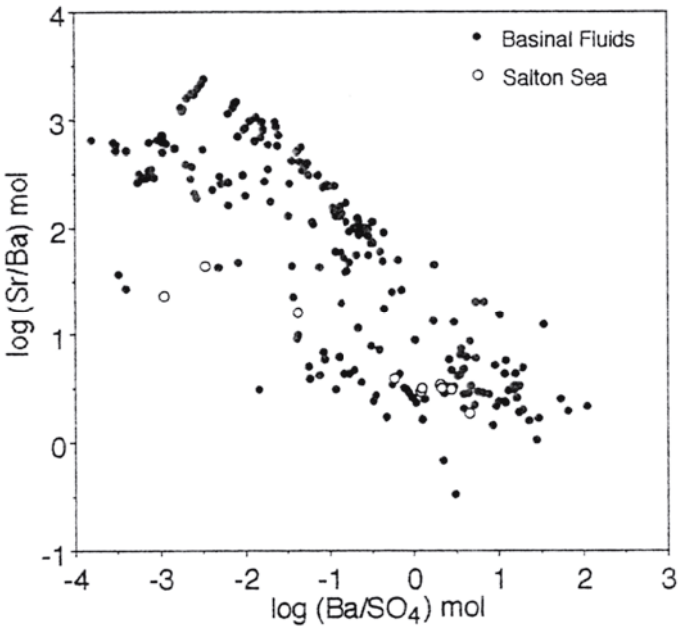

Figure 11. The relation between the Sr/Ba and Ba/SO_4 ratios of basinal waters and Salton Sea rift. Data from Hanor (1994) and McKibben and Hardie (1997).

Mechanisms for the precipitation of barite and celestine

Most barite and celestine has formed in one or more of the following ways:

Barium-rich fluids ascending from deep and mixing with seawater. Such deposits are known as *submarine exhalative* deposits. There are two principal end-member types, *submarine volcanic hydrothermal* deposits, whose formation is directly related to fluid convection driven by magmatic heat, and *sedimentary exhalative (sedex)* deposits, for which no obvious magmatic activity is involved. The Ba-rich fluids are derived from the leaching of oceanic or continental rocks or both. The sulfate in the overlying marine fluids may have undergone partial reduction, thus altering the isotopic composition of residual dissolved sulfate to heavier values, which are reflected in the precipitated barite. Sedex deposits include economically important occurrences of Pb and Zn as well as barite, and the submarine volcanic hydrothermal deposits include a wide range of *volcanic-hosted massive sulfide (VMS)* deposits, many of which contain barite, as well.

Biologically mediated precipitation of barite and celestine. A number of marine and freshwater organisms are known to induce the precipitation of barite or celestine from the Ba, Sr, and sulfate present in ambient water (e.g. Dehairs et al. 1980, Bernstein et al. 1992). There is also evidence that release of Ba and/or sulfate through degradation of biologically precipitated materials can create microenvironments favorable for the precipitation of barite.

Reaction of barium- or strontium-rich fluids with non-seawater sulfate. These include reactions involving Ca-sulfate evaporite minerals, sulfate-bearing waters derived from the subaerial evaporation of seawater and/or the dissolution of evaporites, sulfate derived from the oxidation of sulfides, and magmatic sulfate. Examples of barite formed this way include the carbonate-hosted *Mississippi Valley Type* and *Irish Type* ore deposits, vein deposits occurring along continental rifts, and innumerable examples of dispersed barite in the form of concretions and cements. Most of the largest deposits of celestine in the world have formed in specialized environments in which Sr-rich fluids have reacted with sulfate in an evaporate-carbonate environment. Other examples include replacement of gypsum and anhydrite in salt dome caprock by barite and celestine and the

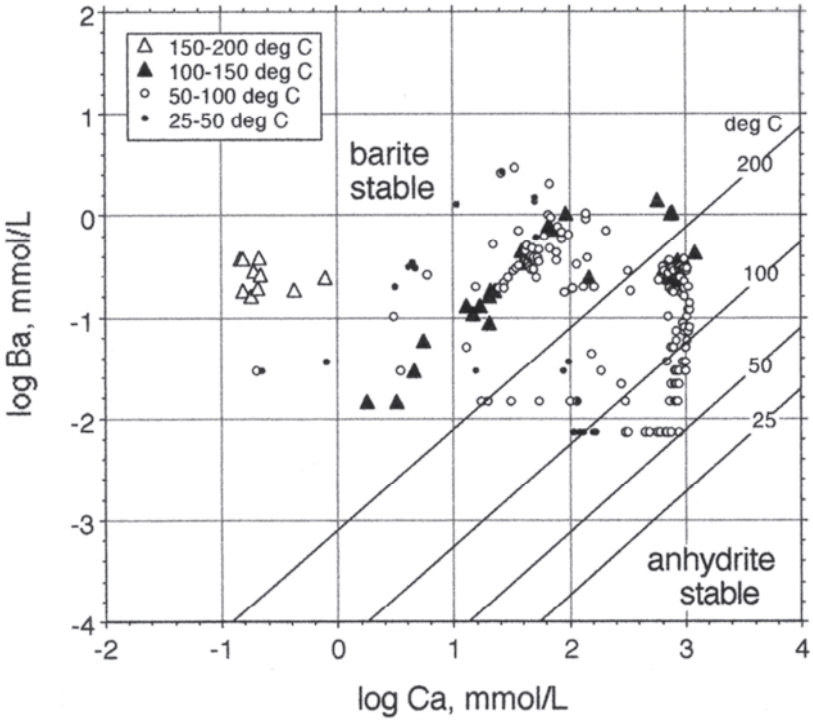

Figure 12. Variation in dissolved Ba and dissolved Ca in basinal waters world-wide. Sloping lines delineate approximate stability fields of barite and anhydrite as a function of temperature as determined from data in Table 3.

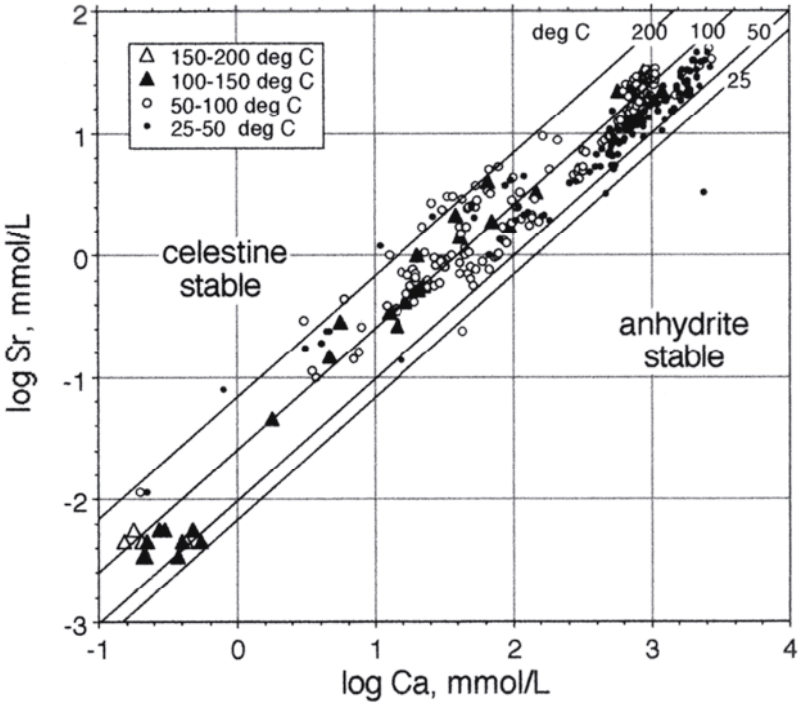

Figure 13. Variation in dissolved Sr and dissolved Ca in basinal waters world-wide. Sloping lines delineate the approximate stability fields of celestine and anhydrite as a function of temperature as determined from data in Table 3.

apparent discharge of barium-rich ground waters into sites of active subaerial evaporation of seawater. Figures 12 and 13 show the variations in dissolved Ba and Sr with dissolved Ca in sedimentary basins and the phase relations between barite and celestine with anhydrite calculated from Table 3 for typical basinal P–T conditions (Fig. 1). Composition-temperature-pressure relations for many of these waters favor replacement of anhydrite by barite or celestine. Decreasing temperature and pressure also favors replacement of anhydrite.

Decreasing solubility resulting from changes in fluid pressure and temperature. Precipitation of barite and celestine can result from changes in pressure and temperature. Barite shows a reduction in solubility through lowering of pressure at any temperature, and below 100°C a lowering of temperature. The hydrolysis constant for barite decreases by about an order of magnitude for an ascending fluid following a typical basinal *P-T* trajectory (Fig. 1). Celestine, because of its strongly retrograde solubility, is less likely to be precipitated by ascending fluids undergoing cooling.

Release of Sr during diagenesis of marine carbonates. In the presence of interstitial marine sulfate, release of Sr during diagenetic alteration of a Sr-rich carbonate, such as aragonite, to a carbonate-poor carbonate such as calcite or dolomite, can produce celestine (Baker and Bloomer 1988).

Relation of barite and celestine occurrences to global tectonics and regional hydrogeology

Most major occurrences of barite and celestine have formed in response to the development of tectonic regimes which have driven waters carrying Ba and Sr derived from depth into shallow, oxidizing conditions where sulfate is stable. As reviewed by Garven and Raffensperger (1997), fluids within sedimentary basins and the continental crust are subjected to a variety of forces which can cause large-scale fluid migration. The types of flow associated with these forces are sometimes grouped into topography-driven flow, free convection (e.g. thermohaline overturn), and forced convection (Cathles 1997). Fluid flow in the oceanic crust, in contrast, is dominated by thermal convection induced by high heat flow associated with magmatic activity.

Extensional faulting has played a key role in the localization of many barite deposits. Such faults occur in a wide variety of tectonic settings, including even compressional continental margins. Many barite deposits occur along areas of extension in compressional, passive, and strike-slip continental margins, continental rift basins, and oceanic crust.

Relation of barite and celestine occurrences to the secular evolution of sedimentary rock types

During the early Archean, most marine sulfate was probably derived from local magmatic activity, and barite precipitated in sedimentary-volcanic environments now preserved in greenstone belts.The progressive oxidation of the Earth's atmosphere and oceans during the Precambrian was important in creating large quantities of oxidized sulfur which in turn led to the formation of two reservoirs of sulfate which subsequently have been involved in barite precipitation: sulfate in marine waters and Ca-sulfates in evaporite sequences (e.g. Warren 1997). The development of organisms that could precipitate massive quantities of platform and epicontinental carbonates in the Paleozoic resulted in the formation of thick and regionally-extensive carbonate-evaporite sequences. Some of these carbonates served as regional aquifers during crustal deformation, permitting fluids from depth to react with sedimentary sulfate. The appearance of Ca-rich sediments also provided a mechanism for concentrating Sr and creating high Sr/Ba environments necessary for precipitating celestine. Since the Jurassic, however, the principal locus of carbonate deposition has shifted from the shallow marine coastal environment into the pelagic realm.

Marine versus continental barite

Goldberg et al. (1969) introduced the concept, which continues to be invoked in the literature, that there are demonstrable differences between what they termed marine and continental barite, i.e. barite presently found on or near the seafloor and barite found in rocks that now make up part of the continental crust, respectively. Unfortunately, this classification obscures the sources of Ba and sulfate and the mechanisms by which barite precipitates.

Barite precipitated with seawater sulfate as the principal source of sulfur has several distinct modes of formation in modern marine environments, including: (1) biologically-mediated pelagic precipitation in near-surface waters; (2) precipitation related to oceanic submarine hydrothermal activity; (3) precipitation related to submarine discharge of fluids from continental margins and in epicontinental marine basins. Each type of barite has been referred to in the literature by different authors as "marine barite."

The term "continental barite" has no genetic connotation other than barite which is presently part of a continental terrane, even if it originally precipitated in a marine environment on oceanic crust. Of the four examples of continental barite discussed by Goldberg et al. (1969), one is from a Precambrian metamorphosed sedex deposit that formed in a marine setting, two are from carbonate-hosted MVT deposits, and one is a magmatic-hydrothermal vein deposit. Of the four examples of marine barite discussed by these authors, two are from the California borderland in a tectonic setting which may involve continental or transitional crust. The other two are dispersed barites from Pacific deep-sea sediments.

CHEMICAL AND ISOTOPIC COMPOSITION OF BARITE AND CELESTINE: AN OVERVIEW

Natural barite and celestine rarely exist as end-member phases. There is a wide variation in Sr/Ba and the incorporation of other cations, such as Ca^{2+}, Ra^{2+}, Pb^{2+}, and K^{+} in the barite-celestine series. These compositional variations have the potential for helping to constrain interpretation of environments of formation. In addition, there is measurable variation in the Sr, S, O, Ra, Pb, and Nd isotopic compositions of barite and celestine. The use of Sr- and S-isotope geochemistry, in particular, has added greatly to our understanding of sources of components and environments of formation of barite and celestine. Finally, both minerals can contain fluid inclusions, which provide information on the salinity, chemical composition, and temperature of the host fluids. Systematics on the controls on the chemical and isotopic composition of barite and celestine are briefly reviewed to provide a background for the later sections of this chapter.

Frequency distribution of compositions in the barite-celestine series

Although a complete solid solution exists between barite and celestine, apparently even at temperatures approaching 25°C, there is a strongly bimodal distribution to the frequency distribution of compositions in this solid-solution series (Hanor 1968, Prieto et al. 1993, 1997). Most barite contains less than 7 mol % $SrSO_4$ and most celestine contains less than 4 mol % $BaSO_4$ (Fig. 14) (Hanor 1968). Intermediate compositions are known in nature (e.g. Burkhard 1978), but they are uncommon.

Hanor (1968) explained this strongly bimodal distribution through a series of model calculations predicting the compositions in the barite-celestine series that would be expected during the progressive titration of Ba and Sr out of an aqueous solution (Fig. 15). The calculations assumed a closed system with respect to Ba and Sr and precipitation following the Doerner-Hoskins fractionation relation (Eqn. 17), i.e. early-formed precipitates do not re-equilibrate with the aqueous solution. In the model results reproduced here, it was assumed that initial aqueous solution compositions between $Ba_{90}Sr_{10}$ and $Ba_{10}Sr_{90}$ occur with equal frequency and that all of the Ba and Sr is eventually precipitated out of solution. A value for the partition coefficient $\lambda_{Sr\text{-}Ba}$ of 0.03 (Eqn. 17) was used which represents an average value of $D_{Sr\text{-}Ba}$ for temperatures between 20 and 80°C and the complete range of solid solution compositions studied by Starke (1964).

During titration of Ba and Sr from a fluid of given initial Sr/Ba content, the first solid to form is highly enriched in Ba, as expected from the small value of the partition

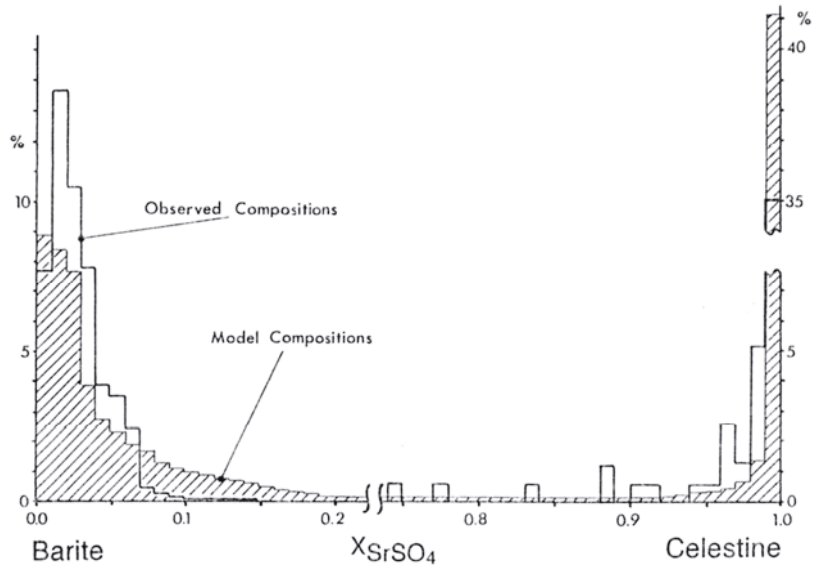

Figure 14. Frequency distribution of observed compositions in the barite-celestine solid-solution series normalized so that the areas under the Ba-rich and the Sr-rich ends of the histogram are the same. Shaded area shows the calculated frequency distribution of compositions formed during closed-system precipitation of Ba and Sr from solution. See text for details. Modified from Hanor (1968).

coefficient. As Ba is removed preferentially over Sr from aqueous solution, the Sr/Ba concentration of the fluid increases, and the Sr/Ba ratio of the next increment of solid to be precipitated has a higher Sr/Ba ratio than the preceding. There is, however a strongly non-linear variation in solid composition with the degree of progress of removal of Ba plus Sr from aqueous solution. There are *three* distinct stages in the evolution of the compositions of the solids as precipitation progresses. In the first stage, a series of Ba-rich, Sr-poor solids is formed (Fig. 15). The Sr content of these solids increases only slightly as precipitation progresses. In the second stage, compositions of the solids swing abruptly from Ba-rich to Sr-rich over a very narrow range of precipitation. In the third stage, the solids precipitated are very nearly pure $SrSO_4$. As a consequence of the strong fractionation of Ba and Sr which occurs during precipitation, most of the solids produced are thus either Ba-rich or Sr-rich. Only a small mass has intermediate compositions. On this basis, Hanor (1968) concluded that the paucity of intermediate compositions in nature does not require the existence of a miscibility gap, but can be simply explained by the strong partitioning of Ba into the solid during precipitation and the eventual formation of a residual fluid having a high Sr/Ba ratio. Subsequent authors have come to the same conclusion (Prieto et al. 1993, 1997).

Nature's modes for titrating Ba and Sr out of solution are far more varied than the above and probably only rarely involve sequential removal of most of the Ba plus Sr from aqueous solution. Submarine exhalative deposits, for example, are systems open with respect to Ba and Sr, where hydrothermal fluids carrying Ba and Sr are injected into an essentially infinite volume of well-mixed sulfate-rich seawater.

It is thus not surprising from the small partition coefficient for Sr incorporation into barite that most barite has only modest concentrations of Sr. More problematic are the venues which can produce celestine in the presence of barium. One mechanism is to start with a fluid whose initial Sr/Ba ratio is high, then precipitate the Ba end-member early in the precipitation history, and then precipitate nearly pure $SrSO_4$, much like the titration curves on the far right of Figure 15.

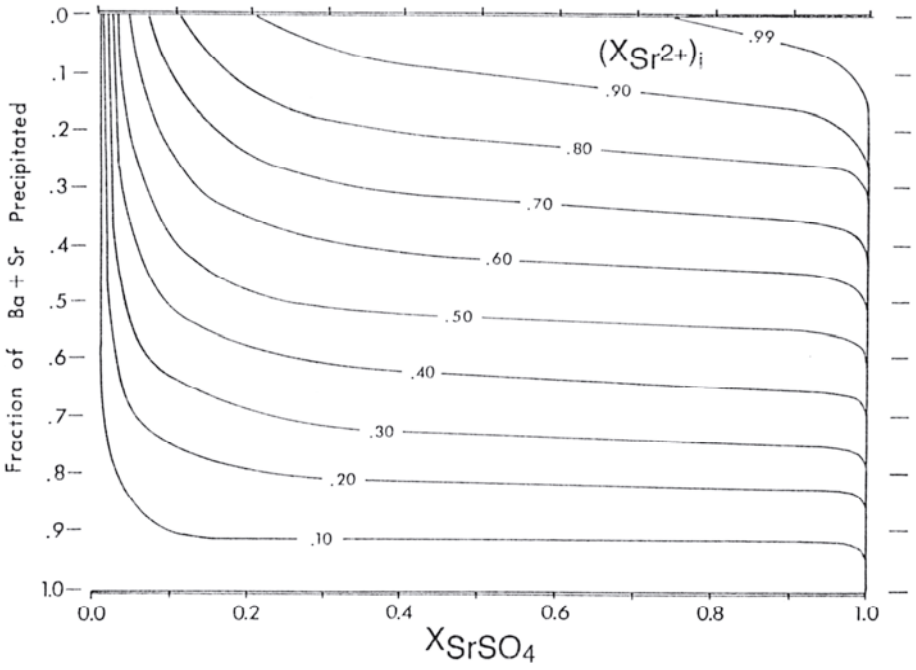

Figure 15. Composition of the last-formed increment of $(Ba,Sr)SO_4$ as a function of the mole fraction of Ba plus Sr precipitated from aqueous solution for a series of initial aqueous solution compositions of varying initial Sr/Ba content. The calculations assume Doerner-Hoskins behavior and $\lambda_{Sr\text{-}Ba} = 0.03$. Solid and liquid compositions are expressed as mole fractions, where $X_{Sr}^{2+} + X_{Ba}^{2+} = 1$ and $X_{SrSO_4} + X_{BaSO_4} = 1$. Modified from Hanor (1968).

Ba-Sr zoning in barite-celestine

The partitioning of Ba and Sr described above has the potential for giving rise to compositional zoning that reflects changes in fluid compositions resulting from fractionation. In addition, because the Ba-Sr partition coefficient is temperature dependent, changes in temperature in time and in space may also give rise to compositional variations. Hanor (1966) and many others (e.g. Starke 1964, Burkhard 1978, Breit et al. 1990) have described compositional zoning in barite which exist on scales from the several micron to the 1000 km.

For example, the Sr content increases from the center outward in some barite concretions, suggesting precipitation from a closed system (Hanor 1966). In contrast, concretions associated with shale-hosted stratiform deposits commonly show reverse zoning, in which Sr decreases from the center outward. This may reflect diffusion-controlled rates of transport of Sr and Ba to sites of precipitation (Okita 1983).

Zoning of Ba and Sr has been described within individual ore districts. At the Julcani Ag-Bi-Pb-S district, central Peru, ore-forming solutions rose vertically and spread laterally from a central zone (Hanor 1966). There is a strong increase in the Sr-content of barite out from this central zone, consistent with partitioning of Ba into the solid phase and an increase in fluid Sr/Ba ratio during fluid flow and precipitation (Hanor 1966). In contrast, Tischendorf (1963) established that the Sr content of barite decreases upward over a vertical distance of 500 m in veins of the Schneckenstein district, Germany. Although Tischendorf does not give an explicit interpretation of this zoning, it could have been produced by a pronounced decrease in temperature of ascending fluids.

Hanor (1966) established that there is a regional zoning in Sr content of barite in the eastern half of North America. The westernmost zone is characterized by barites having

values of from 1 to 2 mol % $SrSO_4$. The central zone, which spatially encompasses the Cincinnati and Findlay arches, is characterized by high Sr values in the range of 6-26 mol % $SrSO_4$. The eastern zone is characterized by intermediate Sr values, ranging from 1.5 to 9.0 mol %. The high-Sr central zone encompasses most of the major occurrences of celestine in the eastern half of North America. The boundary between the central and western zones is also a regional boundary for the occurrence of fluorite mineralization. Barite districts west of this boundary contain no fluorite. Nearly every barite district east of this line contains appreciable fluorite. Hanor (1966) proposed that this regional zoning reflects compositional differences in potential Precambrian source rocks below Paleozoic cover. As an alternative hypothesis, this regional Sr zoning may reflect instead a Paleozoic carbonate, high Sr/Ba source to the east and a Paleozoic siliciclastic, low Sr/Ba source to the south and west.

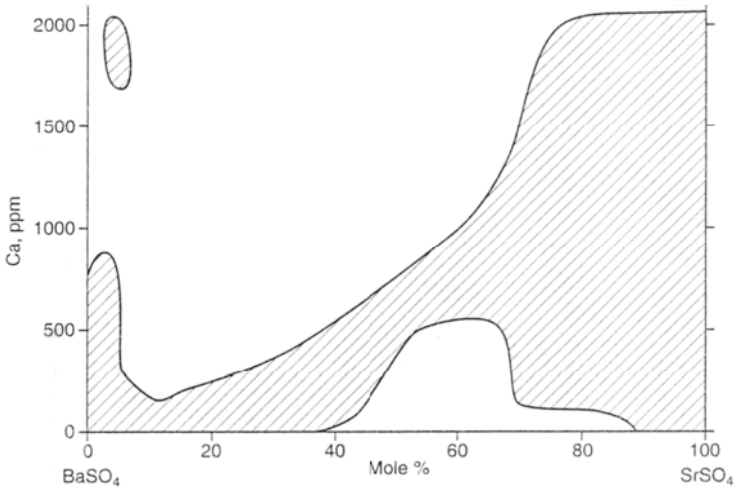

Figure 16. Variation in the Ca content of barite and celestine from the Swiss Alps and Jura Mountains. Data from Burkhard (1978).

Other cations

The elements Ca and K are generally present in quantities of a few hundred to a few thousand ppm in barite (e.g. Church 1970), but other than Burkhard's (1978) extensive documentation of Ca in Alpine barite (Fig. 16), there has been little attempt to date to develop the systematics of their occurrence. Burkhard found higher Ca values to be associated with carbonate host rocks. Lead in the hundreds of ppm range has been reported from some barite, particularly in volcanic-hosted massive sulfide deposits of Japan, and Kajiwara and Honma (1976) have used the Pb content of barite coexisting with galena (PbS) to estimate f_{O_2} conditions prevailing during ore deposition from the equilibrium reaction $PbS_{(s)} + 2O_{2(g)} = PbSO_{4(ss)}$. Takano and Watanuki (1974) have reviewed other aspects of the Pb content of barite.

Radium is close in ionic radius to Ba (Table 1), and has been detected in recent seafloor occurrences in barite (e.g. Moore and Stakes 1990, Paytan et al. 1996), in barite sinter (Cecile et al. 1984), and barite well scale (Fisher 1998). Guichard et al. (1979) described the distribution of rare earth elements of barite, although more recent work suggests some of the REE may be present in a separate phase (Martin et al. 1995).

Strontium isotopic composition

Strontium-isotope analyses have been widely used to constrain the origin of both barite and celestine (e.g. Reesman 1968, Whitford et al. 1992). These minerals are ideal for Sr-isotope work because of their high Sr content and the fact they are depleted in Rb, which eliminates any need for correcting for the in-situ production of radiogenic ^{87}Sr since the time the barite or celestine precipitated. In addition, the very high Sr content makes these minerals insensitive to contamination during their post-depositional history (Whitford et al. 1992).

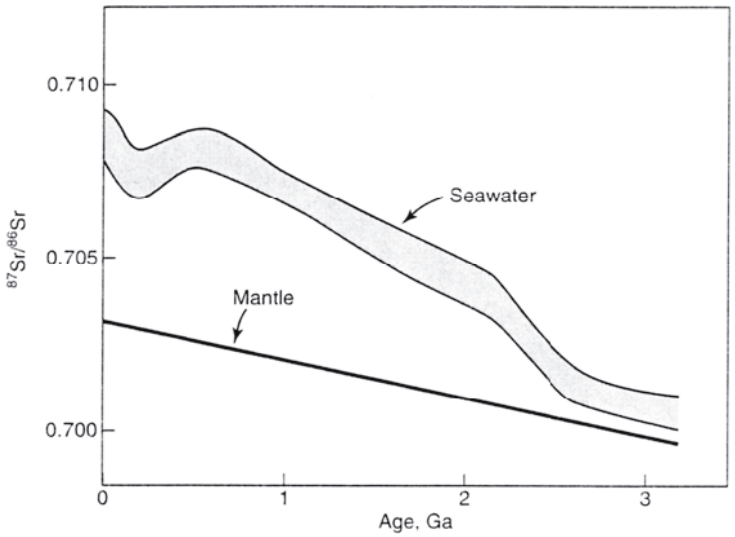

Figure 17. Secular variation in the $^{87}Sr/^{86}Sr$ ratio of the mantle and seawater. Modified from Franklin et al. (1981).

The Sr-isotopic composition of geological materials is expressed as the ratio of $^{87}Sr/^{86}Sr$, which can be measured with great analytical precision. Radiogenic ^{87}Sr is produced by the decay of ^{87}Rb (half-life = 4.88×10^{10} y). Rocks having high initial concentrations of Rb , such as granites, are characterized by high $^{87}Sr/^{86}Sr$ ratios. Rocks derived from materials having low Rb concentrations, such as the mantle (Fig. 17), have low $^{87}Sr/^{86}Sr$ ratios.

Since the Precambrian, the $^{87}Sr/^{86}Sr$ of seawater has fluctuated between approximately 0.7070 and 0.7092 as the result of variations in the rates of input of enriched Sr from continental weathering and depleted Sr from mantle sources (Fig. 17). Sulfate and carbonate minerals ultimately derived from seawater, including pelagic and submarine exhalative barite and celestine, have Sr isotopic compositions which reflect the Sr composition of seawater at the time the minerals or their precursors were formed, unless they have undergone major diagenetic alteration. Silicate minerals, however, have a much wider range of isotopic compositions. For example, some detrital K-feldspar in the North Sea has $^{87}Sr/^{86}Sr$ values in excess of 0.7300, and high Rb/Sr micas can have values in excess of 0.8000 (Whitford et al. 1992). Volcanoclastic sediments and barite derived from volcanic sources, on the other hand, may have $^{87}Sr/^{86}Sr$ ratios lower than contemporaneous seawater if they were sourced from low-Rb rocks having a low initial $^{87}Sr/^{86}Sr$ ratio.

Potential barite-forming fluids in sedimentary basins containing Paleozoic strata commonly have $^{87}Sr/^{86}Sr$ ratios in excess of seawater values contemporaneous or coeval with the depositional age of the current host sediment. This is well illustrated by the data of Connolly et al. (1990) for the Alberta basin, Canada (Fig. 18). The enrichment represents Sr derived from alteration of silicates. Because of the significant increase in $^{87}Sr/^{86}Sr$ with time since the Jurassic, however, some fluids in Cenozoic sedimentary basins actually have $^{87}Sr/^{86}Sr$ ratios lower than contemporaneous seawater values, representing introduction of Sr from older and deeper sedimentary sources (e.g. McManus and Hanor 1988, 1993). Barite derived from such sources, such as barite in recent chimneys in the Gulf of Mexico (Fu 1998), have $^{87}Sr/^{86}Sr$ ratios less than that of coeval seawater.

There is no isotopic fractionation of Sr during sulfate precipitation, and barite-celestine Sr derived from seawater or from the dissolution of a marine evaporite or carbonate phase will thus have an isotopic composition with a marine signature. Many synsedimentary barite and celestine occurrences have Sr isotopic ratios heavier than that of contemporaneous marine water (Fig. 18), representing a partial continental silicate input for Sr and, by extension, Ba.

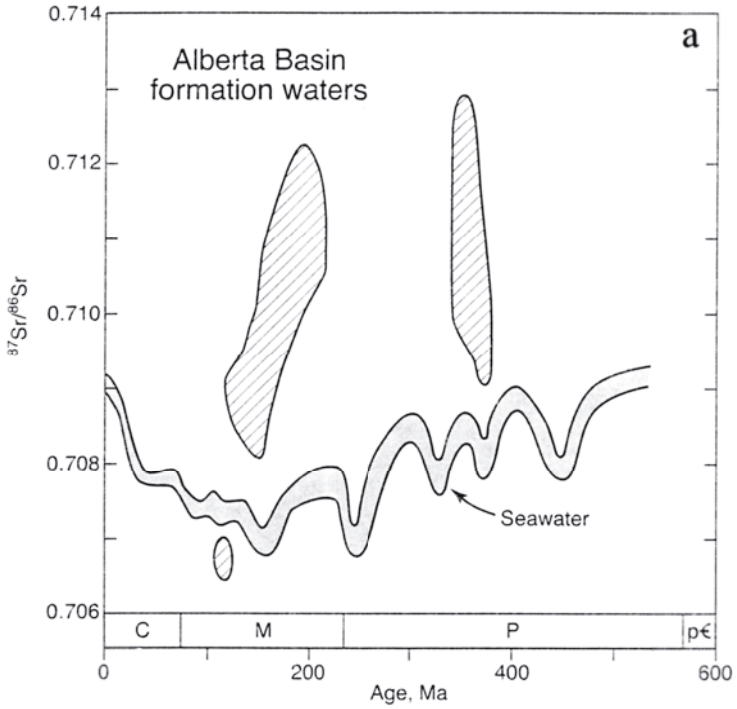

Figure 18a. Strontium isotopic composition of formation waters from the Alberta Basin, Canada plotted according to the age of their present host sediment (Connolly et al. 1990).

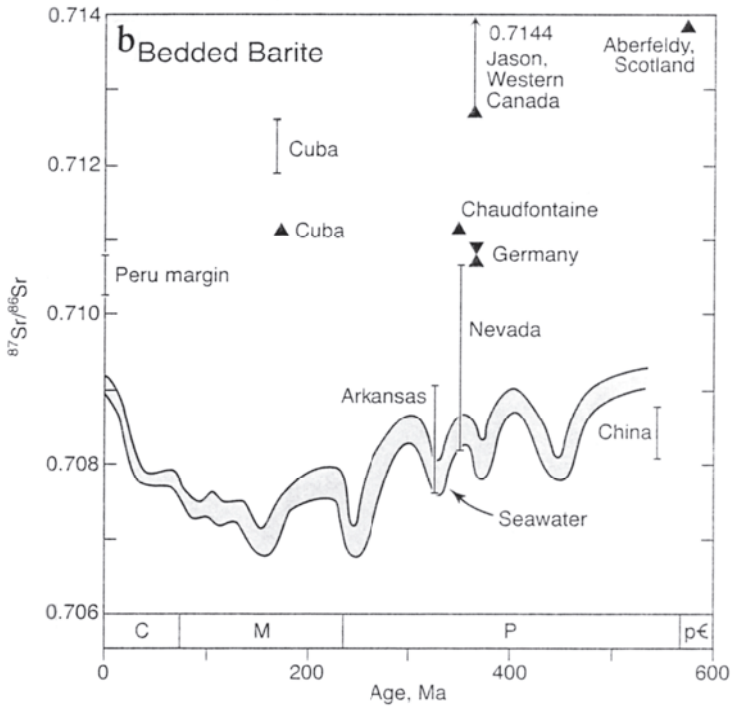

Figure 18b. Strontium isotopic composition of barites from metal-bearing (triangles) and metal-free (lines with bars) sedex barite deposits (Maynard et al. 1995, Jewell 2000). The seawater Sr curve is from Burke et al. (1982).

Sulfur isotopic composition

Sources of sulfate in barite and celestine include seawater sulfate; seawater sulfate modified by microbial reduction; calcium sulfate minerals; magmatic sulfate; and sulfate produced by oxidation of reduced sulfur, including sulfide, elemental sulfur; and organically bound sulfur. The $\delta^{34}S$ isotopic composition of barite and celestine has proved invaluable in the identification of sources of sulfate and environments of deposition (e.g. von Gehlen et al. 1962, 1983; Kusakabe and Robinson 1977, Strizhov et al. 1988).

The isotopic systematics of sulfur are complex because sulfur exists in several redox

states and a variety of fractionation mechanisms exist (Seal et al. this volume). Below approximately 200°C, the rate of isotopic exchange between dissolved sulfate and sulfide is slow, and isotopic equilibrium between the species is rare (Ohmoto and Lasaga 1982). Kinetic effects therefore dominate the isotopic systematics of sulfur in sedimentary basinal conditions. The principal kinetic effect is associated with the reduction of sulfate to sulfide, which can be achieved both microbially and thermochemically. In general, substantial isotopic fractionations occur when sulfate is reduced to sulfide or sulfur, whereas negligible fractionation occurs during oxidation of sulfide (Seal et al., this volume).

The lighter isotopes of sulfur are preferentially partitioned into sulfide during microbial reduction, thereby producing hydrogen sulfide which is much lighter than the precursor sulfate and a residual sulfate which is heavier. Thus, sulfate reduction drives residual seawater sulfate toward higher values. The major factors controlling the sulfur isotopic composition of seawater are the relative proportion of sulfide and sulfate removed from the oceans, and the $\delta^{34}S$ value of average river sulfate, derived from the continental weathering of sulfate and sulfide bearing rocks. Holland (1984) argued that fluctuations in river sulfate is less of a controlling factor than fluctuations in the removal rates of sulfide and sulfate.

The value of $\delta^{34}S$ in gypsum is only approximately 1.65 permil heavier than the aqueous sulfate in solutions from which it precipitates, and the isotopic composition of gypsum deposits precipitated from seawater during evaporation thus track secular changes in seawater isotopic composition. The isotopic composition of seawater sulfur has fluctuated throughout the Phanerozoic from approximately +10 to +30 permil VCDT, based on analyses of gypsum and anhydrite in the geological record (Fig. 19). Late Proterozoic values of $\delta^{34}S$ range from +15 to +25 (Claypool et al. 1980). Because sulfate has a long oceanic residence time, the isotopic composition of sulfur is assumed to have been uniform throughout the oceans at any given time. Waters in anoxic basins or sulfate-bearing brines in evaporite sedimentary basins may have more positive $\delta^{34}S$ values than contemporaneous seawater as a result of bacterial reduction. Thermochemical reduction of sulfate at higher basinal temperatures, on the other hand, typically produces sulfides similar in isotopic composition to the parent sulfate.

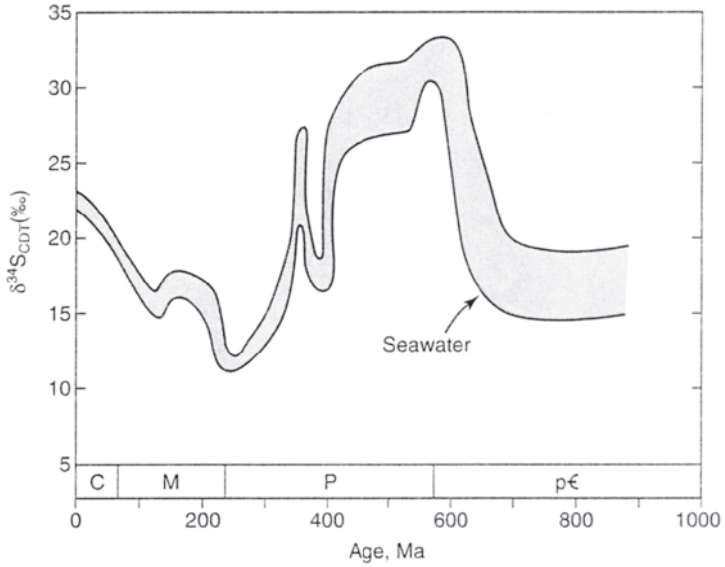

Figure 19. Variation in the sulfur isotopic composition of seawater with time (after Claypool et al. 1980).

Early Archean sulfates in submarine exhalative deposits typically have $\delta^{34}S$ compositions slightly heavier than zero, while coexisting sulfides group around zero. With the later appearance of sulfate-reducing bacteria and the preferential removal of light sulfur, marine sulfate became heavier, and barite compositions reflect this shift. Barite in

many sedex deposits has sulfur isotopic compositions similar to that of coeval seawater sulfate (Fig. 19), indicating that much of the barite was formed by mixing of Ba-bearing hydrothermal fluids with seawater. Sulfide minerals, if present, are generally lighter, reflecting that much or most of the sulfide has been derived by bacterial reduction of marine sulfate (Lydon 1995). Sedex barite formed in slightly anoxic basins has an isotopic composition heavier than coeval seawater (Goodfellow 1999). Barite in carbonate-hosted MVT deposits typically has a sulfur isotopic composition inherited from marine evaporites (Kesler 1996).

Oxygen isotopic composition

The $\delta^{18}O$ of present-day dissolved marine sulfate is +8.6 permil VSMOW, far out of equilibrium with the $\delta^{18}O$ value of ocean water (Seal et al. this volume). Holser et al. (1979) have shown that this difference can be explained by the persistence of non-equilibrium between oxygen in seawater and oxygen in the river input of sulfate, which owes its $\delta^{18}O$ value to the combined effect of the solution of evaporite minerals and the oxidation of sulfides during weathering. It is estimated that the isotopic equilibration time between seawater and dissolved sulfate is greater than 10^9 years, far larger than the oceanic mixing time of approximately 2000 years. An alternative explanation involves equilibrating marine sulfate with seawater oxygen at temperatures of 200°C in mid-ocean ridge hydrothermal systems. The $\delta^{18}O$ of seawater sulfate has varied throughout geological time, with $\delta^{18}O$ values of late Proterozoic and Phanerozoic anhydrites varying generally between 13 and 17 permil, with exception of the Permian when a minimum value of 10 was reached (Holser 1979)**.**

The oxygen isotopic composition of barite is not reported as often as that of □34S. At most diagenetic conditions of temperature and pH, oxygen in dissolved sulfate and in water are not in isotopic equilibrium because of the sluggish kinetics of isotopic exchange. At temperatures above about 150°C and near-neutral pH conditions, the oxygen isotopic composition of sulfate can be used as a geothermometer and to infer conditions under which the sulfate formed (Ohmoto and Lasaga 1982). Under highly acidic conditions, oxygen exchange between sulfate and H2O is more rapid (Seal et al. this volume). However, this is probably not a factor in most barite deposits.

Radium

The several naturally-occurring isotopes of radium, ^{224}Ra, ^{226}Ra, and ^{228}Ra, are produced by the radioactive decay of parents in the U and Th decay series (Fig. 20). All of these isotopes are radioactive and have half-lives ranging from 1622 y to 3.64 d. Radium and Ba are of similar ionic radius, and Ra often occurs along with its various daughters in measurable quantities in recently precipitated barite. Radiometric dating schemes based Th-Ra systematics have been used to date recent hydrothermal deposits of bariite and to calculate sedimentation rates (Kadko and Moore 1988, Paytan et al. 1996). Techniques of Th-Ra dating include the assumption that the $^{228}Th/^{228}Ra$ activity ratio is of the same magnitude as $^{232}Th/^{226}Ra$, and that ^{228}Th produced by decay of ^{228}Ra does not migrate.

Fluid inclusions

Coarse-grained barite typically contains fluid inclusions (Roedder and Bodnar 1997). The study of heating and freezing behavior of primary fluid inclusions in barite can provide valuable information on the temperature of fluid entrapment and on fluid salinity, and chemical analysis of fluid inclusions provides direct information on the details of fluid chemistry in minerals as old as the Early Archean (e.g. Rankin and Shepard 1978). It has been found, however, that many fluid inclusions in barite stretch upon heating, leading to homogenization temperatures that are far higher than true entrapment temperatures (Ulrich and Bodnar 1988). These factors may explain why analyses of fluid inclusions in barite by

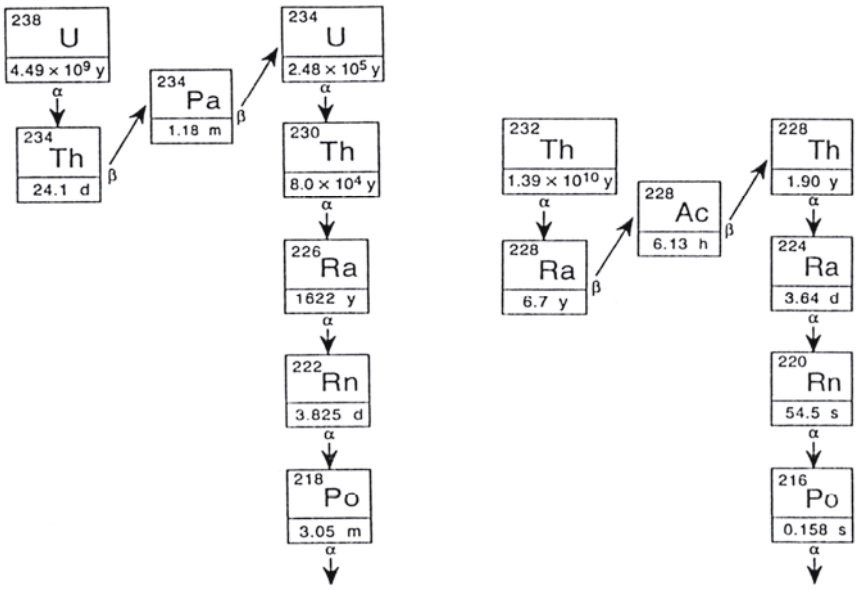

Figure 20. Portions of uranium-238 and thorium-232 decay schemes, showing the Th and Ra isotopes refered to in text. Modified from Fisher (1998).

Ramboz and Charef (1988) for the Les Malines deposit in France yield anomalously high fluid pressures and temperatures.

BARITE IN SUBMARINE VOLCANIC HYDROTHERMAL SYSTEMS

The basic concept of the syngenetic accumulation of massive sulfides and sulfate minerals on the seafloor in direct association with magmatic activity was well established by the late 1950s by Oftedahl (Oftedahl 1958, Franklin et al. 1981, Franklin 1995). The subsequent discovery in the 1970s of presently active seafloor systems has established the general applicability of the model.

Heat from magmatic activity drives deep convective circulation of fluids in the oceanic crust resulting in leaching of Ba from a variety of source rocks. Extensional faults and fractures help to focus upward discharge of hydrothermal fluids onto the seafloor, where they mix with seawater. Principal regions of thermal convection today occur along mid-ocean rises and rifts, seamounts, and back-arc basins (Scott 1997). It is reasonable to include Early Archean barite deposits in this section of the chapter because of their occurrence in volcanic greenstone belts and probable association with volcanic activity, even though their original tectonic setting has been obscured by later geological events.

The basic processes by which volcanic-hosted mineral (VHM) deposits form have been derived both from detailed field examination of ancient deposits exposed through outcrop, the drill bit and mine workings, and from study of modern seafloor examples. The underlying driving force for creating a VHM deposit is the high heat associated with emplacement of magma which generates convective fluid flow in the oceanic crust. Seawater is recharged into the system over a broad area, but the upward discharge is controlled by faults and fractures and is thus much more focused. Seawater is modified in composition as it descends through the crust and is progressively heated. Notable changes in modern seawater systems include the loss of Mg, Sr, Ca, and sulfate as the result of formation of anhydrite, zeolites, and clay minerals (Franklin 1995, Scott 1997). Reaction between modified seawater and basalt at about 385°C causes a lowering of pH and the leaching of metals and sulfide from host rocks (Franklin 1995, Scott 1997). Presumably Ba is leached from source rocks after the loss of sulfate. During the Archean, surface

marine waters were low in sulfate, and presumably there were significantly different chemical pathways taken during seawater-volcanic rock interaction.

Sulfides in modern systems are precipitated on or near the seafloor by rapid cooling of the hydrothermal fluid. Some sulfide minerals are dispersed into the overlying water column in distinctive black plumes or smokers. Isotopic studies have established that the metals and sulfide are transported simultaneously to the seafloor and that, unlike sedex Pb-Zn deposits, reduction of seawater sulfate is unimportant as a source of reduced sulfur (Janecky and Shanks 1988). Precipitation of sulfide and sulfate minerals occurs both as chimneys around vent orifices and in plumes which rise from the vents. In modern deposits dominated by metal sulfides, initial venting produces anhydrite chimneys rapidly precipitated from seawater-sourced Ca and sulfate as a result of the retrograde solubility of anhydrite. The chimneys act as a substrate for subsequent deposition of sulfides. With cooling, the anhydrite chimneys eventually dissolve and collapse. Minerals also precipitate around the exterior of sessile worm tubes in the complex community of vent fauna which populate areas of hydrothermal discharge.

According to Franklin (1995) the presence or absence of barite in vent systems is largely dependent on temperature of discharge. In the high-temperature phase of discharge, most barite is dispersed into the overlying water column in smoke plumes. Lower temperature fluids, T <250°C, which are depleted in base metals and sulfur, form barite-rich chimneys over the vents. Barite is precipitated with seawater as the source of sulfate. In ancient deposits, barite probably formed where hydrothermal systems continued to vent after the peak of high-temperature discharge and where seawater contained abundant sulfate. Modern seafloor hydrothermal fluids generally contain abundant silica which is precipitated upon cooling and/or boiling forming white plumes or smokers rising above discharge vents. Ferruginous chert overlies many deposits and is the product of low temperature discharge of silica- and iron-rich waters. Thus, barite in VHM deposits is often associated with silica-rich sediments and ferruginous cherts.

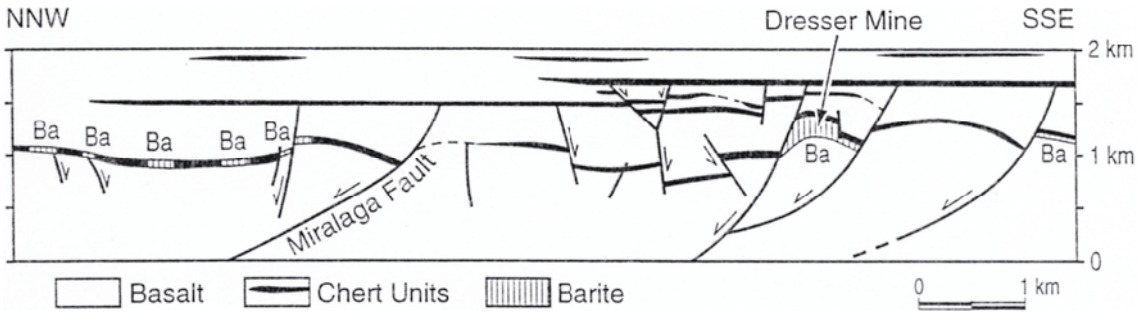

Figure 21. Restored cross-section through the North Pole area, Western Australia, showing the Early Archean North Pole cherts interbedded with basalts, and the relation of the occurrence of barite to synsedimentary extensional faults. Modified from Nijman et al. (1998).

Sulfide-poor barite deposits of Archean age

Barite makes its first documented appearance in the geologic record in a spectacular manner: as large synsedimentary mounds more than 20 m high and 50 m across that were precipitated on the seafloor of the East Pilbara block of Western Australia approximately 3.5 Ga ago (Nijman et al. 1998). The mounds occur as part of a complex of baritic veins and sediments in the North Pole Chert of Early Archean age which crops out over an area of approximately 10 by 15 km. The North Pole Chert itself consists of a series of thin chert units interbedded with thicker basalts in the basal portion of the Warrawoona Group, which in turn overlies older basalts (Fig. 21). It is the lowermost of these cherts which contains

extensive barite. This chert also contains some of the oldest documented stromatolite-like structures and contains possible remains of living organisms. Galena from vein barite in the North Pole Chert gives a model lead age of 3490 Ma (Nijman et al. 1998).

Nijman et al. (1998) documented the existence of synsedimentary extensional growth faults active during the deposition of the North Pole Chert and immediately overlying units (Fig. 21) and coeval with felsic volcanism. Swarms of chert veins fan upward from growth-fault planes in the underlying basalt. The large barite mounds and apparent underlying feeder veins of barite and chert are spatially associated with some of these faults.

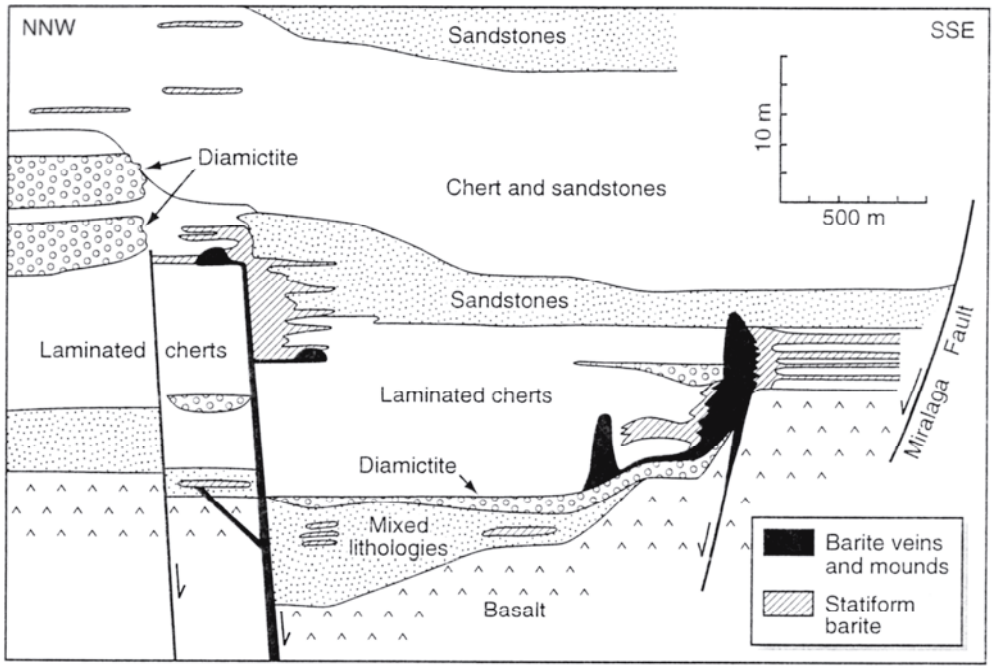

Figure 22. Diagram showing the stratigraphic and structural relations of barite in the northwesternmost part of the cross section in Figure 21. Modified from Nijman et al. (1998).

One very large mound described by Nijman et al. (1998) stands on a base of diamictite, which may have formed by collapse of a submarine fault scarp (Fig. 22). The barite structure is made up of smaller hemispherical mounds of barite deposited in subparallel layers. The layers now consist of bladed crystals of up to 10 cm long. Judging from the diagrams in the paper by Nijman et al. the blades are perpendicular to bedding and may be similar to secondary blades of barite noted in detrital barite deposits of Early Archean age in South Africa (Reimer 1980). Thin chert and Fe-oxide layers separate some successive barite layers. Beds of stratiform barite that are described as sinter occur proximal to some of the mounds (Fig. 22).

There is consensus that the North Pole Chert was deposited within a shallow-water evaporite lagoon behind a barrier of volcanoclastic sand (Buick 1990, Buick and Dunlop 1990). Fluid inclusions in the barite contain CO_2, H_2S, calcite and sphalerite, and there is a large variation in both CO_2 content and gas-bubble size. Nijman et al. (1998) invoke submarine discharge of fluids containing Ba, Si, and sulfide into a 50-m-deep stratified water body. Boiling or degassing and mixing with the overlying water caused rapid oxidation of sulfide into sulfate. Some of the barite occurs as replacement of bladed gypsum thought to be evaporitic in origin (Dunlop and Buick 1990), and some occurs as

detrital beds derived from erosion of the mounds.

Barite in similarly massive quantities also occurs in sediment-hosted deposits in Early Archean portions of the Precambrian shield areas of India, South Africa, Canada, and Russia. Much of this barite was apparently deposited in shallow, high-energy aqueous environments, which resulted in its erosion and reworking into sand-size clasts. Deb et al. (1991), for example, described a detrital stratiform barite occurrence in the Indian Shield which is only 1 m in thickness, but extends 10 km along strike. The barite is interlayered with Cr-rich muscovite-bearing quartzite in the upper amphibolite facies of the Sargur Group (>3.3 Ga). The barite sediments have retained their primary sedimentary stratification, with alternating quartzose layers interbedded with micaceous and pyritic layers. The authors interpreted the barite to have been originally derived from a submarine hydrothermal deposit.

Stratiform barite in Early Archean (>3.2 Ga) metasediments of the Barberton Mountain Land, Transvaal, South Africa, may have had a similar origin. Reimer (1980) described several different major sedimentary barite occurrences which include: 12-m-thick zones of barite with finely disseminated pyrite and other sulfides alternating with chert; lens-shaped deposits of barite within chert; and detrital barite sands containing detrital pyrite, chromite, zircon, magnetite, ilmenite, molybdenite, and gold as accessory minerals. The barite sand was presumably eroded from older deposits and mechanically mixed with the other heavy minerals. Transport distances were probably short. Diagenetic recrystallization has led to the formation of radiating, cauliflower-like large crystals of secondary barite that cut across original bedding. Reimer (1980) envisioned the barite as being formed by hydrothermal solutions containing Ba that reacted with seawater sulfate, with little obvious association with evaporites. DeWit et al. (1982) have identified potential submarine vent features in the vicinity of the barite and at approximately the same stratigraphic horizon.

Isotopic composition and sources of sulfate. Archean barite has low $^{87}Sr/^{86}Sr$ ratios, reflecting primitive mantle compositions (Fig. 17), and $\delta^{34}S$ values just slightly greater than magmatic values (Perry et al. 1971, Lambert et al. 1978). For example, the Archean barite of the Sargur Group in India has a $^{87}Sr/^{86}Sr$ ratio of 0.7018 and $\delta^{34}S$ values of 4.02 to 7.45 permil VCDT (Deb et al. 1991).

One of the more problematic aspects of the Early Archean barite deposits is the source of sulfate in an ocean presumably nearly devoid of free oxygen. One possibility is that the sulfate is magmatic in origin. As discussed by Hattori and Cameron (1986), sulfate in igneous rocks can be formed by the oxidation of primary sulfide in silicate magma and by the hydrolysis of SO_2 gas in igneous-hydrothermal fluids. The amount of Fe is much larger than S in typical melts, and f_{O2} is determined by the ambient Fe^{III}/Fe^{II} ratio. In the first process sulfide is oxidized by a reaction such as

$$S_{2(melt)} + 4H_2O_{(melt)} \rightarrow SO_{4(melt)} + 4H_{2(g)} \quad (26)$$

Degassing of H_2 moves reaction to right. In an aqueous phase, sulfate may be produced by reactions such as

$$SO_{2(aq)} + 2H_2O_{(aq)} \rightarrow H_2SO_{4(aq)} + H_{2(aq)} \quad (27)$$

or

$$4SO_{2(aq)} + 4H_2O_{(aq)} \rightarrow H_2S_{(aq)} + 3H_2SO_{4(aq)} \quad (28)$$

Reaction of sulfate with Ca^{2+} or Ba^{2+} to form anhydrite or barite helps to drive these reactions to the right.

Volcanic-hosted massive sulfide (VHMS) deposits

Barite occurs not only in submarine deposits having low concentrations of associated metals, but is also a common mineral in sulfide-bearing VHMS deposits in submarine volcanic rocks of all ages, from pre-3.4 Ga volcanic strata of the Pilbara Block in Australia (Barley 1992) and Archean gold deposits in Canada (Cameron and Hattori 1985) to modern active spreading centers (Franklin et al. 1981, Franklin 1995). The deposits consist of bulbous to tabular stratiform accumulations of massive pyrite and lesser pyrrhotite with Zn, Pb, and Cu sulfides. The deposits are spatially associated with submarine volcanic rocks and associated sedimentary sequences and are underlain by discordant alteration zones which may occupy synvolcanic faults. VHMS deposits occur in present or former areas of high heat flow that result from magmatic activity. Most deposits are mineralogically simple and contain from 50 to more than 80 vol % sulfides. Pyrite is the dominant sulfide, followed by sphalerite, chalcopyrite, and galena.

One of the earliest known VHMS-barite deposit is the Early Archean Hemlo occurrence in Ontario (Cameron and Hattori 1985). The Cenozoic Kuroko deposits in Japan also contain barite and have been studied in detail (Lambert and Sato 1974, Farrell and Holland 1983). Barite is also commonly associated with gold-rich massive sulfide deposits (Poulsen and Hannington 1995). Hannington and Scott (1989) have shown that gold is effectively transported in hydrothermal fluids by bisulfide complexing and quantitatively precipitated by oxidation of the reduced sulfur. At subcritical seafloor depths of approximately 1900 m or less, boiling of hydrothermal fluids can occur, which causes precipitation of Cu, Fe and Zn as sulfides and produces a fluid enriched in Au, Ba, and Pb. Gold is precipitated during boiling where the ambient seawater is oxidizing. For reasons which are not well understood, barite is less common in Late Archean and Proterozoic deposits (Franklin 1995, Lydon 1995). Huston (1999) proposed this may be the result of low total concentrations of sulfur in Precambrian seawater.

Modern submarine hydrothermal barite

Prior to the recognition in the late 1960s of the relation between mid-ocean rises and ridges, seafloor spreading, and plate tectonics, Arrhenius and Bonatti (1965) and Boström and Peterson (1966) had suggested the possible existence of magmatic-hydrothermal activity along the East Pacific Rise. They noted that the areas of maximum barite concentrations in Pacific pelagic sediments do not coincide with areas of biologically high productivity under the Peru current but rather with the East Pacific Rise, and they suggested the possibility of the existence of active magma chambers discharging Ba-rich fluids on the seafloor. Direct observation of seafloor venting of hydrothermal fluids was first made in the mid-1960s in the Atlantis II Deep of the Red Sea (Degens and Ross 1969) where dense warm brines overlie metalliferous muds. With the development of submersible research vessels, hydrothermal venting has since been found at more than 100 oceanic sites (Scott 1997).

***Tectonic setting*.** Barite is a major component of submarine hydrothermal deposits in modern back-arc basins, such as the Lau Basin, the Okinawa trough, and the Mariana trough (Bertine and Keene 1975, Herzig et al. 1993, Scott 1997). Barite is also abundant in the Guaymas Basin in the Gulf of California, where it makes up approximately 15% of the precipitated minerals (Peter and Scott 1988), and on the Galapagos ridge (Varnavas 1987). In contrast, barite is usually only a minor component or is absent from many sediment-starved mid-ocean ridges and from seamounts. Back-arc rocks are commonly more enriched in Ba than are mid-ocean rise tholeiites, which may account for the more common occurrence of barite with the former (Scott 1997).

All of the sites, except for the seamounts, are located in extensional or rifted terranes,

and all of the sites, including the seamounts, are characterized by high heat flow. Modern hydrothermal deposits are mineralogically complex and diverse, but basically consist of two general types: sulfide and Fe-Si-Mn oxide deposits. The deposits can consist of a single vent chimney a few centimeters high to coalesced mounds hundreds of meters wide and topped by chimneys several tens of meters high. Most important to the size and composition of deposits and to the geochemistry of the vent fluid is the type and amount of host volcanic rocks and the sediments through which the fluids have passed. These, in turn, are dependent on the tectonic setting of hydrothermal activity (Scott 1997).

Mineralogy of submarine hydrothermal barite deposits. An example of modern submarine hydrothermal barite deposits is provided by the chimneys of the Mariana trough, which are composed of barite, sphalerite, galena, chalcopyrite, and silica (Scott 1997). Well-formed polyhedra of barite appear to have formed from recrystallization of early fine-grained barite on the outer side of chimneys. The basic framework of the chimneys consists predominately of euhedral lathlike crystals of barite ranging from than 1 mm across to large crystals up to 5 mm across. Crystal size and morphology change rapidly across centimeter-dimension regions of the chimney. Barite crystals commonly form radiating bundles or sector-zoned euhedral minerals that project into open vugs and contain vermicular inclusions of the sulfides sphalerite, chalcopyrite, and galena.There is no petrographic evidence that the barite crystals have been dissolved or leached.

Urabe and Kusakabe (1990) described barite-bearing silica chimneys and crusts in the back-arc basin in the Izu-Bonin arc, northwestern Pacific. The deposits occur on the flank of a rhyolite lava dome along the rift axis. The chimneys are composed of filamentous amorphous silica and minor amounts of barite and amorphous Fe oxide. Barite $\delta^{34}S$ values range from 21.7 to 22.3 permil, and are only slightly higher than seawater sulfate of 20.2 permil. The range in isotopic composition is similar to that barite from the Mariana backarc basin (Shikazono 1994) and the Kuroko deposits (Farrell and Holland 1983). Seawater sulfate is thus the dominant source of sulfate in all three barite deposits.

Thorium-radium systematics. The young age of many of the barite chimneys has lent them to Th-Ra dating (Moore and Stakes 1990, Kadko and Moore 1988). Kadko and Moore calculated the ages of barite chimneys on the Endeavor Ridge to be 2.0 to 3.9 years. Low $^{226}Ra/Ba$ ratios in marine bottom waters and high ratios in the chimneys preclude bottom-water as a major source of Ba.

SEDIMENTARY EXHALATIVE (SEDEX) DEPOSITS OF BARITE

A different type of submarine barite deposit consists of barite formed by ascending barium-rich fluids venting into a marine environment where there is no obvious magmatic source of heat to drive fluid flow. The terms *sedimentary-exhalative* and *sedex*, used here to describe these deposits, are employed in their broadest context and do not have as a requirement the presence of base metals such as Pb, Zn, and Cu. Some of the largest sedex barite deposits in the world, such as the Arkansas deposits, contain only trace amounts of base metals (Howard and Hanor 1987).

Many sedex deposits of barite, particularly those associated with base metals, occur in sedimentary basins controlled by tectonic subsidence associated with intracratonic or epicontinental marine rift systems (Goodfellow 1999). The deposits occur in shallow-water sediments deposited during the stage of thermal subsidence that follows active extension and fill by coarse clastics, turbidites, and volcanics. Where the structural setting can be reconstructed, these deposits are generally spatially associated with synsedimentary faults in small basins and depressions situated within larger rift basins. Although the deposits may have been located in areas of high heat flow, there is little

evidence to support direct crustal heating by intrusion of magma.

Other sedex deposits of barite occur within a wide variety of continental margin settings, including collisional margins, passive margins, and strike-slip margins. Many of these barite deposits are devoid of associated base metals. Faulting, however, appears to be a universal requirement for the transport and focusing of subsurface fluid flow. Many of the largest and economically most important deposits of barite in the world occur along what were or are today Phanerozoic continental margins (Murchey et al. 1987, Maynard and Okita 1991) in districts that extend hundreds and even thousands of kilometers along strike. Continental margins, of course, are often the locus of tectonic activity, and Ba-bearing fluids released during tectonic activity can ascend vertically into overlying sulfate-bearing marine waters. Phanerozoic continental margins have also been sites of oceanic upwelling and high biological productivity. Because there is a documented association of pelagic barite with biological productivity during the Cenozoic, some have proposed that barite deposits along older continental margins have had a similar origin (Jewell 2000). We will examine here examples of sedex barite deposits occurring within continental margins in convergent, extensional, and strike-slip tectonic settings.

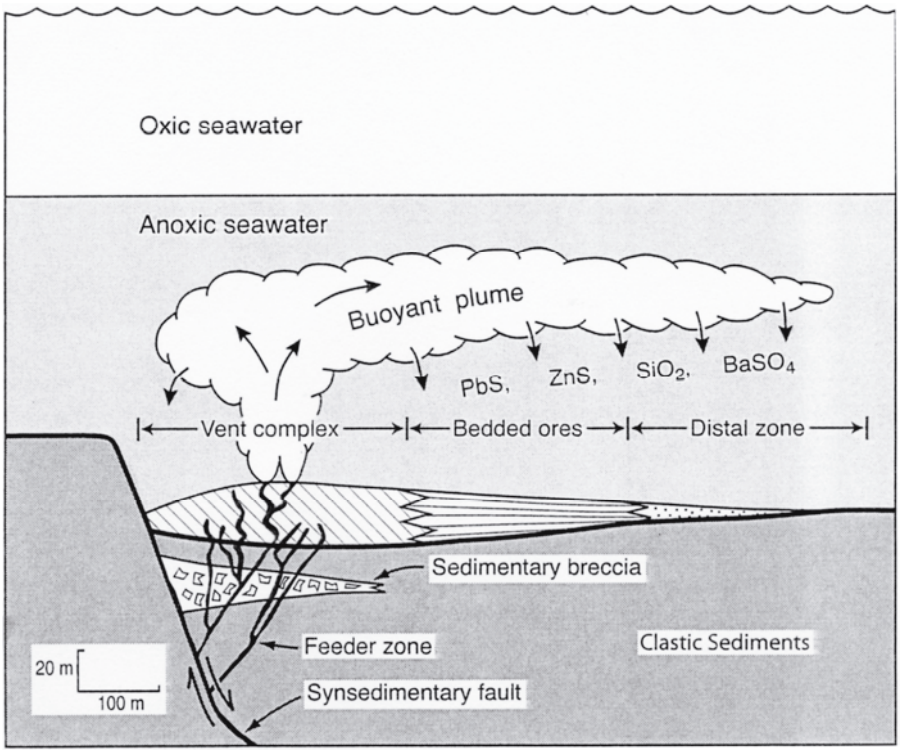

Figure 23. Schematic diagram showing principal features of a sedex sulfide-barite deposit at the time of ore deposition. Based on reconstructions of Lydon (1995) and Goodfellow (1999).

Proterozoic barite

Zn-Pb sedex deposits. The Middle Proterozoic is marked by the first appearance of sedimentary-exhalative sulfide deposits dominated by sphalerite and galena, with barite as a common, though not universally present, accessory. As shown in the schematic illustration modified from Lydon (1995) and Goodfellow (1999) (Fig. 23), who present excellent general reviews of sedex deposits, the Zn-Pb sedex deposits of Proterozoic and younger age typically consist of: (1) a vent complex, which lies above and within a feeder zone of ascending hydrothermal fluids, (2) a zone of bedded ores, which consists of a

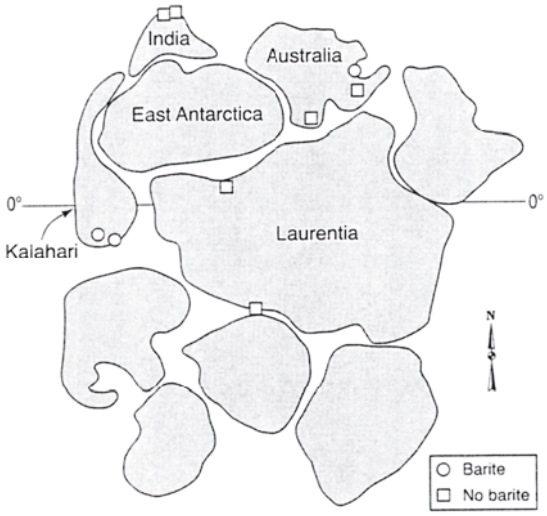

Figure 24. Reconstruction of a mid-Proterozoic supercontintent showing the location of major sedex Pb-Zn and barite deposits. Base from Goodfellow (1999).

compositionally layered apron of hydrothermal precipitates, and (3) a distal facies which lies outside the limits of ore-grade sulfide mineralization. The ratio of barite to heavy metals generally increases laterally away from the vent complex. Barite also occurs at the top of some vent complexes. Sedimentary breccias formed as a result of the collapse of fault scarps. Ore-forming fluids either formed buoyant plumes, as in the example shown, or bottom-hugging brines. Examples of Proterozoic sedex deposits containing barite include the well-documented Lady Loretta deposit, Australia, and several major deposits in the central Bushmanland Group, western Namaqua Province, southern Africa (Lydon 1995). Most Proterozoic Pb-Zn sedex deposits formed during the time period 1650-1700 Ma and seem to be associated spatially (Fig. 24) with possible intracratonic suture systems, which later became continental margins, within a Proterozoic supercontinent (Goodfellow 1999). Many Proterozoic sedex Pb-Zn deposits of northern Australia and elsewhere lack barite, which may reflect transport of metals by brines too high in sulfate to transport significant Ba (Cooke et al. 2000).

Metal-poor sedex barite deposits. There are also metal-poor barite sedex deposits of probable Proterozoic age, including barite and ironstones in Australia (Lottermoser and Ashley 1996). Horton (1989) described massive barite which occurs in layers and pods that range in thickness from a few centimeters to up to 3.7 m in thickness which occur in a 40-km-long zone in quartz-sericite schist and schistose pyroclastic rocks of inferred Late Proterozoic age of the Battleground Formation, Kings Mountain Belt, western South Carolina. The high quartz content and lack of volcanic textures suggest that the schist originated from epiclastic or sedimentary materials and possibly in part from hydrothermally altered volcanic materials. Horton (1989) suggested that the barite may have originated from seafloor hot springs, but was redistributed and locally concentrated in discordant veins during regional metamorphism from greenschist to amphibolite facies.

Phanerozoic convergent continental margins

Some of the largest accumulations of barite in the world, including the extensively studied deposits of Arkansas and Nevada, occur within former Phanerozoic convergent continental margins (Fig. 25). Here, microcrystalline barite occurs as beds and lenses in fine-grained siliceous sedimentary sequences containing shale and some chert (Orris 1986). The more massive, higher-grade beds of barite are commonly laminated. Barite nodules of early diagenetic origin are common in beds containing lower concentrations of barite. Intraformational conglomerates, breccias, and clasts of barite-cemented, fine-grained sediment are common in synsedimentary debris flows within the deposits.

Mississippian Ouachita orogenic belt. The stratiform, siliciclastic-hosted barite deposits of the Ouachita region, Arkansas, USA, were long an economically important source of barite. The Chamberlain Creek deposit alone yielded approximately 25% of the world's production for a total of nearly 8 Mt during the period from 1939 to 1972 (Shelton

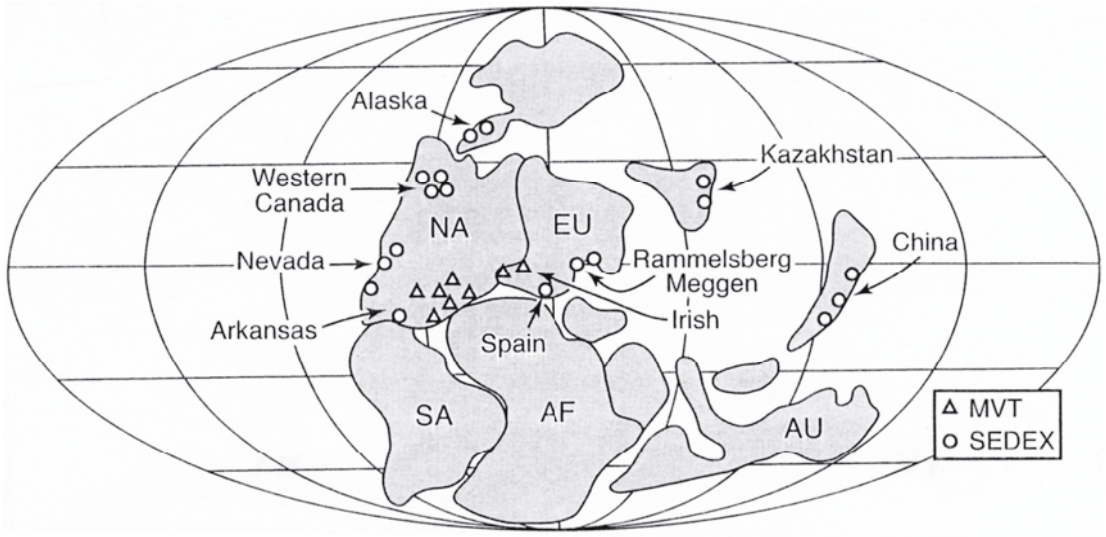

Figure 25. Devonian continental reconstruction showing the location of major Paleozoic sedex (circles) and MVT and Irish-type (triangles) barite deposits. Base from Goodfellow (1999) with additional deposits from the literature.

1989, Brobst 1994). The Fancy Hill deposit in western Arkansas (Okita 1983, Howard and Hanor 1987) still contains large reserves of barite.

Barite in the Ouachitas occurs as conformable, stratiform lenses and disseminations in shales and siltstones of the lowermost Stanley Group of Middle Mississippian age. Individual deposits are lenticular and range from <1 m to 30 m in maximum stratigraphic thickness and from 40 to over 7500 m in outcrop length. The barite content exceeded 85 wt % in portions of the Chamberlain Creek deposit, but the maximum concentrations of barite are less in most other deposits in the region.

The barite occurs primarily as disseminated single crystals <150 μm in a shale or carbonate matrix; as dense, finely crystalline laminae; and as nodules of spherically radiating crystals. On the basis of the spatial proximity of the Chamberlain Creek deposit to the Magnet Cove alkali intrusive complex, Park and Branner (1932) originally postulated that the deposit was a hydrothermal replacement related to the nearby igneous intrusive complex. Scull (1958) expanded the concept to include all of the Ouachita deposits. In 1964, however, Zimmerman and Amstutz (1964) presented a series of arguments based on pioneering textural and sedimentological studies that convincingly demonstrated that the barite was deposited penecontemporaneously with the host silts and clays. Locally, there are textures reflecting primary precipitation from bottom waters, early diagenetic replacement of other minerals by barite, and penecontemporaneous mechanical transport and redeposition of clasts of barite. Many of these features have been described in further detail by Zimmerman (1970) and Okita (1983).

Hanor and Baria (1977) proposed the following model for the genesis of the Ouachita barite deposits. During Middle Mississippian time, compressive regional deformation and a change in tectonic regime along the Ouachita continental margin (Thomas 1976) resulted in an increased influx of clastic materials into the Ouachita basin and the development of submarine depressions on the seafloor near the base of the continental slope (Fig. 26). Hanor and Baria (1977) in considering potential sources for the Ba, rejected a pelagic source on the basis that the rate of supply would have been too slow. Calculations by Boström et al. (1973) showed that present maximum documented fluxes of Ba to the seafloor are only on the order of 10 mg Ba cm^{-2}/1000 yr. At these rates, it would have required approximately 500×10^6 years to have produced a Chamberlain Creek deposit.

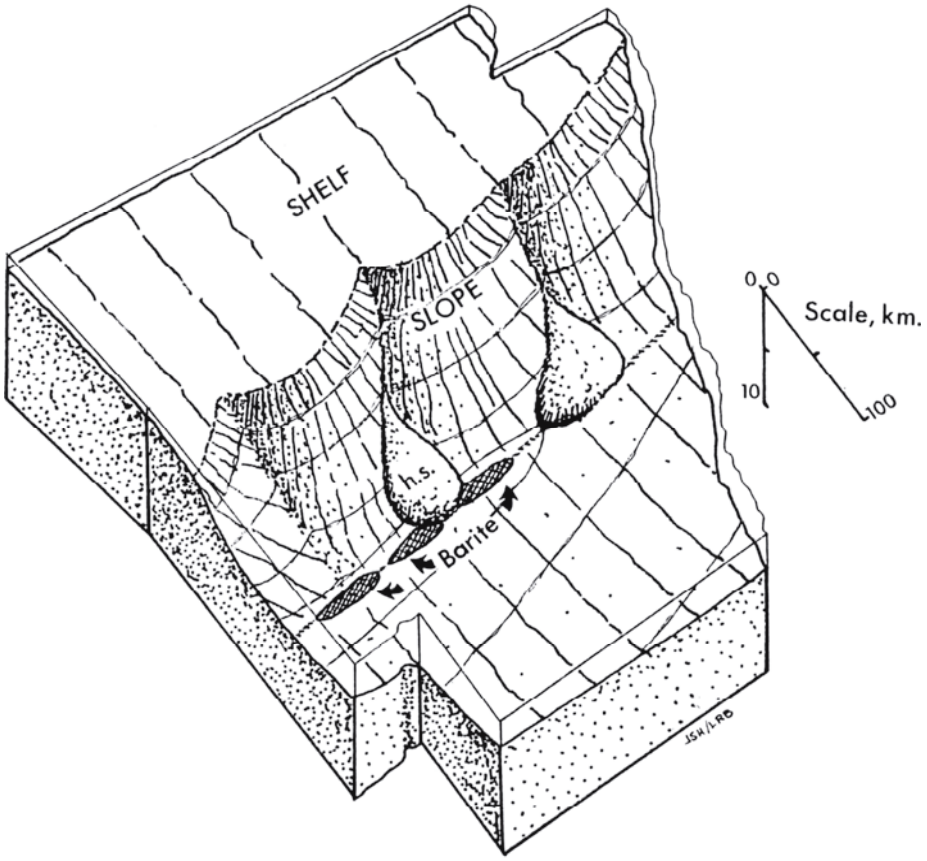

Figure 26. Conceptual model for the origin of the stratiform barite deposits of Arkansas. Ba-rich brines pooled in local depressions near the base of the continental slope between lobes of the Hot Springs sandstone (h.s.). Modified from Hanor and Baria (1977).

Hanor and Baria (1977) thus concluded that it was necessary to invoke a submarine source.

Hanor and Baria then considered mechanisms for the concentration of barite in stratiform lenses and proposed that the tectonically active nature of the Ouachita trough favored the formation of local submarine depressions (Fig. 26). Faults provided conduits for formation water in underlying sediments to migrate upward and mix with overlying marine waters, precipitating barite. Fluids more dense than seawater would pond in these depressions, and much of the precipitation of barite would thus be confined to localized areas. It was thought that injection of a buoyant fluid directly into seawater as a plume would have produced a highly dispersed and economically unimportant precipitate. Removal of barite from a brine pool could be accomplished by precipitation at the brine-seawater interface (Fig. 27). These authors estimated that approximately 1.6×10^{14} L of a normal formation water containing 200 mg/L Ba would have been necessary to form a deposit the size of Chamerlain Creek. The isotopic composition of a barite sample from Chamberlain Creek is $\delta^{18}O$ = 13.2 permil (SMOW) and $\delta^{34}S$ = 18.3 permil (VCDT) (Hanor and Baria 1977), values consistent with seawater sulfate of Middle Mississippian age, the estimated age of the host sediment. Sr isotopic values range from 0.7077 to 0.7092 (Maynard et al. 1995) or from approximately coeval seawater values to moderately radiogenic levels (Fig. 18).

Ordovician-Devonian Roberts Mountain allochthon, Nevada

The Nevada barite belt has been called the areally largest barite province in the world (Papke 1984, Dube 1986, 1988), but it is really a subpart of a much larger Paleozoic barite

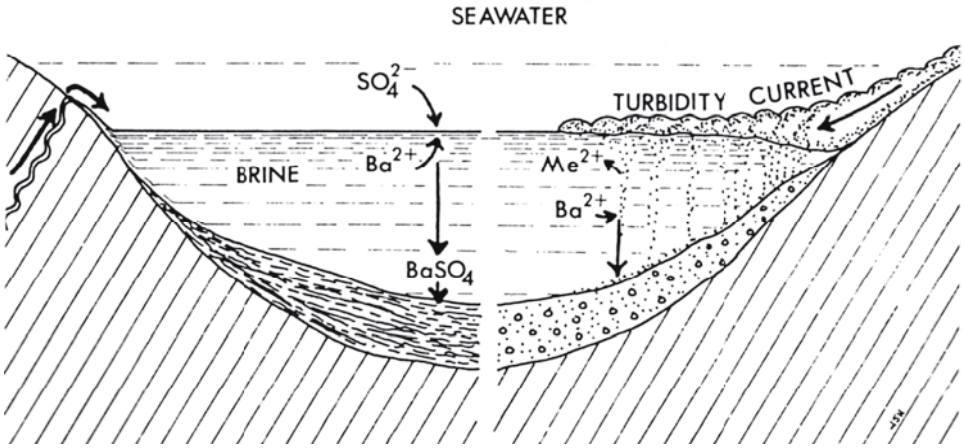

Figure 27. Dissolved Ba in a brine pool reacts with seawater sulfate to form barite. Ba-rich clay beds may have formed as clays settling through the brine. Modified from Hanor and Baria (1977).

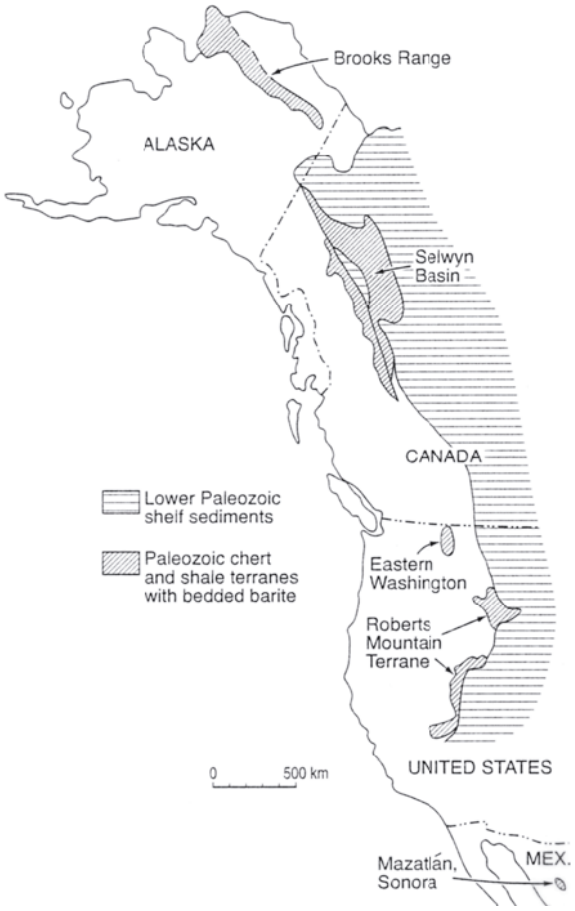

Figure 28. Map of western North America showing the distribution of terranes or regions with Paleozoic chert, shale, and barite. Location of barite from Murchey et al. (1987). Location of shelf sediments and shelf edge from Turner et al. (1989).

province (Fig. 28) which extends from northwestern Mexico through southern Nevada, and northward into Alaska (Murchey et al. 1987). In addition to the deposits discussed by Murchey et al., the bedded barite deposits of eastern Washington State (Mills et al. 1971) should be placed in this group.

As summarized by Dube (1986, 1988), bedded barite in Nevada is hosted by sediments that range in age from Cambrian to Early Mississippian. Most deposits, however, occur in Late Ordovician and Late Devonian host sediments. The barite bodies are lensoid, have thicknesses of up to 75 m, and have high thickness to width (length) ratios (Shawe et al. 1969). Single large deposits contain up to nearly 15 Mt of barite (Dube 1986). Horton (1963) noted that most of the barite deposits of Nevada lie in a belt that spatially coincides with the Antler orogenic belt, which is now known as the Roberts Mountain allochthon.

The $\delta^{34}S$ compositions of massive and laminated barite in East Northumberland Canyon, Nevada range from 20.9 to 28.6 permil, with most values around 25.0 permil (Rye et al. 1978). These values are typical of Upper Devonian marine sulfate, and because of this, seawater is thought to be the source of the sulfate (Rye et al. 1978). Although

there is general agreement that the bedded deposits are syngenetic and that the sulfate is marine, there has been disagreement as to the source of Ba.

Some of the criteria used by Dube (1986, 1988) to support a sedex origin for the Nevada deposits are the stratiform, lens-like form of the orebodies: massive to laminated textures; coarse or angular sedimentary units near ore horizons, suggesting faulting; and presence of vent fauna in the form of fossil tube worms and brachiopods. Barite conglomerates are present in some of the deposits, suggesting slumping at proximal fault scarps near feeder zones. The high thickness to length ratio of many of the barite lenses suggests that the fluid from which the barite precipitated may have been ponded against fault scarps, perhaps within minibasins.

Jewell and Stallard (1991) and Jewell (1992) proposed instead that the Nevada bedded barite is ultimately the result of the concentration of Ba by pelagic organisms thriving in a coastal upwelling system in the Late Devonian ocean. These authors have cited the high levels of P (see Graber and Chafetz 1990) and organic carbon in barite-bearing sections relative to non-barite sections, and low Al/(Al+Fe+Mn) and low Fe/Ti bulk-sediment values indicative to them of a terrigenous rather than a hydrothermal source for the Ba. In their model, barite produced by Paleozoic pelagic organisms sank into underlying anoxic waters and then dissolved. Barite was then reprecipitated on the continental slope at an interface between sulfate-rich oxic and Ba-rich anoxic waters. Although this is a hypothesis worth testing further, there are difficulties in reconciling it with the strong field evidence for a sedex origin discussed by Dube (1986, 1988) and others. It is also unclear whether pelagic processes have ever been dynamic enough in the geological past to generate Ba fluxes large enough to produce localized, million metric ton orebodies of barite. The association of barite with phosphorites and cherts in some deposits may simply reflect deposition of barite in elevated concentrations during times of low background clastic sedimentation.

Further evidence cited by Jewell (2000) to support a biological origin for Pb- and Zn-free bedded barite in general, including deposits in Nevada, Arkansas, and China, consists of "...$^{87}Sr/^{86}Sr$ analyses that are comparable to contemporaneous seawater...". However, while some analyses do approach those of coeval seawater, most of the Sr-isotopic signatures (Maynard et al 1995, Jewell 2000) of the Nevada bedded barites and other bedded barite deposits are not comparable. Many of the Arkansas and Nevada analyses show enrichment in radiogenic Sr, and the Chinese barite is less radiogenic than coeval seawater (Fig. 18). The Pb- and Zn-free bedded barite from Cuba is highly radiogenic (Maynard et al. 1995).

Murchey et al. (1987) proposed a hybrid origin for the barite deposits along the western North America Paleozoic continental margin. They have suggested that the barite deposits are sedex, but that the source sediments from which Ba was derived by hydrothermal leaching were enriched in Ba derived from pelagic processes at the time of deposition.

Central convergent margin: Peru. The present convergent margin of Peru is characterized by an extensional tectonic regime and the lack of a well-developed accretionary prism. What have been described as "massive" barite deposits actually consist of crusts of barite a few millimeters thick, concretions, and chimneys up to 15 cm in height at two active vent sites (Dia et al. 1993, Torres et al. 1996a, Aquilina et al. 1997). Venting fluids sampled during deep submersible dives show an enrichment in Na, Cl, Ba, and radiogenic Sr ($^{87}Sr/^{86}Sr$ = 0.710151 to 0.711186) relative to modern seawater (Fig. 18) (Aquilina et al. 1997). Values for $\delta^{34}S$ range from 10.7 to 29.7 permil. One site is close to sea water in sulfur isotopic composition and the other is enriched in heavy sulfur. The venting fluids and barite have similar isotopic ratios of S, O, and Sr. Torres et al. (1996a)

proposed that the Ba was derived by remobilization of non-detrital barite deposited in area of high biological productivity along the continental margin. Aquilina et al. (1997), in contrast, proposed that the Ba was derived from mainly continental sources.

Phanerozoic passive continental margins and epicontinental rifts

Selwyn basin, Canada: Cambrian-Mississippian. The Selwyn basin is an elongated epicontinental marine rift basin that extends from northeastern British Columbia, Canada, to Alaska. It is one of the best known sedex mineral districts because of excellent outcrop and the extensive and detailed work done there by the Geological Survey of Canada and others. Much of the development of general conceptual models for sedex deposits by Lydon (1995), Goodfellow (1999), and others stems from the study of these deposits.

The Selwyn basin was initiated in the Cambrian as result of extension along the northwest American passive margin and was terminated during the Mississippian by infilling with clastics. Stratiform Pb-Zn deposits were formed within the basin during three major periods, early(?) Cambrian, early Silurian, and middle to late Devonian. Sulfide deposits in early Cambrian and Devonian sediments are typically interbedded with barite and are often commonly capped by barren barite. Early Silurian deposits, in contrast, contain no barite. Stratiform barite deposits without significant metals commonly occur in rocks of Devonian and Mississippian age. Goodfellow (1999) noted that an important characteristic of sedex-bearing rifts in general is that they were long-lived and have a sedimentary record that spans hundreds of millions of years. Rift-bounding faults were periodically reactivated (Fig. 29), resulting in several hydrothermal events within the same sedimentary basin.

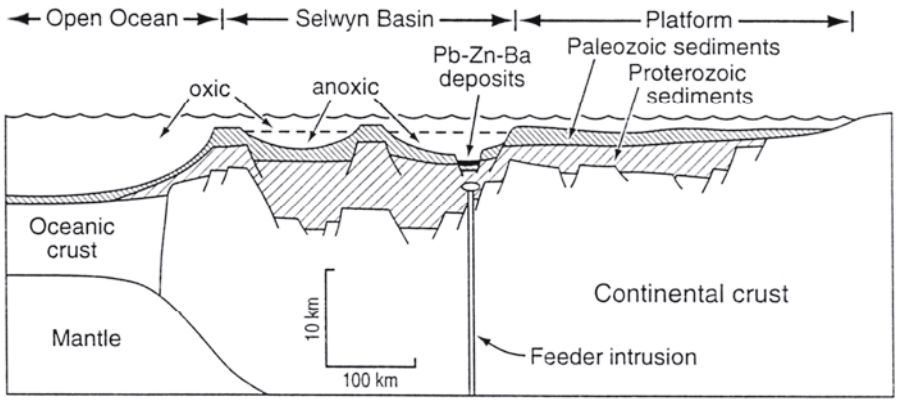

Figure 29. Schematic cross section of the Selwyn basin showing location of anoxic bottom waters and sedex sulfide-barite deposits. Intrusive activity may have been involved in the generation in ore-forming fluids but not in driving fluid expulsion. After reconstructions by Goodfellow et al. (1993) and Goodfellow (1999).

All major sedex deposits in the Selwyn basin formed during periods of anoxic bottom-water conditions (Figs. 23, 29). The $\delta^{34}S$ values for barite are consistently 10 to 15 permil more positive than the global values for marine evaporites indicating partly restricted circulation between the Selwyn basin and open seawater and/or vertical stratification within the water column (Cecile et al. 1983). Isotopic values of sulfide minerals are generally lighter, reflecting that much or most of the sulfide has been derived by bacterial reduction of marine sulfate (Goodfellow et al. 1993, Lydon 1995). The Sr isotopic composition of the barite is highly radiogenic, reflecting a sialic crustal source for the ore-forming fluids.

On the basis of fluid-inclusion and field data Goodfellow (1999) concluded that

hydrothermal fluids in the Selwyn basin vented into sea water both as buoyant plumes (Fig. 23) and as dense bottom-hugging brines (cf. Fig. 27). Deposits formed from plumes are mound-shaped and are characterized by rapid changes in thickness and mineralogy away from the discharge vents. In contrast, deposits formed from dense brines tend to be more uniform in thickness, are laterally widespread, and are delicately bedded. Heating by magma injection into the lithosphere (Fig. 29) may have played an important role in generating ore-forming fluids, but was not responsible for the driving forces which caused fluid expulsion.

Sedex deposits of late Paleozoic age occur in the Alaska basin (Murchey et al. 1987). Most completely studied have been the Red Dog sedex Pb-Zn-Ba deposits of Carboniferous age that occur in northwesternmost Alaska. The Upper Carboniferous to Middle Jurassic Etivuk Group includes baritic shales which record a change to low sedimentation rates and oxygenated conditions and the continuation of low-temperature hydrothermal activity long after the formation of the Red Dog deposits (Edgerton 1997).

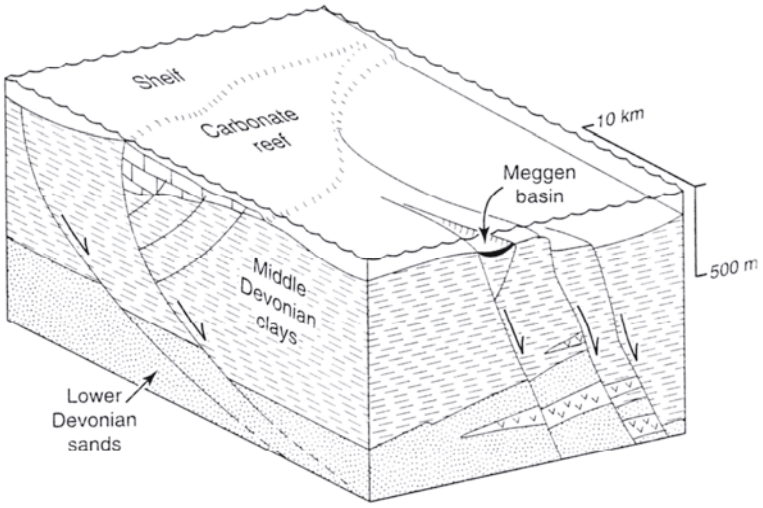

Figure 30. Block diagram showing a paleo-structural reconstruction of the Meggen region, Germany, at the time of submarine-hydrothermal Zn-Pb-Ba mineralization. Modified from Krebs (1981).

Meggen and Rammelsberg, Devonian, Gemany. Meggen and Rammelsberg, Germany are two important sedex sulfide-barite deposits in Devonian host sediments and have been studied since the mid-1850s. Meggen is noteworthy for having been the first barite deposit in which the use of sulfur isotopes established Devonian seawater as the source of sulfur in the barite and hence a synsedimentary origin for the deposit (Buschendorf et al. 1963). According to Krebs (1981) the deposit formed when warm metalliferous basinal brines were driven toward syndepositional growth faults and ascended to the seafloor. Metal and barite precipitation occurred in restricted, fault-bounded sub-basins (Fig. 30). The Rammelsberg ore bodies are similarly associated with a major growth fault (Hannak 1981). Sawkins and Burke (1980) noted the relation of the occurrence of mid-Paleozoic massive sulfide deposits in Europe with extensional tectonic features.

China and Kazakhstan, Cambrian; Spain, Silurian. Large bedded barite deposits of apparent sedex origin exist over an area of approximately a million square kilometers in Lower Cambrian strata in China (Wang and Li 1991) and in Cambrian sediments in central Kazakhstan (Vinogradov et al. 1978). The Kazakhstan barite has fluid inclusions which yield homogenization temperatures of 150 to 250°C, which are interpreted by Vinogradov et al. to preclude a synsedimentary origin. It cannot be determined from the published description of these deposits, however, whether the inclusions exist in coarse, secondary barite, and whether stretching and/or the presence of dissolved methane has contributed to high homogenization temperatures. In other respects the Kazakhstan

deposits closely resemble sedex deposits described above. The Chinese and Kazakhstan deposits constitute some of the largest reserves of barite in the world (Clark et al. 1990). The literature is sparse on these occurrences, but one hopes that additional studies will be performed and published.

Moro and Arribas (1981), in a review of stratiform barite deposits worldwide, included a brief description of several bedded barite districts in Spain. Host rocks are siliciclastic and volcanic sequences of Silurian age. Their field outcrop photos and photomicrographs document sedimentary features very similar to those observed in the Arkansas and Nevada deposits (Zimmerman 1970, Graber and Chafetz 1990).

Northwest Africa, Cretaceous. Dean and Schreiber (1977) described the occur-rence of rosettes, lenses and laminae of barite in Lower Cretaceous sediments at two DSDP sites along the continental margin of northwest Africa. Salinities of interstitial porewaters increase downward at both sites in response to suspected underlying evaporites of Jurassic age. Dean and Schreiber suggested three possible sources of sulfate: seawater sulfate, sulfate formed by oxidation of pyrite, and sulfate derived from evaporites. Sulfur isotopic work would help resolve probable sources. They concluded that the main source of Ba was from oxidation of organic matter.

Northern Gulf of Mexico, Recent. Although the northern Gulf of Mexico sedi-mentary basin is technically a passive continental margin, it is active both tectonically and hydrologically (Hanor and Sassen 1990). Sediments both onshore and offshore are undergoing active deformation as a result of salt tectonics, subsidence, and extensional growth-faulting. The combination of topographically-driven fluid flow, thermohaline instabilities resulting from the dissolution of salt and perturbation of thermal gradients, and overpressuring have given rise to dynamic and complex regional subsurface fluid flow (Hanor and Sassen 1990, Hanor 1999a). It is not surprising, therefore, that brine seeps exist on the seafloor in the Gulf of Mexico and that some of these have barite associated with them.

Fu (1998) described several minor occurrences of barite chimneys and crusts associated with brine seeps in the offshore Louisiana Gulf of Mexico. On the basis of $^{228}Th/^{228}Ra$ dating the chimneys studied by Fu are recent, from 0.5 to 6.5 years old, and the crusts from 9 to 23 years old at the time of sampling. Chimney $\delta^{34}S$ and $\delta^{18}O$ values are similar to that modern seawater, but the crusts are enriched in heavy S and O, reflecting sulfate that has been derived from seawater that has undergone bacterial reduction (Fu 1998). The $^{87}Sr/^{86}Sr$ ratio of the barite is lower than that of modern seawater, consistent with strontium derived from anhydrite in Jurassic salt (McManus and Hanor 1993), which forms domes and allochthonous sheets in the offshore Louisiana Gulf of Mexico.

Cenozoic strike-slip margins

Southern California borderland. Occurrences of barite are common in proximity to fault scarps in the California borderland (Lonsdale 1979). The barite occurs as cones, columns and irregular piles of mineral debris on the seafloor. At one location, barite occurs as spherical and cylindrical concretions, the latter appearing to be baritized worm burrows (Hanor, unpublished). Some of the deposits studied by Lonsdale (1979) stand 2 to 3 m above the seafloor, but one mass has an estimated height of 10 m. Dense colonies of tube worms occur around some of these deposits. The barite is thought by Lonsdale and others who have studied similar occurrences (see references in Lonsdale 1979) to be the result of submarine discharge along faults. An active hydrothermal circulation system has been proposed for the San Clemente fault zone on the basis of the pattern of heat flow. Lonsdale proposed convective circulation of seawater within the San Clement fault zone, with sulfate removed by reduction and Ba added by leaching. As cited by Lonsdale, basaltic rocks of

the region are notable for their high concentrations of Ba. Widespread submarine fluid expulsion occurs further north along this translational continental margin within Monterey Bay, although the presence of barite has not yet been identified (Orange et al. 1999).

Cortecci and Longinelli (1972) measured oxygen-isotope variations in one of several large barite slabs from this offshore region. These values, and isotopic analyses reported by Goldberg et al. (1969) and Church (1970), indicate the barite is enriched in ^{18}O and ^{34}S relative to seawater sulfate. The relative fractionation of sulfur to oxygen follows the 4 to 1 ratio observed experimentally in the bacterial reduction of dissolved sulfate (Mitzutian and Rafter 1969).

Sedex barite deposits in active marine evaporite settings

Precipitation of barite can apparently occur contemporaneously with seawater evaporation. Such may be the case for the Chaudfontaine barite deposit in Belgium (Dejonghe 1990, Dejonghe and Boulvain 1993), where barite, pyrite, sphalerite, and galena formed in small shallow pools that evolved under evaporitic conditions in a Devonian carbonate bioherm. According to Dejonghe and Boulvain, much of the barite grew at the sediment–water interface from marine S and non-marine Ba and Sr. Similar deposits may occur in Argentina (Brodkorb et al. 1982). Given the low concentration of Ba in normal seawater, however, it is unlikely that significant amounts of barite could ever be precipitated by direct evaporation only.

The question of metal-bearing and metal-free bedded barite deposits

There has been considerable interest in determining why some bedded barite deposits, such as Meggen, Rammelsberg, and many of the Selwyn basin deposits, are spatially associated with significant amounts of metal sulfides, whereas other barite deposits, such as the Arkansas, Nevada, and many Chinese deposits are not. Maynard and Okita (1991) attempted to explain this difference on the basis of differences in tectonic setting. They proposed a dual classification of "continental margin type" and "cratonic rift type" barite deposits. In the continental margin type deposit barite was deposited without associated metal sulfides in small ocean basins lying between subduction zones and passive continental margins. Sulfide-bearing deposits, in contrast, formed in cratonic rifts and have a continental geochemical signature. Turner (1992) noted, however, that metal-free barite deposits occur in the Selwyn basin along with Pb-Zn-Ba deposits. Turner further noted that most Cambrian to Devonian age stratiform Pb-Zn-Ba deposits world-wide formed in a continental margin setting rather within cratonic rifts.

Maynard et al. (1995) presented an extensive compendium of Sr-isotopic analyses of bedded barite and concluded that barite associated with Pb and Zn is much more radiogenic than coeval seawater than Pb-Zn-free barites (Fig. 18). They suggested that these differences in Sr-isotopic composition of barite could be used to screen exploration targets for the possible occurrence of heavy metals. They further explained the occurrence of barite-only deposits in intracratonic rift settings by the exhalation of ore-forming fluids into sulfide-free oxic seawater.

Other variables to consider in the relation between barite and metal sulfides include temperature and salinity. Elevated temperature and salinity facilitate the mobilization and transport of lead and zinc through the formation of chloro-complexes (Hanor 1996b, 1999b), whereas the mobilization of Ba under basinal conditions is more critically dependent on the presence of low concentrations of sulfate (Fig. 6). Terranes or sedimentary sequences with halite may be more likely to generate metal-bearing sedex fluids than those without. As noted above, an alternative explanation for the origin of Pb- and Zn-free bedded barite deposits has been proposed by Jewell (2000), who has advocated a biological origin for the Ba.

CENOZOIC PELAGIC BARITE AND DISPERSED BARITE IN DEEP SEA SEDIMENTS

The final types of barite to be discussed which have seawater as the principal source of sulfate are: pelagic barite, a term restricted in this chapter to barite produced in the shallow part of the water column of the open ocean, and fine-grained barite regionally dispersed in deep-sea sediments in environments spatially removed from localized submarine hydrothermal vents. The term *pelagic*, derived from the Greek word *pelagos*, referring to the level surface of the sea, is used here in its strict sense. Barite dispersed in deep-sea sediments may include pelagic barite, barite precipitated at the sediment–water interface, and particulate barite derived from distant hydrothermal sources. As discussed earlier, the term *marine barite* by itself is ambiguous and includes a wide variety of barite deposits. Some have coined the term *biobarite* to refer to pelagic barite thought to originate from biologically mediated processes, but this is not appropriate because some benthic organisms can also precipitate barite.

Probably no types of barite have received more attention in the recent literature than pelagic barite and barite in deep-sea sediments, because of their potential as paleo-productivity indicators and because of their potential use in tracking secular changes in the isotopic composition of seawater. The literature on these types of barite and on Ba in seawater is large, and some highlights are reviewed here.

Barite in seawater

Particulate barite is nearly ubiquitous in seawater. Dehairs et al. (1980) found barite particles in all water samples they investigated in an areally extensive sampling of the Atlantic, Antarctic, and Pacific oceans. Barite concentrations ranged from 10 to 100 ng/kg of seawater, with most water samples containing several tens of ng/kg. Barite is particularly abundant in waters underlying areas of high surface productivity.

The barite studied by Dehairs et al. (1980) consists of aggregates of submicrometer grains with or without a crystalline habit, sub-spherical particles, and particles with a distinct crystalline habit. Dehairs et al. reported a wide range of Sr concentrations, with 67% of the barite samples containing <10 mol % $SrSO_4$, 22% containing from 10 to 50% $SrSO_4$, and 11% containing over 50% $SrSO_4$. Barium-free, Sr- and S-rich particles are also present as biogenic Acantharian celestine debris or as smaller particles with no obvious biogenic morphology. The suspended barite particles contain minor amounts of K.

Stroobants et al. (1991) found that barite particles in the upper 10-20 m of the water column occurred as bioaggregates without distinct crystalline habit. Below these surface waters, however, barite existed in bioaggregrates containing microparticles with a crystalline habit. At water depths below a few hundred meters barite crystals, were present as free discrete particles, possibly as a result of breakup of aggregates by bacterial activity. The free microcrystals settle much more slowly than the carrier-aggregates, and local concentration of suspended barite within the water column at mid-depth can result (Dehairs et al. 1992). Bertram and Cowen (1997) observed three distinct crystalline forms of barite in plankton tows and net tows and on artificial seafloor substrates in the central Pacific. Microcrystalline aggregates of barite contained no detectable Sr, whereas ovoid and hexagonal-type crystals contained variable, and some high, Sr concentrations. The microcrystalline aggregates may be formed passively within abiotic microenvironments, and certain hexagonal crystals are precipitated by benthic forams.

Mode(s) of precipitation of pelagic barite

The exact mechanisms of formation of pelagic barite in the upper water column are still unknown and a subject of debate. The following mechanisms have been proposed.

Inorganic precipitation. Most authors argue that highly variable Sr/Ba ratios of pelagic barite are inconsistent with inorganic precipitation from surface seawater, which has a restricted range of Sr/Ba ratios (e.g. Dehairs et al. 1980). Inorganic precipitation has been deemed unlikely because most near-surface seawater is also undersaturated with respect to pure $BaSO_4$ (Fig. 8) (Monnin et al. 1999). Bernstein et al. (1992) estimated saturation indices for celestine and barite in ocean surface waters to be 0.16 and 0.14 respectively. Calculations by Hanor (1969), based on the Sr-Ba partition coefficients determined by Starke (1964), however, showed that Sr-enriched barite is significantly less soluble than pure $BaSO_4$, and that seawater could be nearly saturated with respect to a strontian-barite containing 33 mol % $SrSO_4$.

Precipitation in sulfate-enriched microenvironments. Bishop (1988) proposed that barite forms in microenvironments enriched in sulfate released from decaying diatom organic matter. According to Bishop, the C:Si ratio of a diatom is 2:1, and the C:S ratio is approximately 100:1. Therefore the Si:S ratio of a diatom is approximately 50:1. Dissolved Si and Ba covary in seawater in a ratio of 1300:1. According to Bishop, the reaction of organically bound S with dissolved Ba in seawater need only be 4% efficient if diatoms are the only source of S for barite. In addition, other plankton groups can contribute to the pool of S. Fresh diatom silica surfaces may adsorb Ba better than other biogenic organic phases (Bishop 1988) thus enhancing the formation of microenvironments conducive for barite precipitation.

Incorporation of Ba into skeletons of siliceous plankton. Because of the excellent correlation between dissolved Ba and Si in the marine water column, it has been suggested that the distribution of both elements is governed by the dissolution of Ba-enriched siliceous frustrules. However, plankton samples from the Pacific described by Martin and Knauer (1973) had low Ba levels.

Biogenic precipitation of barite by other planktonic organisms. A number of freshwater and marine organisms are known to precipitate barite. These include the benthic marine Rhizopoda of the class Xenophyophorida (Arrhenius 1963, Tendal 1972, Gooday and Nott 1981, Gooday et al. 1995, Hopwood 1997), benthic foraminifera (Dugolinsky et al. 1977), marine algae in the Mediterranean (Fresnel et al. 1979, Gayral and Fresnel 1979), freshwater protozoa (Hubert et al. 1975, Finlay et al. 1983, Fenchel and Finlay 1984), and freshwater desmid algae (Brook et al. 1980, 1988; Wilcock et al. 1989). Finlay et al. (1983) speculated that the intracellular precipitation of ~4 μm size spherical barite granules by the freshwater protozoa of the genus *Loxodes* in the English Lake District of England, may be instrumental in gravitropic responses. A related marine form, *Remanella*, precipitates celestine, however, not barite (Bishop 1988). Production of pelagic barite by direct intracellular biological precipitation has not yet been demonstrated.

Dissolution of acantharian debris. Acantharians are an abundant planktonic species of radiolaria which secrete shells or tests of celestine (see section in this chapter on celestine). Bernstein et al. (1992, 1998) argued that the uptake of Ba in the celestine acantharian shells and its subsequent release during ingestion of acantharians by zooplankton may result in the precipitation of barite. Despite the abundance of acantharians in the euphotic zone, celestine remains have apparently not been reported in either the gut contents or fecal material of zooplankton. However, siliceous remains are common. Bernstein et al. speculated that the absence of acantharian debris may be the result of rapid dissolution of celestine skeletons and cysts. The authors calculated that the dissolution of a single acantharian or acantharian cyst of 1 μg mass containing 5.4×10^{-9} mol $SrSO_4$ would saturate a 10-μL volume of water with respect to $SrSO_4$, while supersaturating the water with respect to $BaSO_4$ by seven times.

Fate of barite in the water column

Undersaturation of seawater with respect to $BaSO_4$ almost everywhere in the water column (Fig. 8) (Monnin et al. 1999) induces the dissolution of suspended barite. Nearly all suspended barite particles are affected by dissolution to varying degrees (Dehairs et al. 1980). The edges of euhedral particles are rounded in the process, and particles become progressively ellipsoidal and spherical. There is also etching of crystal surfaces. Some pelagic barite dissolves completely as it sinks through the water column, and there is a decrease in the number of suspended barite particles with water depth. Most of the barite, however, is transported rapidly within fecal pellets to the seafloor where it accumulates in bottom sediments. The interstitial pore water of these sediments rapidly becomes saturated with respect to barite, inhibiting further dissolution. Bertram and Cowen (1997) observed that both size and Sr content of suspended barite particles decrease from surface water to the seafloor in the central Pacific, suggesting that the particles undergo dissolution and preferential removal of Sr-rich barite.

High concentrations of dissolved Ba possibly derived from the dissolution of pelagic barite are found in marine anoxic basins, including the Cariaco trench, Framvaen Fjord, Black Sea (Falkner et al. 1993), and the Mediterranean (de Lange et al. 1990a,b). Barium distribution is not strongly affected by adsorption or uptake on Mn or Fe oxyhydroxides formed at the redox interfaces of these basins. However, microbial activity just above the O_2/H_2S interface in the Black Sea promotes breakdown of settling particulate matter and the release of barite. Dissolution of barite in the marginal sediments of these basins also probably contributes to the small Ba maxima observed at the redox interface.

Barite in deep-sea sediments

Occurrence. Barite is a common constituent of those deep-sea sediments whose mineralogy is dominated by non-terrigenous sources. The high content of Ba in east equatorial Pacific sediments was first described by Revelle (1944), who suggested Ba may have been deposited in biogenic carbonate on the basis of the correlation between the abundance of Ca carbonate and Ba. Arrhenius et al. (1957) identified the existence of small (1 μm) crystals of high refractive index and high alpha activity as possibly barite in north equatorial Pacific sediments. Since that study, barite has been identified in deep-sea sediments ranging in age from Recent to Cretaceous (Dean and Schreiber 1977).

Arrhenius and Bonatti in their 1965 paper on neptunism and volcanism in the oceans showed that maximum concentrations of barite, 7 to 9 wt % on a carbonate-free basis, coincide spatially with the East Pacific Rise and not with the area of high productivity along the Peru current to the east (Fig. 31). According to Church (1970, 1979) barite occurs in three different types of deep-sea sediments, those characterized by: (1) abundant calcareous and siliceous biological debris; (2) abundant Mn and Fe phases in nodular and dispersed forms, and (3) altered volcanic debris with montmorillonite, palygorskite, and clinoptilolite. The order of frequency of occurrence of these three types of barite is about 10:2:1. Euhedral crystals typically 1 to 2 μm in size can comprise up to 2% of the sediments underlying productive areas of the eastern equatorial Pacific. Barite crystals ranging in size from 25 to 100 μm are occasionally found in deep-sea sediments containing altered volcanic debris or manganiferous phases. In their survey of barite reported in sediment samples collected during the Deep Sea Drilling Project, Dean and Schreiber (1977) noted the common occurrence of barite both in the 2 to 20 μm and <2 μm grain size fractions.

Chemical composition. The first detailed and extensive study of the chemical composition of barite in deep-sea sediments was performed by Church (1970). In contrast to pelagic barite, which has a wide range of Sr concentrations, Sr in deep-sea barite from

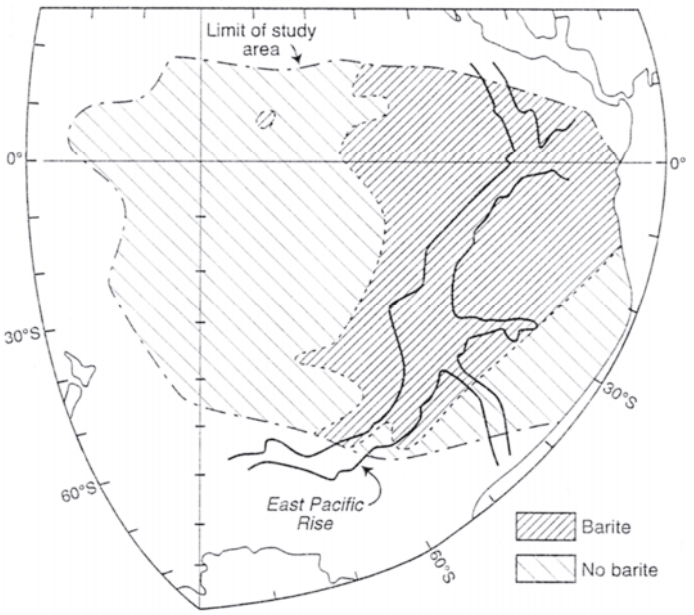

Figure 31. Distribution of barite in near surface sediments in the southeastern Pacific based on a study by Church (1970).

the Pacific ranges from 0.2 to 3.4 wt % and averages 1%. Calcium and K are present in levels of 0.01 to 0.1 wt %, with no correlation to each other, Sr content, or crystal size. Church found no evidence for high levels (100-1000 ppm) of Cr, Zn, Pb, and Zr earlier reported by Arrhenius (1963).

Strontium isotopic composition. The relatively high concentrations of Sr in barite has permitted use of very small samples of deep-sea barite for Sr-isotope studies. Goldberg et al. (1969) determined that barite crystals from Pacific surface sediments had Sr isotopic compositions similar to that of present day seawater. With the advent of more precise Sr-isotopic techniques there has been considerable refinement in the understanding of the Sr-isotopic compositions of pelagic barite (Paytan et al. 1996). Martin et al. (1995) found that all samples from near the core tops in eastern equatorial Pacific sediments have values close to modern-day seawater (0.709175). The $^{87}Sr/^{86}Sr$ ratios for barite from Late Miocene to Pliocene sediments deeper in the cores agree very well with published Sr-isotope data for carbonates over the past 36 Ma. The crystal morphology of barite over these depth intervals shows no noticeable change, and the barite has not re-equilibrated with pore fluids in terms of Sr isotopic composition. Martin et al. (1995) thus concluded that marine barite may be useful for Sr-isotopic stratigraphy and correlations in epochs for which the seawater curve for Sr is known and in times or environments where Ca carbonate has either undergone diagenetic alteration or is absent. However, barite separates in two sites north of the productivity maximum had consistently slightly lower $^{87}Sr/^{86}Sr$ ratios than coexisting foraminifera and fish teeth, thus suggesting the presence of small amounts of oceanic hydrothermal barite in these sediments (Martin et al. 1995).

Neodymium isotopic compositions and REE. Guichard et al. (1979) reported relatively high Nd concentrations (5-100 ppm) for barite in deep-sea sediments, which would make it a useful mineral for Nd-isotope studies of seawater. However, Martin et al. (1995) observed Nd isotopic values of barite in pelagic sediments to be significantly different than values for contemporary seawater. The Nd values appear instead to be dominated by an unidentified aeolian contaminant having a high Nd concentration and low $^{143}Nd/^{144}Nd$ ratios. Martin et al. (1995) concluded that while deep-sea barite is potentially useful as a recorder of Nd paleo-seawater compositions, its utility for both REE and Nd studies may be hampered by the presence of various refractory contaminants, such as rutile, anatase, zircon, and titanite, which are not easily removed using standard chemical

separation techniques.

Radium and thorium. Some of the results of early studies of Ra, Pb, Th, and U in barite samples from pelagic sediments suggested rapid exchange and remobilization of these elements after burial (Church and Bernat 1972, Borole and Somayajulu 1977). Church and Bernat (1972) concluded from the high $^{228}Th/^{232}Th$ they measured in barite near core tops that ^{228}Ra in barite was in rapid exchange equilibrium with pore waters. Borole and Somayajulu (1977) measured excess ^{226}Ra in barite samples too old to contain excess ^{226}Ra, and concluded that barite must be continually growing in the sediment column. However, there was no increase in size in the barite crystals with depth in the sediment.

More recent work by Paytan et al. (1996) sheds new light on Th and Ra systematics in barite in pelagic sediments. Concentrations of U in the barite are less than 0.5 ppm, negligible in comparison to that of Th, indicating essentially all the ^{230}Th in barite is unsupported. $^{230}Th/^{232}Th$ activity ratios range between 20 and 190, with a mean of ~100, which is consistent with the bulk sediment ratio. The exponential decrease in ^{226}Ra of barite in the upper 25 cm of the sediment suggests that barite behaves as a closed system and is not affected by exchange or recrystallization. The lack of detectable ^{228}Th, ^{228}Ra, and ^{224}Ra activities in any of the barite samples indicates that no significant barite growth is occurring below the bioturbated zone.

Paytan et al. (1996) ascribed problems in the earlier results for Ra and Th in marine barite to the use of milder sequential leaching procedures that did not remove all detrital material and oxyhydroxide coatings from the barite. An extreme HF leach step is necessary to remove detrital components, and special precautions are needed to remove surface coatings of Fe-Mn oxyhydroxides from barite surfaces.

Origin of barite in deep-sea sediments. There are still uncertainties regarding the origin(s) of this type of barite, despite the large amount of work which has been done on it. A spatial association between the occurrence of Ba in deep-sea sediments and areas of high biological productivity was made early on. The high content of Ba in east equatorial Pacific sediments was first described by Revelle (1944), who suggested that Ba may have been deposited in biogenic carbonate, because of the correlation between the abundance of Ca carbonate and Ba. Arrhenius (1952) tested the hypothesis that rate of accumulation of Ba is a function of the rate of organic production in the euphotic zone by measuring variations in BaO/TiO_2 ratios with depth in sediment cores, and assuming that the rate of TiO_2 accumulation is uniform in space and time. Arrhenius concluded that the rate of Ba accumulation is approximately 20 times higher under the equatorial divergence high productivity zone between 10°N and 10°S than outside this zone. Arrhenius (1952) also established that there has been a marked variation in the rates of Ba accumulation with time.

Church (1979) proposed that the flux of particulate barite down through the water column could account for approximately half the sedimentary barite he observed. According to Church, the remainder appears to grow in surface sediments as a consequence of further organic degradation. Church (1970) suggested that barite deposition on the East Pacific Rise is correlated with high concentrations of $CaCO_3$ and organic matter. However, Boström et al. (1973) indicated that these $CaCO_3$ data do not agree with earlier studies on the areal distribution of carbonates.

Although it is sometimes stated in the literature that barite is particularly abundant both in the water column and underlying sediments in areas of high biological productivity, Arrhenius and Bonatti (1965) showed that maximum concentrations of barite, 7 to 9% on a carbonate-free basis, coincide spatially with the East Pacific Rise and not with the area of high productivity along the Peru current. Boström et al. (1973) determined the

concentration of Ba in more than one thousand sediment samples from the Pacific, Indian, South Atlantic and Arctic oceans and determined Ba accumulation rates in the Pacific (Fig. 32). Some barite may form by release of Ba during alteration of volcanics. There is some correlation of Ba accumulation rates with accumulation rates of opaline silica (Fig. 32), particularly in the equatorial Pacific, but there is remarkably little Ba in sediments underlying high productivity regions off the coast of Japan and South America. All high Ba values are located on the active ridge system in the Indian and Pacific oceans. Regions of high productivity in the north Pacific, eastern Pacific, and east Indian oceans lack Ba-rich sediments.

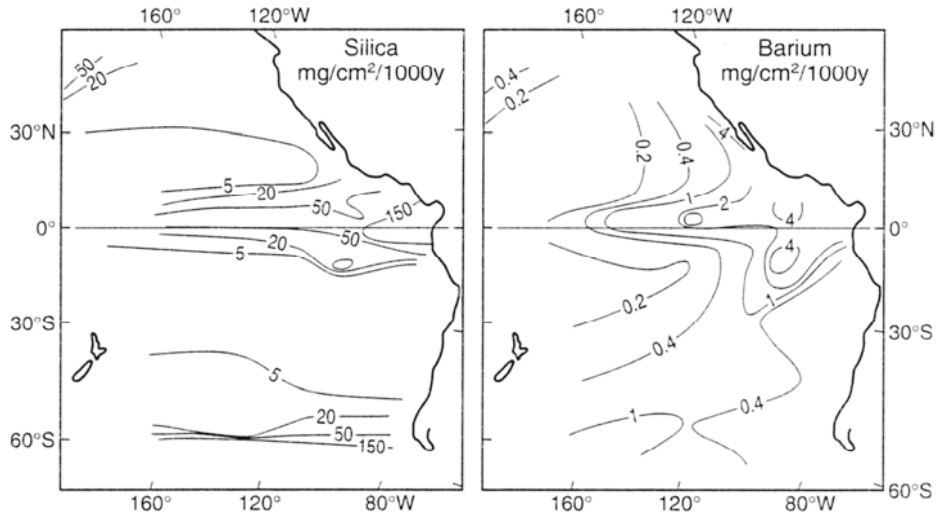

Figure 32. Accumulation rates for (a) opaline silica and (b) Ba in sediments of the Pacific. Both diagrams modified from Boström et al. (1973).

An unknown, but possibly significant amount of barite is generated by xenophyophores, a group of bottom-dwelling protozoans closely related to foraminifera (Tendal 1972, Tendal and Gooday 1981). Pictures of the seafloor taken from submersibles in the Atlantic Ocean suggest that these protozoans are quite common. Gingele and Dahmke (1994) concluded that the barite secreted by the xenophyophores cannot be distinguished from barite dispersed in sediments in terms of size and morphology. The quantitative contribution of the xenophyophores to the barite budget remains unclear. Perhaps these organisms ingest rather than secrete barite.

There would thus appear to be multiple origins for the barite dispersed in deep-sea sediments. Among these origins are the more Ba-rich of the pelagic barites which settle intact through the water column; barite precipitated at the sediment-water interface, perhaps by dissolution of other forms of biogenic minerals or recrystallization of pelagic barite; particulate barite derived from distant hydrothermal sources; and barite secreted by benthic organisms.

Paleoenvironmental significance. A number of authors have concluded that barite in deep-sea sediments has utility as a paleoenvironmental indicator (Schmitz 1987, Andrew et al. 1990, Dymond and Collier 1996). Dymond et al. (1992) developed an algorithm for computing absolute paleoproductivity rates from rates of barite accumulation. Barite accumulation rates show cyclical variations in which maxima correspond to glacial and minima correspond to interglacial stages (Gingele and Dahmke 1994).

The association between barite accumulation rates and primary productivity seems well established for Pacific equatorial waters, but as noted above, there are areas where there is no correlation. The accuracy of the calculations is further limited by the precision

in distinguishing between biogenic barite and the background barium which increases with increasing concentration of terrigenous matter. In addition, secular variations in the concentration of Ba in the water column could affect barite production and dissolution rates. That absolute concentrations of Ba in seawater have fluctuated in the past is evidenced by variations in Ba/Ca ratios of benthic foraminifera. Schroeder et al. (1997) concluded that total Ba in equatorial Pacific carbonate sediment is not a good proxy for barite because of the association of Ba with terrigenous input. It is possible that the non-barite Ba is adsorbed on grain surfaces. McManus et al. (1998) noted that barite can be reduced under suboxic conditions. They proposed that the accumulation of authigenic U may serve as an indicator of when the Ba record may be unreliable.

EPIGENETIC BARITE DEPOSITS AND EVAPORITES

This section explores a diverse group of barite deposits in which sulfate is sourced not from seawater, as in the previous examples, but from marine evaporites and/or buried evaporative marine waters.

Carbonate-hosted barite deposits

The evolution in sedimentary rock types over geological time manifests itself in the Late Proterozoic and Paleozoic with the appearance of laterally extensive biochemical continental margin and epicontinental platform carbonate sediments, many of which have served as hosts for ore deposits. The Paleozoic thus marks the development of new types of carbonate-hosted ore deposits, the Mississippi Valley type (MVT) and Irish type deposits, which have no known Archean or Lower Proterozoic counterparts. During low stands of sea level, the platform carbonates formed karsts and transformed into aquifers of regional extent which then served to focus fluid flow during large-scale deformation of the platform margins. Marine evaporites that are commonly associated with these carbonates provided potential sources of S for the formation of both barite and associated metal sulfides.

Mississippi Valley type deposits occur as epigenetic cavity fill and replacements by galena, sphalerite, fluorite, and barite in lithified and diagenetically cemented limestones and dolomites deposited in platform environments. Most MVT deposits were formed from 10 to 100 Ma after deposition of the host sediment (Hitzman 1999). Most deposits are related spatially to regional unconformities, and the timing of mineralization is related to large-scale orogenic events. Barite commonly occurs late, after the main stage of base metal mineralization.

Irish type Pb-Zn-Ba deposits occur in non-argillaceous, shallow marine carbonates and include syndiagenetic to epigenetic mineralization (Hitzman and Beaty 1996). A distinguishing feature of the Irish type deposits is their occurrence in carbonate environments that have undergone extension. The deposits are located adjacent to normal faults that served as fluid conduits, and mineralization occurred within 1 to 10 Ma after deposition of the host rocks. Barite is typically early, in contrast to the late deposition in many MVT deposits. Ore fluids were typically hot, 120-280°C, and had salinities of 10-25 wt % NaCl equivalent. Deposits apparently formed from the mixing of two fluids, one metal rich and hot with moderate salinities, and the other of lower temperature and salinity and which may have contained the sulfur.

Since the Jurassic, the principal locus of carbonate deposition has shifted from the shallow marine environment into the pelagic realm. There are no sediments being deposited today that are strictly comparable to those that host the MVT and Irish type deposits.

An extensive review of carbonate hosted lead-zinc-barite deposits world-wide is contained in the volume edited by Sangster (1996). Representative examples of MVT and

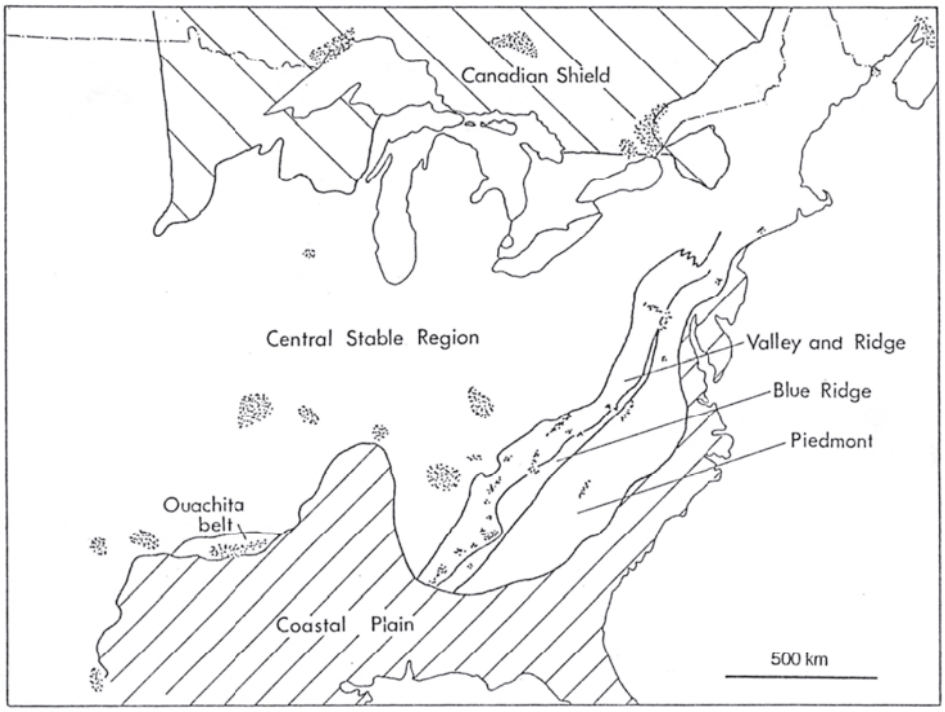

Figure 33. Map showing the distribution of barite deposits (stippled areas) in the central and eastern United States and Canada. From Hanor (1966).

Irish type deposits of eastern North America are described below.

Carbonate-hosted MVT deposits of the Appalachian orogen. The Appalachian orogen of eastern North America has had a complex tectonic history with three extended periods of orogeny in the Cambrian-Ordovician (Taconic, Penobscottian), Devonian (Acadian) and Mississippian through Permian (Alleghanian). There followed a period of rifting during the Triassic and Jurassic. Kesler (1996) provided a comprehensive review of the continental-scale MVT mineralization which extends throughout the Appalachian orogen as exposed in the Valley and Ridge province (Fig. 33) from Alabama through Quebec (Williams-Jones et al. 1992, Paradis and Lavoie 1996) to Newfoundland. The mineral deposits contain various combinations of sphalerite, galena, barite, fluorite, dolomite, calcite, and quartz and are most abundant in thicker stratigraphic sections along the strike of the orogen. Each of the four units which host significant MVT mineralization (Fig. 34) were important paleoaquifers that focused fluid flow during proximal tectonic events.

Barite, largely without significant amounts of sulfides, occurs in the Upper-Precambrian, Lower Cambrian Clastic Sequence with major deposits in the Cartersville District of Georgia. The Late Cambrian-Early Ordovician Knox-Beekmantown-St. George groups constitute the most important MVT paleoaquifer in the Appalachians and host large deposits of sphalerite. Barite occurs with or without fluorite in districts, such as the Sweetwater district, Tennessee, peripheral to zinc deposits. Farther to the west, MVT mineralization, including barite, is present in the Knox Group along the crest of the Cincinnati arch in central Tennessee and central Kentucky.

Possible sedimentary exhalative barite occurs in the Athens Shale in the Tennessee embayment of the Upper Ordovician Clastic Sequence and in foreland basin shales in the Pennsylvania embayment (Nuelle and Shelton 1986, Clark and Mosier 1989). MVT mineralization in Pennsylvanian and Permian sediments is confined to nodules and veinlets of sulfide and local barite, commonly associated spatially with coal layers. MVT

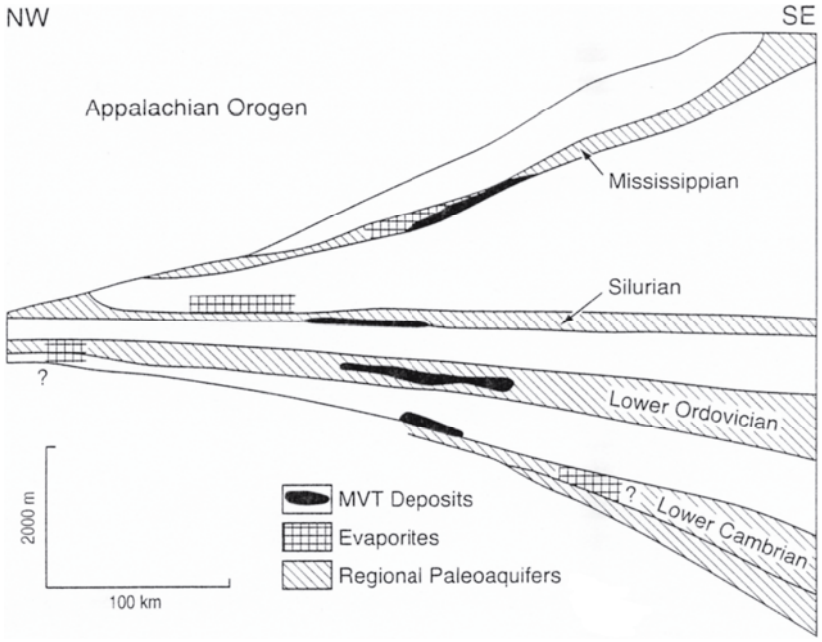

Figure 34. Schematic cross-section through the southern and central Appalachians showing the location of MVT deposits and evaporites in relation to principal paleoaquifers. Based on Kesler (1996).

mineralization is zoned on a regional scale throughout the Appalachians, with barite much more common in the southern part of the orogen. Most mineralization in the southern Appalachian orogen seems to have formed during Devonian time, presumably in response to the Acadian orogeny.

Information on the nature of the mineralizing fluids has been obtained from fluid-inclusion studies. Freezing temperatures yield fluid salinities in sphalerite of 20 to 26 equivalent wt % NaCl, and homogenization temperatures from <100 to >200°C. Some homogenization temperatures for Appalachian barite range from 200 to 300°C, unusually high relative to the other minerals. The temperatures may be artifacts produced by either stretching of the inclusions (Ulrich and Bodnar 1988) or the presence of dissolved methane (Hanor 1980).

Kesler (1996) presented chemical evidence for the presence of several distinctly different mineralizing brines in the orogen. Fluid-inclusion leachates from east Tennessee have very low Na/Cl and Cl/Br ratios, typical of brines that have undergone extreme evaporation to the point of precipitation of sylvite and other non-Na salts, but not typical of brines that have formed as the result of dissolution of halite. Kesler et al. (1995) thus concluded that the high salinities observed in the inclusions are the result of seawater evaporation rather than the subsurface dissolution of halite. An alternative explanation to that of Kesler et al. (1995) would be the dissolution of bittern salts high in Br.

Sulfur-isotope studies indicate that the most likely sources of S in both sulfide and sulfate minerals are buried seawater sulfate and evaporite sulfate. Sulfate S in barite was derived directly from these marine sources with a fractionation of only a few permil. Sulfide sulfur was derived almost entirely from H_2S produced by bacterial and thermochemical reduction of marine sulfate. Studies of most MVT deposits show that $^{87}Sr/^{86}Sr$ increases with decreasing age in the paragenetic sequence in a given deposit. Some ratios exceed that of enclosing carbonate host rocks and probably reflecting the introduction of Sr from a siliciclastic source. In the Sweetwater district of Tennessee, however, $^{87}Sr/^{86}Sr$ values for early fluorite and barite are actually less than those for

enclosing rocks and coeval seawater (Kesler 1996). Schrijver et al. (1994) have presented Pb-isotopic evidence supporting a siliciclastic source for both Pb and Ba in Taconic Orogen of Quebec.

Intracratonic MVT deposits. More problematic in origin than the MVT deposits of the Paleozoic Appalachian orogen are the carbonate-hosted MVT deposits of the intracratonic area of North America (Fig. 33), including the eponymous MVT district of the Upper Mississippi Valley region of southeastern Wisconsin and adjacent areas of Illinois and Iowa, the MVT districts of central and southeast Missouri, central Kentucky, and central Tennessee, and the Pine Point deposit of northwest Canada. These deposits are very similar in mineralogy and host rock setting to MVT deposits of the Appalachian orogen, but problematic in origin because of their greater distance from orogenic belts whose deformation might have driven ore-fluid transport (Garven and Raffensperger 1997). Some districts, such as the Cave-in-Rock fluorite district, which also contains barite, may be related to intracratonic igneous activity (Ruiz et al. 1988). Barite typically occurs as a late-stage mineral whose presence may not be related to the deposition of earlier base metals (Misra et al. 1996).

One of the more completely documented barite districts in the continental interior of North America is that of southeast Missouri (Kaiser et al. 1987). Lead-Zn-Ba-quartz mineralization is localized in flat-lying, elongate structures called runs, which represent high permeability zones formed at the intersection of near-vertical faults and areas of intense jointing within the subhorizontal Upper Cambrian Potosi and Eminence cherty dolomites. Fluids moved through these areas of high permeability depositing sulfides and barite in the central core areas of the runs and additional barite in sediments peripheral to the runs. Barite becomes progressively finer-grained and plumose laterally away from these core areas.

Fluid-inclusion studies indicate that the main stage of sulfide mineralization was deposited from warm saline Na-Ca-Cl fluids having temperatures from 70 to 105°C, salinities of 20 to 26 equivalent wt % NaCl, and carrying isotopically light S. Galena and sphalerite have $\delta^{34}S$ values which range from 3 to 16 permil.

In contrast, main-stage barite was deposited following sulfide deposition, from fluids far less saline (0 to 14 equivalent wt % NaCl). Temperatures of barite deposition are difficult to determine because most of the inclusions are single phase and the few two-phase inclusions analyzed apparently stretched upon heating. Barite $\delta^{34}S$ values range from 21 permil near the faults to approximately 32 permil laterally away from the faults. Fluid-inclusion and O-isotope evidence suggests that the barite was precipitated when a warm saline fluid flowing through the runs mixed with a cooler, less saline ambient fluid. Sulfate was derived from two distinctly different sources, oxidized H_2S from near the runs, and a heavier sulfate derived from the host Cambro-Ordovician carbonates. Uplift of the Ouachitas in late Paleozoic time apparently initiated MVT mineralization in the Ozark region through development of a continental-scale fluid-flow regime in which topographically-driven flow was initiated (Garven and Raffensperger 1997).

Leach (1980) determined that barite in the Central Missouri district was deposited as open-space filling in carbonates from fluids having salinities ranging from 4 to 10 wt % NaCl at temperatures of less than 40 to 50°C. Both salinities and Sr-content fluctuated during the growth of many of the barite crystals examined by Leach, who proposed that the barite was precipitated by mixing of a barium-rich and sulfate-rich fluid in near-surface environments affected by the seasonal introduction of sulfate-bearing water.

Hanor (1966) noted that major occurrences of barite in the mid-continent region of North America are spatially related to domal uplifts (Fig. 35). There is no exposed dome in

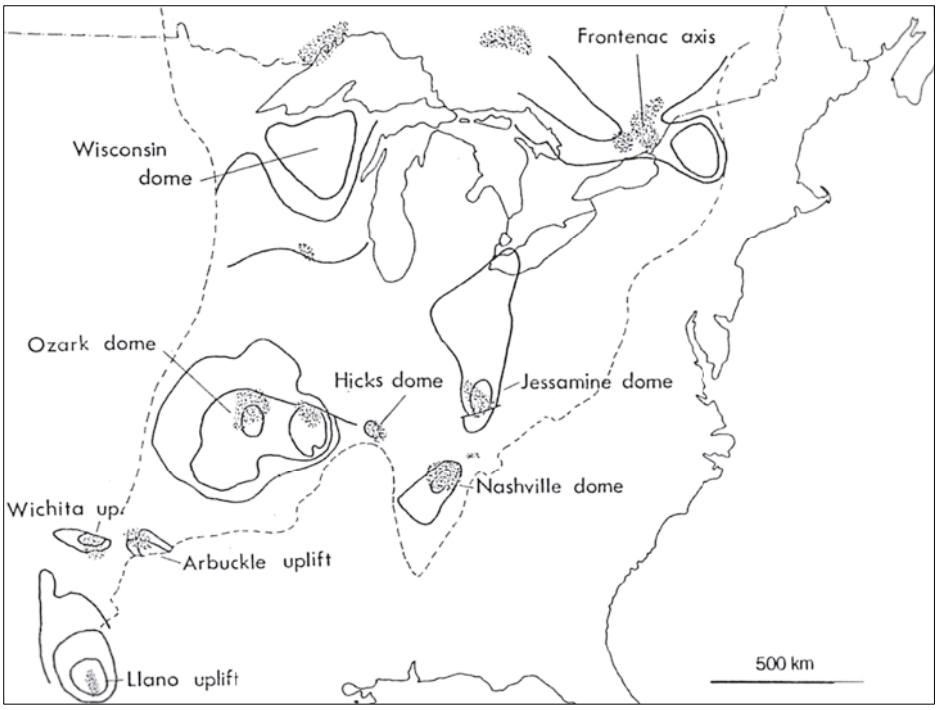

Figure 35. Map showing the relation between the occurrence of barite deposits (stippled areas) and domal uplifts in the central interior of the United States (Hanor, 1966).

this region which does not have some barite mineralization associated with it. Nearly all of the host rocks are Upper Cambrian and Ordovician carbonates. Carbonate solution features associated with the uplifts provided channelways for transport and sites of deposition of Ba. Barite may have been formed in the latter stages of hydrothermal activity when there was greater influx of ambient oxygenated shallow groundwaters circulating through the domal uplifts.

Irish Type deposits. Hitzman (1999) has provided an overview of Irish type base-metal and barite deposits world-wide. In the Walton and Gays River districts of Nova Scotia, Canada, Irish-type sulfide and barite deposits are restricted to areas of synsedimentary faults. Base metals and barite replace host rocks and occlude porosity. Sulfides and barite form stratiform bodies at Walton and discordant bodies at Gays River. Mineralization apparently occurred just prior to the Appalachian orogeny ~320 to 300 Ma when high-temperature high-salinity ore fluids discharged from depth and mixed with cooler, lower-salinity waters. Local evaporites provided the source of sulfur (Mossman and Brown 1986, Sangster et al. 1998, Chagon et al. 1998, Hitzman 1999) (Fig. 36).

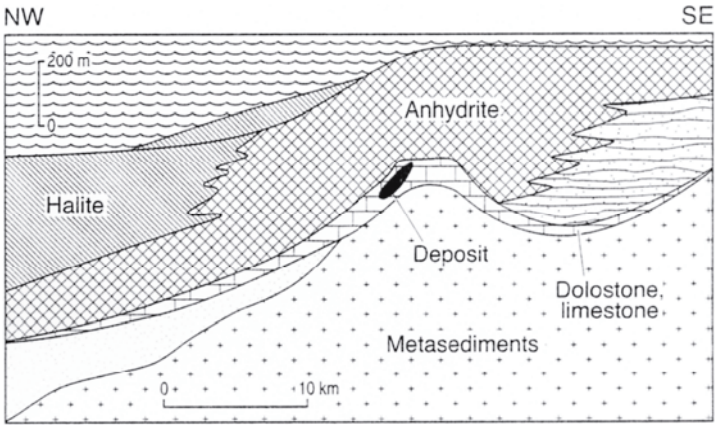

Figure 36. Schematic cross-section through the Gays River Zn-Pb-barite deposit, Nova Scotia, showing the relation of ore to the presence of evaporites. Based on a reconstruction of Chagon et al. (1998).

Continental rifts

Not all barite deposits associated with continental rifts occur in the immediate proximity to continental margins or active marine basins. The continental rifts discussed here are distinguished from the epicontinental marine rift basins discussed earlier in that the barite was deposited in epigenetic veins rather than in a syndepositional marine setting.

As noted by Robinson and Woodruff (1988), the margins of continental rift basins commonly host base-metal and barite vein deposits. Examples cited by Robinson and Woodruff include: the Late Proterozoic rift basins in the Lake Superior region of Ontario, Canada; the Cretaceous Benue Trough, Nigeria; the Paleozoic Midland Valley, Scotland; rift basins associated with the Rhine Graben, Germany; the Grenville Front, Canada; and rifts proximal to the Rhodesian craton, South Africa. Two of the more completely described settings are the Mesozoic rift basins of the eastern United States (Robinson and Woodruff 1988) and the Rio Grande rift (McLemore and Lueth 1996).

Mesozoic rift basins of the eastern United States. The Mesozoic rift basins of the eastern United States include 92 ore deposits in 14 districts extending from New Hampshire to northern Virginia (Fig. 37). This is a tectonic environment characterized by basinal subsidence and crustal extension in a continental setting. The vein deposits are spatially associated with regional faults.

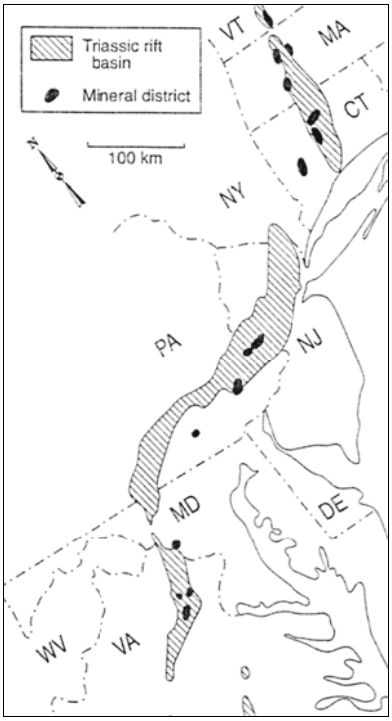

Figure 37. Map showing the location of sulfide-barite deposits in relation to Triassic rifts of the eastern United States. Modified from Robinson and Woodruff (1988).

Mineralization is characterized by quartz, galena, sphalerite, chalcopyrite, minor pyrite and tetrahedrite, and local barite, fluorite, and carbonate minerals. Barite occurs as open-space fill in high-angle faults and fractures. Host rocks for the barite range from Precambrian through Jurassic and represent a wide range of lithologies, including gneiss, schist, diabase, sandstone, shale, granite, and basalt. Fluid-inclusion evidence establishes that vein mineralization was deposited from moderately saline brines having from 10 to 16 equivalent wt % NaCl with a temperature range of 100 to 250°C.

The early Mesozoic basins of the eastern United States containing red-bed sediments may be important as sources of both saline brines and leachable metals (Zielinski et al. 1983). The deposits appear to be the result of transport of brines from within the basins and adjacent basement rocks to shallow sites of mineral precipitation. Fluid migration may have been be the consequence of dynamic and changing stresses that developed during the Middle Jurassic separation of North America from Africa. Seismic pumping may have been important as a drive for fluid flow. Principal mechanisms of deposition (Robinson and Woodruff 1988) appear to have been cooling, sulfate reduction, wallrock reaction, and possibly fluid mixing. Pre-existing fractures and faults were apparently important in localizing vein development.

Rio Grande rift deposits. According to McLemore and Lueth (1996) barite deposits of the Rio Grande rift in New Mexico (Fig. 38) formed from basinal brines having slightly higher temperatures but lower salinities than those responsible for typical MVT deposits. Paleozoic carbonate rocks host veins, breccia cements, and cavity fillings adjacent

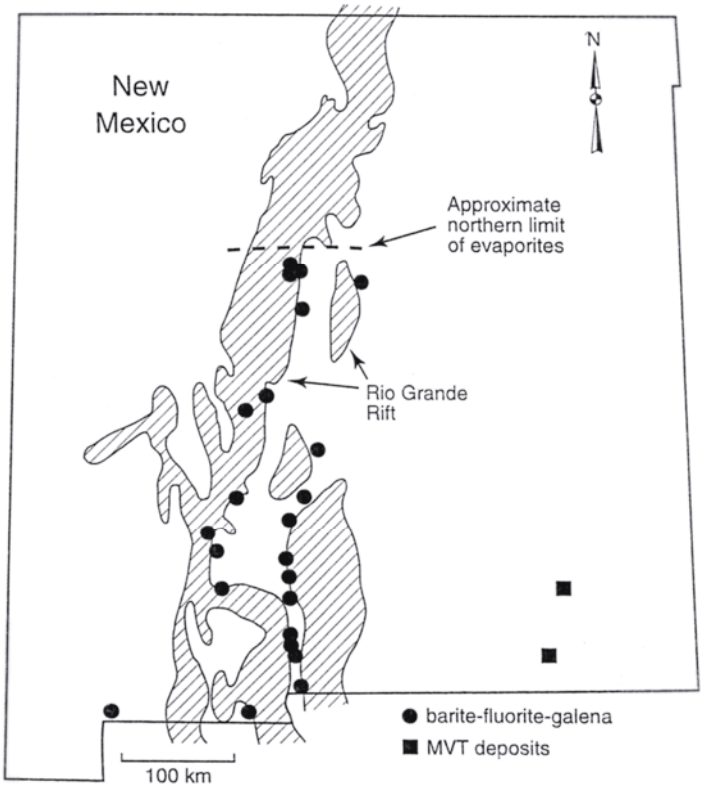

Figure 38. Map showing the distribution of Rio Grande Rift barite-fluorite-galena deposits. After McLemore and Lueth (1996).

to or within faults related to the Basin and Range. The barite deposits occur in the southern two-thirds of the rift, where there are evaporites in the section. Lead-isotope data indicate that the metals were derived from upper crustal sediments. Brines were ejected along fractures, faults, and unconformities. Fluid-inclusion homogenization temperatures and salinities vary widely. For the region as a whole, temperatures range from 95 to 341°C and salinities from 0 to 18 equivalent wt % NaCl; however, the ranges are typically more constrained within a given deposit. At the Hansonburg barite deposit, for example, homogenization temperatures range from 125-210°C and salinities from 10-18 wt % NaCl. McLemore and Lueth (1996) stated that there is no obvious association of the barite deposits with magmatic or volcanic activity, but some of the high homogenization temperatures must be related to high regional heat flow associated with extension of the rift.

Barite in late-stage thrust belts

Numerous studies have been done on barite in European orogenic belts, where the barite commonly exists in vein deposits (e.g. Burkhard 1973, Frimmel 1990, Frimmel and Papesch 1990). For example, Barbieri et al. (1982) documented the Sr geochemistry of late-orogenic epithermal barite deposits of late Triassic age in northern Tuscany, Italy. The $^{87}Sr/^{86}Sr$ values for barite range from 0.7101 to 0.7102, reflecting a large contribution of radiogenic ^{87}Sr derived from a continental source, identified by Barbieri et al. as the Verrucano Formation in the Paleozoic Basement. Phyllites of the Verrucano Formation of Paleozoic age have an initial isotopic composition of 0.7100. These metasediments also have Ba contents of up to 7000 ppm. Formation of barite is attributed to the interaction of ascending Ba-bearing solutions with sulfate-bearing evaporitic rocks. According to Barbieri et al. (1982) mineralization is genetically related to a granitic pluton that intruded sedimentary terranes during the late stage of the Apenninian orogeny. The high $^{87}Sr/^{86}Sr$ values rule out precipitation of barite either from coeval seawater Sr in which $^{87}Sr/^{86}Sr$ ranged from 0.7073 to 0.7090, or from waters that leached marine limestones of similar Sr isotopic composition. Additional Sr isotopic information on barite deposits in Sardinia and

Sicily is given by Barbieri et al. (1984, 1987).

Burkhard (1973, 1978), Frimmel (1990), and Frimmel and Papesch (1990) described the occurrence and composition of barites and celestines from the Alpine fold belt and Jura Mountains.

Dispersed cements and nodules of barite

Barite is common in minor quantities in proximity to marine evaporites, either as a direct replacement of gypsum or anhydrite or as a reaction product formed as a result of mixing of Ba-rich waters with waters derived from the dissolution of Ca sulfate. Variants on this theme are examined briefly in this section.

Dispersed barite cements, Colorado Plateau. Barite is dispersed over a 250 by 250 km area in Late Jurassic sandstones of the Morrison Formation, Colorado Plateau (Breit et al. 1990). Barite abundance ranges from <0.2 g/kg of rock to >4 g/kg. The region of highest concentration of barite coincides approximately with the areal extent of bedded evaporites in underlying Hermosa Formation of Pennsylvanian age, 2 km below. The $\delta^{34}S$ values of the barite range from 8 to 14 permil, similar to the isotopic composition of gypsum and anhydrite in the Hermosa. Breit et al. postulated that sulfate-bearing fluids moved up through faults, altered the overlying arkosic sandstone which contained Ba adsorbed on clays and in carbonate cements, and precipitated barite. Breit et al. (1990) found high Sr contents (2 to 6 wt %) in barite near faults, and low Sr (~0.4 wt %) in the western area of the Colorado Plateau where barite is sparse. In the area of the Dolores fault zone, in western Colorado, a principal feeder for ascending fluids, the combination of Sr content and Sr isotopic composition of the barite supports the hypothesis that sulfate-rich, high-Sr fluids having $^{87}Sr/^{86}Sr$ values close to 0.7100 mixed with a low-Sr source having an $^{87}Sr/^{86}Sr$ value of 0.7080 over a distance of nearly 12 km laterally from the fault zone.

Gluyas et al. (1997) documented, on the basis of the S and O isotopic composition of sulfates, the precipitation of barite and anhydrite cements in the southern North Sea, where inversion of normal faults promoted mixing of sulfate-rich waters derived from the Zechstein evaporites of the Upper Permian with Ba-rich waters derived from underlying Carboniferous coal measures. Precipitation of these cements has resulted in pervasive cementation of the Rotliegend Sandstone, causing degradation of reservoir quality and poor production of natural gas. Considerable volumes of fluid may have been involved. Savage has calculated that as much as from 2.6 km^3 to 26 km^3 of fluid containing from 5000 to 500 mg/L Ba is required to account for the barite cements found in the Amethyst Field, North Sea (David Savage, pers. comm. 2000).

Other examples of barite dispersed in sediments in the form of nodules and cements are provided by Bogoch et al. (1987), Khalaf and El Sayed (1989), Hill (1992), and Stamatakis and Hein (1993).

Salt domes. Barite is a minor, but common mineral in salt dome caprock. The concentration of Ba in most primary marine evaporites is low, and the Ba near salt has presumably been transported in from other sources. For example, Esch (1995) documented pseudomorphs of barite-celestine after anhydrite in the Eugene Island 128 salt dome, offshore Louisiana. Replacement by Sr appears to occur first, followed by conversion to nearly pure $BaSO_4$. Bedded sands surrounding the dome contain barite, among other diagenetic phases. Samuelson (1992) described pervasive barite in the caprock over the top of the Bolling salt dome in Texas. There is an abrupt boundary between the spatial distribution of barite and occurrence of hauerite (MnS_2), sphalerite, and galena, which probably marks a paleoredox front.

Table 4. Abundance of Ba and Sr in common igneous rocks and sediments.

Material	Ba, ppm	Sr, ppm	Ref. *	Material	Ba, ppm	Sr, ppm	Ref.*
Igneous Rocks				*Sediments*			
anorthosite	171	639	*1*	chert	450	250	*1*
kimberlite	847	906	*1*	phosphorite		600	*1*
gabbro	246	293	*1*	gypsum		850	*1*
diabase		175	*1*	anhydrite		2,000	*1*
diorite	714	472	*1*	halite		100	*1*
granodiorite	811	457	*1*	Holocene carbonate		6,000	*1*
granite	732	147	*1*	deep sea sediment		1,000	*1*
carbonatite	3,800	2,350	*1*	Paleozoic carbonate		400	*1*
tholeiite, ridge	15	124	*1*	carbonate	90		*1*
tholeiite, island	246	329	*1*	shale	546		*1*
alkali basalt	613		*1*	sandstone	316		*1*
basalt		393	*1*	pelagic clay, Atlantic	1,260		*1*
andesite	703	442	*1*	pelagic clay, Pacific	4,160		*1*
olivine basalt	613	626	*1*				
ultramafic rocks	1	6	*2*	shale	580	300	*2*
basalt	315	452	*2*	sandstone	10	20	*2*
high-Ca granite	420	440	*2*	carbonate	10	610	*2*
low-Ca granite	840	100	*2*	deep sea clay	2,300	180	*2*

*References: *1*= Puchelt (1972), Faure (1972); *2* = Faure (1998)

BARITE OF CONTINENTAL IGNEOUS AND IGNEOUS-HYDROTHERMAL ORIGIN

Barite has been described as an accessory mineral in carbonatites, dacites, and rhyolites. Barite is also common in a wide variety of metal deposits related to continental igneous activity. Some examples are reviewed here.

Carbonatites

Both barite and celestine are common in carbonatites, which have the highest average bulk Ba and Sr content of common igneous rocks (Table 4). Carbonatitic barite is late magmatic to more commonly hydrothermal (Heinrich and Vian 1967). Barite is most common in late-generation carbonatites that are mineralogically and texturally complex, particularly those containing REE carbonates and phosphate minerals, fluorite, sulfides, and quartz. Heinrich and Vian (1967) list 23 occurrences of carbonatitic barite, including those at Magnet Cove, Arkansas, the Arkansas River area of Fremont County, Colorado, and Mountain Pass, California.

The Sr/Ba ratio of barite in carbonatites varies widely, from 0.01 to 0.43. The barite is deposited relatively late, largely after magmatic calcite and dolomite, both of which are typically both rich in Ba and Sr. The deposition of barite was followed in a few deposits by deposition of celestine and strontianite. Carbonatitic celestine occurs, for example, at Mountain Pass, California; Nano-Vara, former USSR; and Tamazeret, Morocco. Heinrich and Vian (1967) proposed the following geochemical history of Ba and Sr during formation of a carbonatite: some Ba is removed early in the crystallization history by early K-silicates, such as feldspar and micas; there is then subsequent removal of large amounts of both Ba and Sr by carbonates with preferential removal of Sr. This increases the Ba/Sr ratio of the fluid. As barite with trace amounts of Sr is deposited, the Ba/Sr ratio is reversed, leading to late-stage precipitation of celestine.

Other magmatic examples

Fine grains of barite-celestine occur in feldspar porphyries in the Late Archean Kirkland Lake alkaline igneous province (Hattori 1989). Most grains contain from 15 to 20 mol % $BaSO_4$. The $\delta^{34}S$ values are low (6.0 to7.0 permil), reflecting a magmatic source of S, and coexisting sulfides are lower. Values for $^{87}Sr/^{86}Sr$ range from 0.70271 to 0.70403, consistent with the Late Archean age of the rocks. Estimated temperatures of formation exceed 400°C. Hattori concluded that barite-celestine formed instead of anhydrite because of low bulk Ca/Sr and Ca/Ba ratios of the host intrusive and the high P_{CO_2} of the fluid. Other examples include magmatic barite in vesicles in a rhyolite porphyry in Precambrian rocks at Pilot Knob, Missouri (Frank and Moynihan 1947), in a high-K dacite from Bulgaria (Marchev 1991), and in a diorite at Ratagain, Kintail district, Scotland (May et al. 1963).

Hydrothermal barite in the Cordilleran of the western United States

Small deposits of vein barite occur widely through much of the western United States, some in association with porphyry Cu and Cu-Mo deposits, with polymetallic vein deposits (Tooker 1991), and with W vein deposits (Worl 1991). Barite deposits in California lie in a belt that is spatially coincident with the Nevadan batholithic and metamorphic belt. The time of deposition of most of the barite occurrences has not yet been established. Weber (1963), however, has suggested that the deposits may be temporally and genetically related to batholithic intrusions.

In the Rocky Mountain region, barite is largely confined to Laramide orogenic belts. Although barite shows a preference for Tertiary uplifts in the easternmost belt, not all uplifts are mineralized. The tectonic setting of the western Laramide belt has been largely obscured by complex Cenozoic subsidence and faulting. Dunham and Hanor (1967) noted that barite deposits in Laramide Tertiary uplifts are preferentially spatially associated with areas characterized by diorite-granodiorite and latite-monzonite associations, and are generally absent from basaltic provinces, the extensive trachyte-phonolite and alkaline provinces, and the spilite-keratophyre province of the western United States. Barite deposits are not spatially associated with the most Ba-rich igneous rocks. Dunham and Hanor (1967) proposed that these relations may reflect the general geochemical behavior of Ba during the crystallization of melts of various bulk compositions.

If plagioclase is the first feldspar to crystallize from a melt, then Ba is enriched in the residual melt. As long as the melt becomes saturated with water before K-feldspar or biotite begin to crystallize, much of the Ba present in the initial melt should be available for incorporation into a fluid phase. On the other hand, if K-feldspar crystallizes early and before the melt becomes saturated with water then a large portion of Ba present in the initial melt will be captured in the earliest fraction of K-feldspar to crystallize. The behavior of barium during crystallization is thus dependent on the following characteristics of the initial bulk composition of the magma: (1) Ca-content of magma. High Ca is generally associated with high Na/K ratios. Hence plagioclase crystallizes before K-feldspar. (2) Na/K ratio. If the Na/K ratio is low and Ca is low, K-feldspar crystallizes early, capturing Ba. (3) Water content. Water content and confining pressure will determine the stage at which magma becomes saturated with water and a vapor phase is evolved.

In general, most deposits of barite associated with igneous activity in the western United States are small. Some of the deposits included by Dunham and Hanor (1967) in their analysis are probably not directly related to igneous activity. For example McLemore and Lueth (1996) stated that there is no obvious association of major barite deposits in New Mexico with magmatic or volcanic activity, although some of the high homogenization temperatures in fluid inclusions may be related to high regional heat

flow associated with the extension of the Rio Grande rift (Fig. 38) or with deep circulation of the ore-forming fluids. The metaliferous deposits in New Mexico that are associated with volcanic rocks include typical Pb-Zn-Cu-Ag Laramide skarn and replacement deposits formed by mixing of meteoric waters with local magmatic fluids derived from Late Cretaceous to Miocene calc-alkaline or Oligocene to Miocene alkaline igneous rocks. Barite in these deposits is only minor at best.

Barite from outer space

As cited by Chang et al. (1996), barite has been identified in chondritic interplanetary dust particles by Rietmejer (1990).

BEHAVIOR OF BARITE DURING WEATHERING, DIAGENESIS, AND METAMORPHISM

Barite is stable over a wide range of *P-T-X* and redox conditions. In the absence of a sink for sulfate, say by reduction to sulfide, barite is refractory during weathering, diagenesis, and metamorphism, although it can undergo recrystallization and remobilization. Barite is readily destroyed, however, in reducing environments. Some examples are presented below.

Formation of barite in soil environments

Barite has been identified as an authigenic mineral in some soils (Stoops and Zavaleta 1978, Darmody et al. 1989, Davis et al. 1990). Hanor et al. (1995) described the occurrence of authigenic barite in contaminated soils at a hazardous waste disposal site in southwestern Louisiana.

Subaerial weathering of barite

Not surprisingly, barite is highly resistant to subaerial weathering in oxidizing environments because of its low solubility. During weathering of carbonate-hosted MVT deposits, it is not uncommon to have near-surface host limestone and dolomite in temperate climates completely removed by dissolution, leaving behind a residuum of red clay, chert, and barite. In some instances, the concentration of residual barite is sufficient to create an economically-viable ore deposit. Well-known examples are found in southeastern Missouri, in the Cartersville District, Georgia, and in the Sweetwater District, Tennessee (Brobst 1994). Oxidation of coexisting sulfide minerals, such as pyrite, galena, and sphalerite, produces sulfuric acid, which not only enhances destruction of carbonate minerals but helps to stabilize barite through an increase in the activity of sulfate ion.

Some of the Ba dissolved during weathering may be preferentially adsorbed by clays making the Ba available for reprecipitation as secondary barite if a source of sulfate, for example by the oxidation of pyrite, is available. Strontium can be preferentially lost in the process (Hanor 1966).

Solution and reprecipitation of barite in diagenetic redox fronts

Barite is unstable in strongly reducing environments and can dissolve during diagenesis. For example, Bjorlykke and Griffin (1973) reported pseudomorphs of hyalophane after barite in carbonaceous Lower Ordovician shales of the Oslo region, Norway. Sedex deposits of massively bedded barite commonly contain beds of nodular or concretionary barite of early diagenetic origin. Examples include the Arkansas and Nevada bedded sedex deposits (Okita 1983, Graber and Chavetz 1990). The nodules typically contain pyrite as an accessory mineral, and it is likely that these nodules represent the reductive dissolution of barite by bacterial respiration and subsequent reprecipitation under more oxidizing conditions.

Clarke and Mosier (1989) described similar nodules in Devonian shale and mudstone in western Virginia. Instead of a submarine source for the Ba, however, they invoked a pelagic source, where settling particles of barite(?) were dissolved in anoxic bottom waters. Barite nodules then precipitated at the interface between the anoxic waters and overlying dysaerobic waters. The high S and O isotopic compositions of these nodules relative to Devonian seawater (Nuelle and Shelton 1986) reflect a reduced marine sulfate source.

Redox fronts have been reported in rapidly accumulating hemipelagic sediments containing high concentrations of organic matter. Torres et al. (1996b) determined that microcrystalline barite recovered by deep-sea drilling on the Peru Margin and in the Japan Sea is enriched in heavy sulfate up to a $\delta^{34}S$ value of +84 permil. Concentrations of barite of between 10 and 50% are locally present as layers within the cores. On the basis of depth profiles of dissolved barium and sulfate in interstitial pore waters, it was proposed by Torres et al. that barite remobilization is operating at several sites along the continental margins of the circum-Pacific. In the absence of advective flow, upward diffusion of Ba into the overlying sulfate-reducing zone leads to in-situ formation of barite where there is sufficient downward diffusion of sulfate to cause supersaturation. Torres et al. considered this barite to be an analog of barite in ancient rocks of similar lithology, including some sedex deposits. A diagenetic layer of barite was found by Gingele and Dahmke (1994) in sediments of the Angola slope, Africa, southwestern Atlantic ocean. McManus et al. (1998) further discuss the remobilization of Ba in continental margin sediments.

Unusually high concentrations of Ba have been reported from streams draining barite and witherite mining areas (Klein 1959). Bolze et al. (1974) showed through experiment that microbial reduction of barite can occur in systems where barite is the only source of sulfate available, and it was proposed that sulfate reduction may account for the increase in dissolved Ba content of streams that drain barite mining areas.

Behavior of barite during metamorphism

Recrystalzatin. During metamorphism barite commonly recrystallizes to equigranular textures resembling marble. There has been little study of chemical changes barite might undergo during diagenetic or metamorphic alteration. One exception is barite in the deposits at the Cartersville district, Georgia (Hanor 1966). Carbonate-hosted barite and surrounding sediments have been metamorphosed to amphibolite facies (Kesler and Kesler 1971) and inclusion-free grains of barite have been broken, rotated, and partly replaced by fine-grained, inclusion-rich, equigranular barite. The older barite contains from 7 to 9 mol % $SrSO_4$ (Hanor 1966). The younger barite, in contrast, contains 1.6 to 2.0 mol % $SrSO_4$. It is thus possible that Sr was preferentially removed during recrystallization.

Remblzatin. Massive barite occurs in layers and pods ranging in thickness from a few centimeters to up to 4 m thick in 40-km-long zone in quartz-sericite schist and schistose pyroclastic rocks of greenschist to amphibolite facies in the Battleground Formation, Kings Mountain belt, western South Carolina. Horton (1989) suggested the deposits may have originated from seafloor hot springs, but that barite was redistributed and locally concentrated in discordant veins during regional metamorphism.

Stallty in silcate systems. Potential reducing agents for barite at elevated *P-T* conditions include CH_4, H_2, CO, NH_3, and solid carbon. Calculations by Kritsotakis and von Platen (1980) showed that reduction of barite is favored by temperatures in excess of 200°C, low pH, and high gas fugacities. Despite the results of these theoretical calculations, there is abundant field evidence of the remarkable stability of barite during metamorphism.

As an example, metal-rich metasediments which include layers and lenses of massive barite, occur in graphitic quartz-muscovite schist of the Ben Eagach Schist of

Lower Cambrian age in Aberfeldy, Scotland (Coats et al. 1980, Fortey and Beddoe-Stephens 1982). The sequence was subjected to amphibolite grade metamorphism during the Caledonian orogeny. The area has been of interest because associated with the barite are barium silicates, among which are the Ba-K feldspars celsian (>80% cn) and hyalophane (25 to 40% cn), cymrite, $BaAl_2Si_2(O,OH)_8 \cdot H_2O$, and a barian muscovite.

The barite typically occurs as anhedral or polygonal to irregular crystals 1-2 mm across with textures reminiscent of marble. Coats et al. (1980) found no evidence for net input of Ba into the mineralized zone during metamorphism and no evidence for reaction between barite and other Ba-bearing rocks. The high thermal stability of barite and favorable f_{O2}-f_{S2} conditions could explain the survival of barite during amphibolite grade metamorphism

Coats et al. (1990) considered the deposit to be synsedimentary exhalative and to have formed by the introduction of Ba, Fe, Zn, Pb, Mn, and Si from a brine into a black-shale environment. Reaction produced an area of sulfide-rich carbonate deposition, precipitation of barite by mixing with sulfate-bearing seawater, and either the formation of a Ba-Al-Si rich gel under reducing conditions or the precipitation of silica with a Ba zeolite. Additional reaction of Ba-rich pore fluids with clay minerals on the periphery of the deposit formed barian mica. In contrast to many sedex deposits in which barite is the dominant Ba mineral, the barite at Aberfeldy represents only a minor amount of the total Ba present in the deposit. Barium feldspars and muscovite are the product of metamorphic crystallization of Ba-rich clays and or a Ba-bearing chert formed from a Ba-Al-Si gel.

Kribek et al. (1996) described barite-hyalophane sulfide ores in the Bohemian Massif, Czech Republic, which are metamorphosed equivalents of black-shale-hosted submarine exhalative deposits. Despite high temperatures of metamorphism, 600-700°C, it is possible to reconstruct environments of both formation and metamorphism. Kribek et al. (1996) compared these deposits to submarine hydrothermal deposits of the Guaymas basin, Gulf of California, where barite, carbonates, and silica have been deposited in organic-rich sediments (Scott 1997).

CELESTINE IN SEDIMENTARY ENVIRONMENTS

The number of occurrences and modes of occurrence of celestine is far more limited than those of barite. Because of the strong preferential partitioning of Ba into the barite-celestine solid solution, celestine can form only where some process discriminates against the co-precipitation of barium or from sources that have extremely high Sr/Ba ratios. We examine here examples of both: the biological precipitation of celestine in which the organisms involved discriminate against Ba and sedimentary environments that produce fluids with high Sr/Ba ratios.

Pelagic celestine

Bernstein et al. (1992) presented an excellent discussion of the marine production of celestine by Acantharians, from which much of the following description is based. Acantharians are marine planktonic protozoans and are the only marine organism that uses $SrSO_4$ as a major structural component. Other marine organisms apparently can contain celestine, because Bernstein et al. (1992) observed numerous $SrSO_4$ crystals 10 μm long inside a colonial radiolarian from the family *Collosphaeridae*. Hollande and Martoja (1974) and Hughes et al. (1989) also described celestine occurring in radiolaria.

Acantharian life cycle. Both the skeletons (Wilcock et al. 1988) and cysts of acantharians consist of celestine. Prior to reproduction certain acantharians resorb their spines and undergo active $SrSO_4$ metabolism to produce a $SrSO_4$ cyst that surrounds the acantharian cytoplasm. The cytoplasm within the cyst eventually differentiates into

numerous flagellated spores or gametes approximately 5 μm long. These subsequently exit the cyst through a pore. Bernstein et al. (1992) proposed that each spore/gamete contains one or more $SrSO_4$ granules, which possibly serve as nuclei for subsequent skeletal growth or buoyancy adjustment.

Acantharians are low on the food chain, and one mode of their demise is ingestion by other zooplankton. Celestine remains have apparently not been reported in either zooplankton gut contents or fecal material. However, siliceous remains are common. Bernstein et al. have speculated that acantharian skeletons and cysts dissolve rapidly within the predator after ingestion. Fecal material would then contain fluid having elevated concentrations of Sr, Ba, and SO_4, which might serve as a microenvironment for precipitating barite.

Abundance and fate in water column. Acantharians and their cysts are present in most of the world's oceans, and the acantharians are frequently more abundant in the euphotic zone than either radiolaria or pelagic foraminifera. Bernstein et al. (1992) found that the greater than 63 μm size fraction of particulate matter in the Sargasso Sea was composed almost exclusively of acantharian cysts. The <63 μm fraction contained numerous discrete particles of $SrSO_4$ approximately 1 to 3 μm in length which may be fragments of spores or gametes. Beers et al. (1975) reported 7200-16,000 celestine fragments/m^3. Sea water is undersaturated with respect to celestine, and rapid dissolution of acantharian celestine with depth limits the export of Sr beyond intermediate depths. The Sr released is thus rapidly recycled.

Composition. The reported molar Ba/Sr ratio in acantharians ranges from 3×10^{-3} to 4×10^{-3} (Bernstein et al. 1992). These ratios are approximately an order of magnitude higher than the surface seawater molar ratio of 3.3×10^{-4}. Because Sr/Cl depletions in upper ocean are as large as 5%, there is thus the possibility of significant acantharia-mediated Ba depletion in surface waters as well (Bernstein et al. 1992).

Carbonate sediments

Carbonate sediments of pelagic origin consist primarily of calcitic forams and coccoliths and aragonitic pteropods. These sediments thus contain several times less Sr than typical shallow water marine carbonates, where Sr-enriched aragonite is commonly the predominant carbonate. Nonetheless, the submarine dissolution of pelagic carbonates and precipitation of inorganic calcite do release significant Sr into pore fluids (Sayles and Manheim 1975). Rates of release are often slow because of low rates of reaction, low rates of accumulation, or because of Sr uptake by underlying basement rocks. Where carbonate accumulation rates are high, a higher fraction of reactive carbonate reaches the seafloor. Under some conditions, dissolved interstitial Sr/Ca reaches a plateau value that is approximately 25 times the Sr/Ca ratio of the biogenic calcite (Baker and Bloomer 1988)

Baker and Bloomer (1988) have described celestine nodules of unspecified size and morphology recovered at several sites on DSDP Leg 90 from the Lord Howe Rise in the southwest Pacific. The host sediments are predominately very pure calcareous oozes and chalks of Middle Miocene to Early Pliocene age which have undergone relatively rapid burial diagenesis. This has resulted in the expulsion of Sr from biogenic calcite into the ambient interstitial waters. As a result of microbial sulfate reduction, dissolved sulfate decreases down-core. The down-core increase in Sr, however, is proportionally higher than the sulfate decrease, and celestine precipitates at depths of approximately 100 m below the seafloor at each of four sites. The nodular celestine contains 4 to 8 mol % $BaSO_4$, 2-6 mol % $CaSO_4$, 1100-2,600 ppm Al and 400-750 ppm K. The isotopic composition of this celestine has not yet been determined. Calculations of saturation state showed that the porewaters are saturated with respect to celestine and are undersaturated with respect to

barite.

According to Kinsman (1969), celestine is a common early diagenetic mineral of coastal sabkas and is abundant in areas of intense dolomitization. The celestine forms during replacement of aragonite (7000-8000 ppm Sr) by dolomite (600-700 ppm Sr). Examples include the Persian Gulf, Baja California, and shallow lagoons in southwestern Australia.

Celestine and salt domes. Celestine is a common accessory mineral in the caprocks of salt domes (Saunders et al. 1988), where it can exist as a replacement of anhydrite or gypsum. Esch (1995), in a study of diagenesis at the salt-sediment interface in an offshore Louisiana salt dome, observed celestine replacing anhydrite within a matrix of halite. Some of the celestine pseudomorphs are partly replaced by barite.

Celestine in coastal carbonate-evaporite sequences

General features. The largest and most massive occurrences of celestine are invariably in coastal carbonates and evaporites, usually with up-dip or overlying clastics (Scholle et al. 1990). Host rocks range in age from Silurian to Miocene. There is variable evidence of associated hydrothermal activity. Lower Permian deposits in the former USSR and Cretaceous deposits in Mexico have associated barite, but most of others do not. Six of the largest known celestine deposits have proven reserves of 0.5 to 8 Mt. These include (Scholle et al. 1990): Montevive, Spain; Molkabade, Iran; San Augustin, Mexico; Cifteagil, Turkey; Yate, England (Nickless et al. 1975, Wood and Shaw 1976); and Lake Enon, Nova Scotia, Canada (Andrews and Collins 1991). Current principal producers are Spain, Turkey, Mexico, Iran, and the United Kingdom.

Example: East Greenland. Scholle et al. (1990) provided an instructive description of a major celestine deposit in central eastern Greenland. An estimated 25-50 Mt of celestine-bearing sediment having an average grade of 50-60% $SrSO_4$ occur in Upper Permian algally laminated limestones, limestone breccias, and karstified units that surround an isolated gypsum deposit of probable salina origin. This deposit has not yet been mined because of its remote location.

Deposition of the host sediments took place in shallow subtidal to supratidal environments including evaporitic hypersaline lagoons and algal shoals. The main occurrences of celestine are confined to limestone in the proximity of the evaporite lagoon. Here, celestine replaces calcite, dolomite, and gypsum in algally laminated sediment and as replacement of algally laminated limestone clasts as cements, veins, and cave fillings in overlying conglomerate and karst sediments. Celestine almost always appears to be the last stage of replacement of rocks that are dominated by early diagenetic features.

Strontium isotopic ratios of the celestine range from 0.7130 to 0.7137, and all celestine formed roughly at same time and from same pore fluids. Seawater coeval with the host sediments had an $^{87}Sr/^{86}Sr$ ratio of 0.7068 to 0.7070, and the highly radiogenic Sr cannot be the result of diagenetic alteration of associated aragonitic limestone. Gypsum also shows slight enrichment in radiogenic Sr (0.7074 to 0.7082) relative to contemporaneous seawater values, possibly the result of diagenetic alteration.

The $\delta^{34}S$ isotopic composition of celestine is 15.0 to 19.6 permil and is considerably heavier than that of the spatially associated gypsum deposits, which range from 9.1 to 11.4 permil. These values seem to be beyond the range of the effects of simple isotopic fractionation expected during dissolution of gypsum and precipitation of celestine. Isotopically heavier S has also been noted in Mexican celestine deposits by Kesler and Jones (1981), who invoked possible inorganic fractionation or limited enrichment of gypsum sulfate by bacterial reduction. Halas and Mioduchowski (1978) have invoked

bacterial reduction of sulfate in similar celestine deposits.

Scholle et al. (1990) call on precipitation of celestine by mixing of near-surface meteoric waters which had been involved in calcitization or dissolution of evaporites, and thus were rich in sulfate, with rising basinal waters rich in Sr. Such a mechanism was also invoked by Kesler and Jones to explain the more radiogenic Mexican deposits. Other workers have invoked the continental groundwater alteration of limestones to supply Sr.

A radically different mechanism for forming celestine deposits was proposed by Müller (1962), who called on direct evaporation of seawater for the origin of the Himmelte West celestine deposit of Germany, which contains several Mt of celestine. According to Muller, saturation with respect to celestine is reached during progressive evaporation of sea water near the boundary between precipitation of carbonates and gypsum. Brodtkorb et al. (1982) discussed other examples of the possible synsedimentary precipitation of celestine by evaporation of seawater. The difficulty here would seem to be accounting for rock celestine/gypsum ratios significantly higher than seawater Sr/Ca ratios. Additional information on celestine deposits is provided by Carlson (1987), Kushnir (1986). Mitchell and Pharr (1961), Brodtkorb (1989), and Ramos and Brodtkorb (1989, 1990).

Sedimentary venues for forming waters of high Sr/Ba ratios and celestine deposits. The association of large celestine deposits with coastal carbonate-evaporite sequences most likely reflects the difference in geochemical behavior of Sr and Ba in subsurface fluids. As noted earlier in this chapter, the concentration of Sr in subsurface sedimentary fluids is silicate/carbonate-buffered such that the concentration of Sr increases exponentially with increases in salinity. The concentration of Ba, in contrast, is controlled by the concentration of sulfate. The fluids of highest Sr/Ba ratio, and thus those most likely to form celestine rather than barite, are those of high salinity and high sulfate relative to Ba (Figs. 9, 10). Such waters could be produced in coastal evaporitic settings where residual evaporated seawater is saline with appreciable levels of dissolved sulfate. Such waters, if refluxed into underlying sediments, would leach appreciable Sr as the fluids attempted to achieve equilibrium with the host sediments. If such fluids were then discharged back up into shallow gypsum or anhydrite beds, the precipitation of celestine could result. As noted earlier, decreasing temperature and pressure favors celestine stability over anhydrite (Fig. 13).

ENVIRONMENTAL ASPECTS

Barium in potable water supplies

Barium toxicity. High levels of Ba in the human body are potentially toxic. According to Gregus and Klaassen (1996), Ba^{2+} interferes with signaling mechanisms for neurotransmitters by inhibiting Ca^{2+}-activated K^{+} channels in cell membranes. This is accompanied by potentially lethal neuroexcitatory and spasmodic effects. Poisoning associated with ingestion of soluble barium salts has resulted in gastroenteritis, muscular paralysis, decreased pulse rate, and ventricular fibrillation and extra-systoles (Goyer 1974). Stokinger and Woodward (1958) calculated a safe threshold of 2.0 mg/L of dissolved Ba in drinking water on the basis of threshold limiting values in industrial atmospheres, an estimate of the amount absorbed into the blood stream, and daily consumption of two liters of water. However, to provide a safety factor and to allow for possible accumulation in the body, a limit of 1.0 mg/L was initially recommended. The limit has recently been reset to 2.0 mg/L (Fig. 7).

Barium sulfate is sufficiently insoluble that it is routinely used as a radioplaque aid to X-ray diagnosis. Occupational poisoning by Ba is uncommon, but benign pneumoconiosis (baritosis) may result from inhalation of Ba sulfate (Goyer 1974). Baritosis is not

incapacitating and is usually reversible with cessation of exposure.

Strontium apparently does not have the same toxic effects as Ba, and in fact, strontium chloride is routinely used to desensitize teeth in humans. More serious is the potential uptake of radioactive ^{90}Sr by bone. This isotope has a half-life of 21.8 years, however, and has not been reported from naturally occurring celestine deposits, although it could coprecipitate with recent barite.

Barium in drinking water and in municipal wastes. Buffering by barite is an important control on the concentration of Ba in drinking-water supplies (Fig. 7). Dissolved Ba in concentrations of up to 18 mg/L occur in portions of freshwater aquifers of northeastern Illinois (Gilkeson et al. 1981). The area is anomalously depleted in dissolved sulfate as a result of reduction under anaerobic conditions. The reduction of sulfate is accompanied by the presence of dissolved H_2S, increased alkalinity and enrichment of residual sulfate in ^{34}S.

Sewage sludge in Florence, Italy, contains high levels of total Ba (0.4 to 1.6 mg/g) as a result of disposal of barite in hospital wastes (Baldi et al. 1996). Under the reducing conditions, the barite is solubilized and the Ba is partly reprecipitated, probably as witherite ($BaCO_3$) and as BaS.

Barite and the uranium industry

Waters from U mine wastes typically contain an array of radioactive nuclides, including ^{230}Th, ^{226}Ra, ^{210}Pb, and ^{210}Po. According to Paige et al. (1998) ^{226}Ra is the radionuclide responsible for more than 75% of the radioactivity originally present in the ore. The precipitation and the dissolution of Ra-bearing barite are controlling factors in the behavior and mobility of Ra in uraniferous mine wastes. Precipitation of Ba-Pb sulfates on mica and quartz grains is a process which influences the distribution and mobility of ^{210}Pb (Paige et al. 1998).

Beard et al. (1980) described the use of $BaCl_2$ in some U milling operations in Colorado, New Mexico, and Utah to reduce the Ra content of mine and processing wastewaters by coprecipitation with barite. Removal efficiencies ranged from 25 to 99.98% of the dissolved Ra originally present.

Margaritz et al. (1990) used the distribution of dissolved Ba and Sr as proxies of radioactive isotopes to study the potential behavior of nuclear wastes disposed of in the unsaturated zone and/or near the water table. They found a complex distribution of Ba and Sr and a transition from waters saturated to undersaturated with respect to barite over a vertical interval of only 50 cm.

Problems related to oil and gas production

Problems with scaling by barite. Clogging and plugging of production casing by barite scale is a common phenomenon in the oil and gas industry (Weintritt and Cowan 1967). Barite precipitation can be induced during water-flooding operations, particularly if seawater, which contains high concentrations of sulfate, mixes with native formation waters containing high concentrations of Ba. Other mechanisms for precipitating barite include mixing of native formation waters of varying Ba and sulfate concentrations and decreases in temperature and pressure that accompany transport of fluid to the surface. There has been considerable interest in the development of techniques for inhibiting the formation of barite scale, and much of the work done on nucleation and the kinetics of crystal growth of barite (Ali and Nancollas, this volume) stems from these problems.

Radioactive barite scale. Water produced from oil, gas, and geothermal wells can have radioactivity levels approaching those in U mill tailings (Fisher 1995, 1998). The

chief contributors to this naturally occurring radioactive material (NORM) are ^{226}Ra and ^{228}Ra, which are ultimately derived from the decay of ^{238}U and ^{232}Th, respectively (Fig. 20) and which occur as Ra^{2+} in solution. Because of the similarity in ionic radius and electronegativity to Ba^{2+}, some Ra^{2+} is removed from aqueous solution during the precipitation of barite scale in oil field production and processing equipment. In an extensive study of NORM wastes in the hydrocarbon producing fields in Texas, Fisher (1995, 1998) found that ^{226}Ra levels typically ranged from approximately one to several thousand picocuries per liter. The levels of ^{228}Ra are comparable. Highest dissolved Ra values were found in waters whose salinity exceeded 35,000 mg/L or were derived from reservoirs in which volcanic rock fragments are abundant. Well scale contained from 600 to 2700 pCi/g ^{226}Ra and 400 to 4000 pCi/g ^{232}Th. Radium activity correlates with the abundance of Ba in the well scale. Pardue and Guo (1998) reported on the biochemistry of ^{226}Ra in contaminated bottom sediments in oil-field waste pits.

Produced water Produced water released into the environment from oil and gas operations is likely to have substantial concentrations of dissolved Ba and Ra. Mixing of produced waters with ambient groundwaters containing sulfate has the potential for coprecipitating Ba and Ra as radioactive barite and thus creating local areas of elevated radioactivity and radon emission (Fig. 20).

Disposal of barite drilling muds. Dial and Huff (1989) reported levels of dissolved Ba above background in water wells spatially associated with oil-field activities in Ascension Parish, Louisiana. Maximum levels of dissolved Ba, however, were 800 μg/L. These authors cite reports of contamination within two years of when drilling operations began. It is not known whether the increased Ba was due to disposal of produced waters high in Ba or from dissolution of barite drilling muds or cuttings.

Because of the current low cost of barite drilling muds and the cost of separating barite from rock fragments in the cuttings produced by drilling, much barite used in drilling is not recycled. Most wastes in offshore environments are discharged directly into seawater.

In an extensive U.S. Environmental Protection Agency study of barite drilling mud disposal pits at a site in south Louisiana the sole potential risk identified during the site assessment was to future residential children who might ingest the barite wastes on a regular basis. Because potential risks associated with agricultural use of the property were not quantified, it was determined that the property cannot be used for farming or grazing purposes. This means that future use of the property is restricted to industrial purposes.

An example of a "bad rap" for barite

Many scientists and some of the general public are aware of the potential toxicity of Ba. Many are also aware that barite is used in oil and gas operations. Fewer are aware, however, that Ba is between the 12th or 15th most abundant element in the Earth's crust, and that the presence of Ba in rocks and sediments at levels of several hundred ppm is not surprising.

Isphording (1982) provides an instructive example of a case where the public, the oil industry, and state and Federal governments became involved in protracted controversy resulting from the discovery of Ba at levels of several hundred ppm in offshore sediments near the mouth of Mobile Bay, Alabama. This Ba was attributed by some to spillage of barite drilling mud used in offshore oil and gas operations, and concern was raised regarding pollution, wetlands damage, and the destruction of marine life. Subsequent determination (Isphording 1982) of the partitioning of Ba between various minerals of the sediment, however, showed the Ba occurred associated with clay minerals and as a trace element in biogenic carbonate shells. No barite was detected by X-ray diffraction.

CONCLUDING REMARKS

The author's Ph.D. thesis was entitled "The Origin of Barite" (Hanor 1966). The conclusions of that work were based on thermodynamic information available at the time, a new field-sampling and geochemical study of barite deposits in the midwestern and eastern United States, and a synthesis and re-interpretation of the available literature on barite deposits in North America. Because of the major advances in geology which have taken place since 1966, it is now possible in the year 2000 to make much more definitive interpretations regarding the diverse origins of barite and celestine.

These advances include the development of conceptual models and quantitative techniques in plate tectonics, deep-basin hydrogeology, Sr-isotope systematics, compositional systematics and thermodynamics of subsurface brines, ore-mineral age dating, and marine geochemistry, and the direct observation and sampling of deep-sea hydrothermal sites. Critically important also has been the general acceptance among geologists since the mid-1960s of the basic concepts of synsedimentary ore deposition. It is hoped that this chapter has provided an overview of current thought on the properties, occurrence, and origin of barite and celestine as of the year 2000.

Some key areas for future work on the occurrence and origin of barite and celestine include: the conditions under which Ba and Sr are leached from shallow crustal rocks and sediments, the generation and expulsion of barite- and celestine-forming fluids in extensional terranes, the potential significance of the occurrence of major concentrations of barite and celestine as paleo-focal points for discharge of deep fluids, mass-balance constraints to determine much fluid was involved, the factors that result in metal-rich and or metal-poor barite deposits, the mechanisms and rates of precipitation of pelagic barite today and in the geological past, importance of redox fronts in concentrating massive quantities of barite, what Precambrian barite and celestine occurrences can tell us about the early history of the Earth, the role of barite equilibria in determining the concentrations of Ba and Ra in oil and gas exploration and production sites, and the development of new exploration strategies for the location of additional deposits of these economically important minerals.

ACKNOWLEDGMENTS

I thank editors Charlie Alpers and John Jambor and external reviewers George Breit, Christophe Monnin, and Fred DeHairs for their helpful reviews of this chapter. My professional interest in barite goes back to my graduate student days at Harvard, where Ray Siever, Ulrich Peterson, Cliff Frondel, and Bob Garrels helped to guide me along. Further insight was provided by Kurt Boström, Gustav Arrhenius, and Tom Church during a subsequent NSF postdoctoral fellowship at Scripps. My LSU faculty colleague, Lui Chan, and my former graduate students Larry Baria, Larry Bunting, Pat Okita, Kevin Howard, Karen Graber, and Lee Esch have helped me sustain an active interest in heavy divalent cations during my tenure at Louisiana State University. My more recent undergraduate and graduate student research assistants, Kathleen (KT) Moran, Katie Cooper, Romie Coronado, and Kimberly Noble, helped me track down references and put things in order during the preparation of this paper. The recent work on fluids in sedimentary basins reported on here was supported in part by NSF grants EAR 98-05446 and EAR 98-05459.

It is a pleasure to be able to dedicate this chapter to my wife, Leslie, who has been with me since the beginning of all of this.

REFERENCES

Andrew JE, Funnel BM, Jickells TD, Shackleton NJ, Swallow JE, Williams AC, Young KA (1990) Preliminary assessment of cyclic variations in foraminifers, barite, and cadmium/calcium ratios in

early Pleistocene sediments from Hole 709C (equatorial Indian ocean). Proc ocean Drilling Program, Scientific Results 115:611-619
Andrews PRA, Collins RK (1991) Celestine in Canada. Can Inst Mining Metall Bull 84:36-39
Aquilina L, Dia AN, Boulegue J, Bourgois J, Fouillac AM (1997) Massive barite deposits in the convergent margin off Peru: Implications for fluid circulation. Geochim Cosmochim Acta 61:1233-1245
Arrhenius G (1952) Sediment cores from the East Pacific. Rept Swedish Deep Sea Exp, 1947-48, 5:1-120
Arrhenius G (1963) Pelagic sediments. *In* The Sea, vol 3. MN Hill (Ed) Interscience, New York, p 655-727
Arrhenius G, Bonatti H (1965) Neptunism and vulcanism in the ocean. *In* Progress in Oceanography. M Sears (Ed) Pergamon Press, New York, p 7-22
Arrhenius G, Bramlette M, Picciotto E (1957) Localization of radioactive and stable heavy nuclides in ocean sediments. Nature 180:5-86
Baker PA, Bloomer SH (1988) The origin of celestite in deep-sea carbonate sediments. Geochim Cosmochim Acta 52:335-339
Baldi F, Pepi M, Burrini D, Kniewald G, Scali D, Lanciotti E (1996) Dissolution of barium from barite in sewage sludges and cultures of *Desulfovibrio desulficans*. Appl Environ Microbiol 62:2398-2404
Barbieri M, Masi U, Tolomeo L (1982) Strontium geochemistry in the epithermal barite deposits from the Apuan Alps (Northern Tuscany, Italy). Chem Geol 35:351-356
Barbieri M, Masi U, Tolomeo L (1984) Strontium geochemical evidence for the origin of the barite deposits from Sardinia, Italy. Econ Geol 79:1360-1365
Barbieri M, Ballanca A, Neri R, Tolomeo L (1987) Use of strontium isotopes to determine the sources of hydrothermal fluorite and barite from northwestern Sicily (Italy). Chem Geol 66:273-278
Barley ME (1992) A review of Archean volcanic-hosted massive sulfide and sulfate mineralization in Western Australia. Econ Geol 87:855-872
Bautier M, Monnin C, Fruh-Green G, Karpoff AM (in press) Fluid-sediment interactions related to hydrothermal circulation in the Eastern flank of the Juan de Fuca ridge. Chem Geol
Beard, HR Salisbury, HB and Shirts, MB (1980) Absorption of radium and thorium from New Mexico uranium mill tailing solutions. US Bureau of Mines Rept Inv 8463, 14 p
Beers JR, Reid FMH, Stewart J (1975) Microplankton of the north Pacific central gyre. Population structure and abundance, June 1973. Int'l Rev Hydrobiology 60:607-638
Bernstein RE, Byrne RH, Betzer PR, Greco AM (1992) Morphologies and transformations of celestine in seawater: The role of acantharians in strontium and barium geochemistry. Geochim Cosmochim Acta 56:3273-3279
Bernstein RE, Byrne RH, Schijf J (1998) Acantharians: A missing link in the oceanic biogeochemistry of barium. Deep-Sea Res 45:491-505
Bertine KK, Keene JB (1975) Submarine barite-opal rocks of hydrothermal origin. Nature 188:150-152
Bertram MA, Cowen JP (1997) Morphological and compositional evidence for biotic precipitation of marine barite. J Mar Res 55:577-593
Bishop JKB (1988) The barite-opal-organic carbon association in oceanic particulate matter. Nature 332:341-343.
Bjorlykke KO, Griffin WL (1973) Barium feldspars in Ordovician sediments, Oslo region, Norway. J Sed Pet 43:461-465
Blount CW (1977) Barite solubilities and the thermodynamic quantities up to 300 degrees Celsius and 1400 bars. Am Mineral 62:942-957
Bogoch R, Buchbinder B, Nielsen H (1987) Petrography, geochemistry, and evolution of barite concretions in Eocene pelagic chalks from Israel. J Sed Pet 57:522-529
Bolze CE, Malone PG, Smith MJ (1974) Microbial mobilization of barite. Chem Geol 13:141-143
Borole DV, Somayajulu (1977) Radium and lead-210 in marine barite. Marine Chem 5:291-296
Bosbach D, Haal C, Putnis A (1998) Mineral Precipitation and dissolution in aqueous solution: in-situ microscopic observation on barite (001) with atomic force microscopy. Chem Geol 151:143-160
Boström K, Peterson MNA (1966) Precipitates from hydrothermal exhalations on the East Pacific Rise. Econ Geol 61:1258-1265
Boström K, Frazer J, Blankenburg J (1967) Subsolidus phase relations and lattice constants in the system $BaSO_4$-$SrSO_4$-$PbSO_4$. Arkiv Mineral Geol 4:477-485
Boström K, Joensuu O, Moore C, Bostrom B, Dalziel M, Horowits A (1973) Geochemistry of barium in pelagic sediments. Lithos 6:159-174
Bowers TS, Jackson KJ, Helgeson HC (1984) Equilibrium Activity Diagrams. Springer-Verlag, Berlin, 397 p
Breit G, Goldhaber MB, Martin B, Shawe D, Simmons EC (1990) Authigenic barite as an indicator of fluid movement through sandstones within the Colorado Plateau**.** J Sed Pet 60:884-896
Brobst DA (1994) Barium minerals. *In* Industrial Minerals and Rocks (6th ed.). DD Carr (Ed) Soc Mining Metall Explor, Littleton, Colorado, p 125-134

Brodtkorb de MK (1989) Celestite: worldwide classical ore fields. *In* Nonmetalliferous Stratabound Ore Fields. MK de Brodtkorb (Ed) Van Nostrand, New York, p 17-39
Brodtkorb de MK, Ramos V, Barbieri M, Ametrano S (1982) The evaporitic celestite-barite deposits of Neuquen, Argentina. Mineral Dep 17:423-426
Brook AJ, Fotheringham A, Bradly J, Jenkins A (1980) Barium accumulation by desmids of the genus *Closterium* (Zygnemaphyceae). British Phycology J 15:261-264
Brook AJ, Grime GW, Watt F (1988) A study of barium accumulation in desmids using the Oxford scanning proton microprobe (SPM). Nuclear Instr Meth Physics Res B30:372-377
Brower E, Renault J (1971) Solubility and enthalpy of barium-strontium sulfate solid solution series. New Mexico Bureau of Mines and Mineral Resources Circular 116, 21 p
Buick R (1990) Microfossil recognition in Archean rocks: an appraisal of spheroids and filaments from a 3500 m.y. old chert barite unit at North Pole, Western Australia. Palaios 5:411-459
Buick R, Dunlop JSR (1990) Evaporitic Sediments of Early Archean age from the Warrawoona Group, Western Australia. Sedimentology 37:247-278
Burke WH, Denison RE, Hetherington EA, Koepnik RB, Nelson HF, Otto JB (1982) Variation of seawater $^{87}Sr/^{86}Sr$ throughout Phanerozoic time. Geology 10:516-519
Burkhard A (1973) Optische und röntgenographische Untersuchungen am System $BaSO_4$-$SrSO_4$ (Baryt-Celestin). Schweiz mineral petrogr Mitt 53:185-197
Burkhard A (1978) Baryt-Celestin und ihre Mischkristalle aus Schweizer Alpen und Jura. Schweiz mineral petrogr Mitt 58:1-95
Buschendorf F, Nielsen H, Puchelt H, Ricke W (1963) Schwefel-isotopen-Untersuchen am Pyrit-Sphalerit-Baryt-Lager, Meggen/Lenne (Deutschland) und an verschiedenen Devon-Evaporiten. Geochim Cosmochim Acta 27:501-523
Cameron EM, Hattori K (1985) The Hemlo gold deposit: A geochemical and isotopic study. Geochim Cosmochim Acta 49:2041-2050
Carlson EH (1987) Celestine replacements of evaporites. Sed Geol 54:93-112
Carroll JL, Falkner KK, Brown ET, Moore WS (1993) The role of the Ganges-Brahmaputra mixing zone in supplying Ba and ^{226}Ra to the Bay of Bengal. Geochim Cosmochim Acta 57:2981-2990
Cathles LM (1997) Thermal aspects of ore formation. *In* Geochemistry of Hydrothermal Ore Deposits (3rd Edn) HL Barnes (Ed) Wiley, New York, p 191-228
Cecile MP, Goodfellow WD, Jones LD, Krouse HR, Shakur MA (1984) Origin of radioactive sinter, Flybye springs, Northwest Territories, Canada. Can J Earth Sci 21:383-395
Cecile MP, Shakur MA, Krouse HR (1983) The isotopic composition of western Canadian barites and the possible derivation of oceanic sulphate $\delta^{34}S$ and $\delta^{18}O$ age curves. Can J Earth Sci 20:1528-35
Chagon A, St.-Antoine P, Savard MM, Heroux Y (1998) Impact of Pb-Zn sulfide precipitation on the clay mineral assemblage in the Gays River deposit, Nova Scotia, Canada Econ Geol 93:779-792
Chan LH, Edmond JH (1987) Barium. *In* GEOSECS Atlantic, Pacific and Indian Ocean Expeditions, Vol 7, Shore-based Data and Graphics. H Ostlund, H Craig, W Broecker, D Spencer D (Eds) Nat'l Sci Fdn, Washington, DC, p 13
Chan LH, Drummond D, Edmond JH, Grant B (1977) On the barium data from the Atlantic GEOSECS expedition. Deep Sea Res 24:613-649
Chang LLY, Howie RA, Zussman J (1996) Rock-forming Minerals, Second Edition, Vol 5B, Non-silicates: Sulfate, Carbonates, Phosphates, Halides. Longman Group, Harlow, UK, 383 p
Chester R (1990) Marine Geochemistry. Chapman & Hall, London, 698 p
Chow TJ, Goldberg ED (1960) On the marine geochemistry of barium. Geochim Cosmochim Acta 20:192-198
Christy AG, Putnis A (1993) The kinetics of barite dissolution and the precipitation in water and sodium chloride brines at 44-85 degrees Celsius. Geochim Cosmochim Acta 57:2161-2168
Church TM (1970) Marine Barite. PhD dissertation, University of California San Diego, 100 p
Church TM (1979) Marine barite. Rev Mineral 6:175-209
Church TM, Bernat M (1972) Thorium and uranium in marine barite. Earth Planet Sci Lett 14:139-144
Church TM, Wolgemuth K (1972) Marine barite saturation. Earth Planet Sci Lett 15:35-44
Clark SHB, Mosier EL (1989) Barite nodules in Devonian shale and mudstone of western Virginia. US Geol Survey Bull 1880, 30 p
Clark SHB, Gallagher MJ, Poole FG (1990) World barite resources: A review of recent production patterns and genetic classification. Trans Inst Mining Metall B-Appl 99:B125-B132
Claypool GE, Holser, WT, Kaplan, IR, Sakai, H, Zak, I (1980) The age curves of sulfur and oxygen in marine sulfate and their mutual interpretations. Chem Geol 28:199-260
Coats JS, Smith CG, Fortey NJ, Gallegher MJ, May F, McCourt WJ (1980) Strata-bound barium-zinc mineralization in Dalradian schist near Aberfeldy, Scotland. Trans Inst Mining Metall 89:B110-B122

Coffey M, Dehairs F, Collette O, Luther G, Church T, Jickells T (1997) The behaviour of dissolved barium in estuaries. Estuarine Coastal Shelf Sci 45:113-121

Connolly CA, Walter LM, Baadsgaard H, and Longstaffe FJ (1990) Origin and evolution of formation waters, Alberta Basin, Western Canada sedimentary basin. Appl Geochem 5:397-413

Cooke DR, Bull SW, Donovan S, Rogers JR (1998) K-metasomatism and the base metal depletion in volcanic rocks from the McArthur basin, Northern Territory—implications for base metal mineralization. Econ Geol 93:1237-1265

Cooke DR, Bull SW, Large RR, McGoldrick PJ (2000) The importance of oxidized brines for the formation of Australia Proterozoic stratiform sediment-hosted Pb-Zn (sedex) deposits. Econ Geol 95:1-18

Cortecci G, Longinelli A (1972) Oxygen isotope variations in a barite slab from the sea bottom off southern California. Chem Geol 9:113-117

Darmody RG, Hardin, SD, Hassett JJ (1989) Barite authigenesis in surficial soils of mid-continental United States. *In* Water-Rock Interaction (WRI-6). DL Miles (Ed) Balkema, Rotterdam, 183-186

Davis GR, Hale M, Dixon CJ, Bush PR, Wheatley MR (1990) Barite dispersion in drainage sediments in arid climatic regimes. Trans Inst Mining Metall 99:15-20

Dean WE, Schreiber BC (1977) Authigenic barite, Leg 41 Deep Sea Drilling Project. Initial Rept Deep Sea Drilling Proj 41:915-931

de Lange GJ, Boelrijk NAIM, Catalano G, Corselli, C, Klinkhammer G (1990a), Sulphate-related equilibria in the hypersaline brines of the Tyro and Bannock Basins, eastern Mediterranean. Mar Chem 31:89-112

de Lange GJ, Middleburg JJ, van der Weijden CH, Catalano G (1990b) Composition of anoxic hypersaline brines in the Tyro and Bannock Basins, eastern Mediterranean. Mar Chem 31:63-80

Deb M, Hoefs J, Baumann A (1991) Isotopic composition of two Precambrian stratiform barite deposits from the Indian Shield. Geochim Cosmochim Acta 55:303-308

Degens ET and Ross DA (1969) Hot brines and recent heavy metal deposits in the Red Sea. Springer-Verlag, New York, 100 p

Dehairs F, Baeyens W, Goeyens L (1992) Accumulation of the suspended barite at mesopelagic depths and export production in the southern-ocean. Science 258:1332-1335

Dehairs F, Chesselet R, Jedwab J (1980) Discrete suspended particles of barite and the barium cycle in the open ocean. Earth Planet Sci Lett 49:528-550

Dejonghe L (1990) The sedimentary structures of barite: examples from the Chaudfantaine ore deposit, Belgium. Sedimentology 37:303-323

Dejonghe L, Boulvain F (1993) Paleogeographic and diagenetic context of a baritic mineralization enclosed within Frasnian peri-reefal formations—case-history of the Chaudfontaine mineralization (Belgium). Ore Geol Rev 7:413-431

Denis J, Michard G (1983) Dissolution d'une solution solides etude theoretique et experimentale. Bull Minéral 106:309-319

Des Marais DJ (1994) The Archean atmosphere: its composition and fate. *In* Archean Crustal Evolution. KC Condie (Ed) Elsevier, Amsterdam, p 505-523

DeWit MJ, Hart R, Martin A, Abbott P (1982) Archean abiotic and probable biogenic structures associated with mineralized hydrothermal vent systems and regional metasomatism, with implications for greenstone belt studies. Econ Geol 77:1783-1802

Dia A, Aquilina L, Boulegue J, Bourgois J, Suess E, Torres M (1993) Origin of fluids and related barite deposits at vent sites along the Peru convergent margin. Geology 21:1099-1102

Dial DC, Huff GF (1989) Occurrence of minor elements in ground water in Louisiana including a discussion of three selected sites having elevated concentrations of barium. Louisiana Dept Trans Water Res Tech Rept 47, 88 p

Dube TE (1986) Depositional setting of exhalative bedded barite and associated submarine fan deposits of the Roberts Mountains. Geol Soc Am Bull 18:259-267

Dube TE (1988) Tectonic significance of Upper Devonian igneous rocks and bedded barite, Roberts Mountains Allochton, Nevada, USA. Mem Can Soc Pet Geol 14:235-249

Dugolinsky BK, Marhoils SV, Dudley WC (1977) Biogenic influence on the growth of manganese nodules. J Sed Pet 47:428-445

Dunham AC, Hanor JS (1967) Controls on barite mineralization in the western United States. Econ Geol 62:82-94

Dymond J, Collier R (1996) Particulate barium fluxes and their relationships to biological productivity. Deep-Sea Res Part II 43:1283-1308

Dymond J, Suess E, Lyle M (1992) Barium in deepsea sediments: a geochemical proxy for paleo-productivity. Paleooceanography 7:163-181

Edgerton D (1997) Reconstruction of the Red Dog Zn-Pb-Ba ore body, Alaska, implications for the vent environment during the mineralization event. Can J Earth Sci 34:1581-1602

Edmond JM, Boyle ED, Drummond D, Grant B, Mislick T (1978) Desorption of barium in the plume of the Zaire (Congo) River. Netherlands J Sea Res 12:324-328

Edmond JM, Measures C, McDuff RE, Chan LH, Collier R, Grant B, Gordon LI, Corliss, JB (1979) Ridge crest hydrothermal activity and the balance of major and minor elements in the ocean: The Galapagos data. Earth Planet Sci Lett 46:1-18

Eriksson PG, Condie KC Tirsgaard H, Mueller WU, Altermann W, Miall AD, Aspler LB, Catuneanu O, Chiarenzelli C (1998) Precambrian clastic sedimentation systems. Sed Geol 120:5-53

Esch WL (1995) Effects of salt dome dissolution on sediment diagenesis: an experimental and field study. PhD Dissertation, Louisiana State University, Baton Rouge, 219 p

Falkner KK, Klinkhammer GP, Bower TS, Todd JF, Leweis BL, Landing WM, Edmond JM (1993) The behavior of barium in anoxic marine waters. Geochim Cosmochim Acta 57:537-554

Farrell CW, Holland HD (1983) Strontium isotope geochemistry of the Kuroko deposits. Econ Geol Monogr 5:302-319

Faure G (1972) Strontium. *In* Handbook of Geochemistry. KH Wedepohl (Ed) Springer-Verlag, New York, p 38B1-38B35

Faure G (1998) Principles and Applications of Geochemistry. Prentice Hall, Upper Saddle River, New Jersey, 600 p

Felmey AR, Rai D, Moore DA (1993) The solubility of $(Ba,Sr)SO_4$ precipitates: thermodynamic equilibrium and reaction path analysis. Geochim Cosmochim Acta 57:4345-4363

Fenchel T, Finlay BJ (1984) Geotaxis in the ciliated protozoon *Loxodes*. J Exper Biol 110:17-33

Fernandez-Diaz L, Putnis A, Cumberbatch J (1990) Barite nucleation kinetics and the effect of additives. Eur J Mineral 2:495-501

Finlay BJ, Hetherington NB, Davison W (1983) Active biological participation in lacustrine barium chemistry. Geochim Cosmochim Acta 47:1325-1329

Fisher RS (1995) Naturally occurring radioactive materials (NORM) in produced water and scale from Texas oil, gas, and geothermal wells. Texas Bur Econ Geol 95-3, 43 p

Fisher RS (1998) Geologic and geochemical controls on naturally occuring radioactive materials (NORM) in produced water from oil, gas, and geothermal operations. Environ Geosci 5:139-150

Fitch AA (1931) Barite and witherite from near El Portal, Mariposa Co., California. Am Mineral 16:461-468

Fortey NJ, Beddoe-Stevens B (1982) Barium silicates in stratabound Ba-Zn mineralization in the Scottish Dalradian. Mineral Mag 46:63-72

Frank AJ, Moynihan CS (1947) occurrence of the barite at Pilot Knob, Missouri. Am Mineral 32:681-683

Franklin JM (1995) Volcanic-associated massive sulfide base metals. *In* Geology of Canadian Mineral Deposit Types. OR Eckstrand, WD Sinclair, RI Thorpe (Eds) Geol Soc Am, The Geology of North America P-1:158-183

Franklin JM, Lydon JW, Sangster DF (1981) Volcanic-hosted massive sulfide deposits. *In* Economic Geology 75th Anniversary Volume. BF Skinner (Ed) Economic Geology Publishing Co, El Paso, Texas, p 485-627

Fresnel J, Galle P, Gayral P (1979) Résultats de la microanalyse des cristaux vacuolaires ches deux Chromophytes unicellulaires marines: *Exanthemachrysis gayraliae, Pavlova sp*. (Prymnesiophycées, Pavlovacées). Compt Rendus Acad Sciences Paris D 112:823-825

Frimmel HE (1990) Isotopic constraints on fluid rock ratios in carbonate rocks – barite sulfide mineralization in the Schwarz dolomite, Tyrol (Eastern Alps, Austria). Chem Geol 90:195-209

Frimmel HE, Papesch W (1990) Sr, O and C isotope study of the Brixlegg barite deposit, Tyrol (Austria). Econ Geol 85:1162-1171

Fu B (1998) A study of pore fluids and barite deposits from hydrocarbon seeps: deepwater Gulf of Mexico. PhD Dissertation, Louisiana State University, 243 p

Gaines RV, Skinner HCW, Foord EE, Mason B, Rosenzweig A (1997) Dana's New Mineralogy. Wiley, New York, 1819 p

Garven G, Raffensperger JP (1997) Hydrogeology and geochemistry of ore genesis in sedimentary basins. *In* Geochemistry of Hydrothermal Ore Deposits, 3rd edn. HL Barnes (Ed) Wiley, New York, p 797-875

Gayral P, Fresnel J (1979) *Exanthemachrysis gayraliae,* Lepailleur (Prymnesiophyceae, Pavlovales): Ultrastructure et discussion taxinomique. Protistologica 15:217-282

Gilkeson RH, Perry EC, Cartwright K (1981) Isotopic and geologic studies to identify the sources of sulfate in groundwater containing high barium concentration. Illinois State Geol Surv Rept 1981-4, 39 p

Gingele F, Dahmke A (1994) Discrete barite particles and barium as tracers of paleoproductivity in south-atlantic sediments. Paleooceanography 9:151-168

Gluyas J, Jolley L, Primmer T (1997) Element mobility during diagenesis: sulphate cementation of Rotliegeng sandstones, southern North Sea. Marine Petrol Geol 14:1001-1011
Glynn PD, Reardon EJ (1990) Solid–solution aqueous–solution equilibria: thermodynamic theory and representation. Am J Sci 290:164-201
Glynn PD, Reardon EJ, Plummer LN, Busenberg E (1990) reaction paths and equilibrium endpoints in solid–solution aqueous–solution systems. Geochim Cosmochim Acta 54:267-282
Goldberg ED, Somayajulu BLK, Galloway J, Kaplan IR, Faure G (1969) Differences between barites of marine and continental origins. Geochim Cosmochim Acta 33:287-289
Goldish E (1989) X-ray diffraction analysis of barium-strontium sulphate (barite-celestite) solid solutions. Powder Diff 4:214-216
Goldschmidt B (1938) Sur la precipitation mixte des sulfates de baryum et de strontium. Compt Rendu Paris Acad des Sci 206:1110
Gooday AJ, Nott JA (1982) Intracellular barite crystals in two Xenophyophores, *Aschemonella ramuliformis and Galatheammina sp*. (Protozoa: Rhizopoda) with comments on the taxonomy of *A. ramuliformis*. J Mar Biol Assoc UK 62: 595-605
Gooday AJ, Nott JA, Davis D, Mann S (1995) Apatite particles in the test wall of the large agglutinated forminifer *Bathysiphon major* (Protista). J Mar Biol Assoc UK 75:469-481
Goodfellow WD (1999) Sediment-hosted Zn-Pb-Ag deposits of North America. *In* Basins, Fluids and Zn-Pb Ores. O Holm, J Pongratz, P McGoldrick (Eds) Univ Tasmania Centre for Ore Deposits Research (CODES) Spec Pub 2: 59-91
Goodfellow WD, Lydon JW, Turner RW (1993) Geology and genesis of stratiform sediment-hosted (SEDEX) Zn-Pb-Ag sulphide deposits. *In* Mineral Deposit Modeling. RV Kirkham, WD Sinclair, RI Thorpe, JM Duke (Eds) Geol Assoc Canada Spec Paper 40:201-251
Gordon L, Rowley K (1957) Coprecipitation of radium with barium sulfate. Analyt Chem 29: 34-37
Gordon L, Reimer CC, Burit PB (1954) Distribution of strontium within barium sulfate precipitated from homogeneous solution. Analyt Chem 26, 842-846
Goyer RA (1974) Toxic effects of metals. *In* Casarett and Doull's Toxicology: the Basic Science of Poisons. CD Klassen (Ed) McGraw-Hill, New York, p 691-736
Graber KK, Chafetz HS (1990) Petrography and origin of bedded barite and phosphate in the Devonian Slaven Chert of Central Nevada. J Sed Pet 60:897-911
Grahmann W (1920) Uber barytocolestin und das verhaltnis von anhydrit zu colestin und baryt. Neues Jahrb Mineral 1:1-23
Gregus Z, Klaasen CD (1996) Mechanisms of toxicity. *In* Casarett and Doull's Toxicology: The Basic Science of Poisons. CD Klassen (Ed) McGraw-Hill, New York, p 35-74
Grotzinger JP, Kasting JF (1993) New constraints on Precambrian ocean composition. J Geology 101:235-243
Guichard F, Church TM, Treuil M, Jaffrezic H (1979) Rare earths in barites: distribution and effects in aqueous partitioning. Geochim Cosmochim Acta 43:983-987
Gundlach H, Stoppel D, Strubel G (1972) Zur hydrothermalen Löslichkeit von Baryt. Neues Jahrb Mineral 116:321-328
Halas S, Mioduchowski L (1978) Isotopic composition of oxygen in sulfate minerals of calcium and strontium and in water sulfates from various regions of Poland. Ann Univ Mariae Curie-Sklodowska 33:115-130
Hall AJ, Boyce AJ, Fallick AE, Hamilton PJ (1991) Isotopic evidence of the depositional environment of the Proterozoic stratiform barite. Chem Geol 87:99-114
Hannak WW (1981) Genesis of the Rammelsberg ore deposit near Goslar/Upper Harz, Federal Republic of Germany. *In* Handbook of Strata-Bound and Stratiform Ore Deposits, vol 9. K Wolf (Ed) Elsevier, Amsterdam, p 551-642
Hannington, MD and Scott SD (1989) Gold mineralization in volcanogenic massive sulfides: implications of data from active hydrothermal vents on the modern sea floor. Econ Geol Monogr 6:491-506
Hanor JS (1966) The origin of barite. PhD Thesis, Harvard University, 257 p
Hanor JS (1968) Frequency distribution of compositions in the barite-celestite series. Am Mineral 53:1215-1222
Hanor JS (1969) Barite saturation in sea water. Geochim Cosmochim Acta 33:894-898
Hanor JS (1973) Critical comment: The synthesis of barite, celestite, and barium-strontium sulfate solid solution crystal. Geochim Cosmochim Acta 37:2685-2687
Hanor JS (1979) Sedimentary genesis of hydrothermal fluids. *In* Geochemistry of Hydrothermal Ore Deposits, 2nd ed. HL Barnes (Ed) John Wiley and Sons, New York, p 137-168
Hanor JS (1980) Dissolved methane in sedimentary brines: Potential effect on the PVT properties of fluid inclusions. Econ Geol 75:603-609

Hanor JS (1988) Origin and Migration of Subsurface Sedimentary Brines. Society of Sedimentary Geology Short Course No. 21, Tulsa, Oklahoma, 247 p.

Hanor JS (1994) Origin of saline fluids in sedimentary basins. *In* Geofluids: Origin and Migration of Fluids in Sedimentary Basins. J Parnell (Ed) Geol Soc London Spec Pub 78:151-174

Hanor JS (1996a) Variations in chloride as a driving force in siliciclastic diagenesis. *In* Siliciclastic Diagenesis and Fluid Flow: Concepts and Applications. LJ Crossey, R Loucks, MW Totten (Eds) Soc Econ Paleo Mineral Spec Pub 55:3-12

Hanor JS (1996b) Controls on the solubilization of dissolved lead and zinc in basinal brines. *In* Carbonate-hosted Lead-Zinc Deposits. DF Sangster (Ed) Soc Econ Geol Spec Pub 4:483-500

Hanor JS (1999a) Thermohaline porewater trends of southeastern Louisiana revisited. Gulf Coast Assoc Geol Soc Trans 49:273-280

Hanor JS (1999b) Geochemistry and origin of metal-rich brines in sedimentary basins. *In* Basins, fluids, and Zn-Pb ores, 2nd edn. *In* H Holm, J Pongratz, P McGoldrick (Eds) Univ Tasmania, Centre for Ore Deposits Research (CODES) Spec Pub 2:129-146

Hanor JS, Baria LR (1977) Controls on the distribution of barite deposits in Arkansas. *In* Geology of the Quachitas, vol. 2. CG Stone (Ed) Arkansas Geol Commission, Little Rock, p 48-55

Hanor JS, Chan LH (1977) Non-conservative behavior of barium during mixing of Mississippi River and Gulf of Mexico waters. Earth Planet Sci Lett 37:242-250

Hanor JS, Sassen R (1990) Large-scale vertical migration of formation waters, dissolved salt, and hydrocarbons in the Louisiana Gulf Coast. *In* Gulf Coast Oils and gases, Their Characteristics, Origin, Distribution, and Exploration and Production Significance. D Schumacher, BF Perkins (Eds) Proc 9th Ann Res Conf, Gulf Coast Section, Soc Econ Paleo Mineral p 283-296.

Hanor JS, McManus KM, Ranganathan V, and Su S (1995) Mineral buffering of contaminated ground water compositions at a hazardous waste site in southwestern Louisiana: Trans Gulf Coast Assoc of Geol Soc 45:237-243

Hattori K (1989) Barite-celestine intergrowths in Archean plutons: the product of oxidizing hydrothermal activity related alkaline intrusions. Am Mineral 74:1270-1277

Hattori K, Cameron EM (1986) Archaean magmatic sulphate. Nature 319:45-47

Heinrich EW, Vian RW (1967) Carbonatitic barites. Am Mineral 52:1179-1189

Herzig PM, Hannigton MD, Fouquet Y, Vonstackelberg U, Petersen S (1993) Gold-rich polymetallic sulfides from the Lau back-arc and implications for the geochemistry of gold in sea-floor hydrothermal systems of the southwest Pacific. Econ Geol 88:2182-2209

Hill CA (1992) Isotopic values of native sulfur, barite, celestine and calcite: their relationship to sulphur deposits and the evolution of the Delaware Basin (preliminary results). Soc Metall Expl 147-157

Hitzman MW (1999) Characteristics and worldwide occurrence of Irish-type Zn-Pb-(Ag) deposits. *In* Basins, Fluids and Zn-Pb ores, 2nd edn. O Holm, J Pongratz, P McGoldrick (Eds) Univ Tasmania Centre for Ore Deposits Research (CODES) Spec Pub 2: 93-116

Hitzman MW, Beaty DD (1996) The Irish Zn-Pb-(Ba) ore field. *In* Carbonate-Hosted Lead-Zinc Deposits. DF Sangster (Ed) Soc Econ Geol Spec Pub 4:29-57

Holland HD (1984) The Chemical Evolution of the Atmosphere and Oceans. Princeton University Press, Princeton, New Jersey, 582 p

Hollande A, Martoja R (1974) Identification du cristalloide des isospores de radiolaires à un cristal de célestite ($SrSO_4$). Détermination de la constitution du cristalloide par voie cytochimique et à l'aide de le microsonde électronique et du micoanalyseur par émission ionique secondaire. Protistologica 10:603-609

Holser WT (1979) Mineralogy of evaporites. Rev Mineral 6:211-294

Hopwood JD, Mann S, Gooday AJ (1997) The crystallography and possible origin of barium sulphate in deep-sea rhizopod protists (Xenophyophorea). J Mar Biol Assoc UK 77:969-987.

Horton JWJ (1989) Barite in quartz-sericite schist and schistose pyroclastic rock of the Battleground Formation, Kings Mountain Belt. US Geol Survey Prof Paper 1112:115-118

Horton RC (1963) An inventory of barite occurrences in Nevada. Nev Bur Mines Rept 4, 18 p

Howard KW, Hanor JS (1987) Compositional zoning in the Fancy Hill stratiform barite deposit, Quachita Mountains, Arkansas and evidence for lack of associated massive sulfides. Econ Geol 82:1377-1385

Hubert G, Rieder N, Schmitt G, Send W (1975) Bariumanreicherung in den Müllerschen Körperchen der *Loxodidae* (Ciliata, Holotriche). Z Natur 30c:422.

Hughes, NP, Perrry CC, Anderson OR, Williams RJP (1989) Biological minerals formed from strontium and barium sulphates. III. The morphology and crystallography of strontium sulphate crystals from the radiolarian *Sphaerozoum punctatum*. Proc Royal Soc London B238:223-233

Huheey JE (1972) Inorganic Chemistry. Harper & Row, New York, 737 p

Huston DL (1999) Stable isotopes and their signficance for understanding the genesis of volcanic-hosted massive sulfide deposits: A review. Rev Econ Geol 8:157-180

Isphording WC (1982) Misinterpretation of environmental monitoring data—a plague on mankind! Gulf Coast Assoc Geol Soc Trans 32:399-411
Janecky DR, Shanks, WC III (1988) Computational modelling of chemical and sulphur isotopic reaction processes in seafloor hydrothermal systems: chimneys, massive sulfides, and subjacent alteration zones. Can Mineral 26:805-826
Jeandel C, Dupré B, Lebaron G, Monnin C, Minster JF (1996) Longitudinal distributions of dissolved barium, silica and alkalinity in the western and southern Indian ocean. Deep-Sea Res 43:1-31
Jebrak M, Smejkal V, Albert D (1985) Rare earth and isotopic geochemistry of the fluorite-barite vein deposits from the western Rouergue district (France). Econ Geol 80:2030-2034
Jewell PW (1992) Hydrodynamic and chemical controls of Paleozoic phophorite and barite in the western Cordillera of North America. *In* Water-Rock Interaction (WRI-7). Y Kharaka, A Maest (Eds) Balkema, Rotterdam, 1235-1238
Jewell PW (2000) Bedded barite in the geologic record. Soc Econ Paleo Mineral Spec Pub 66:147-161
Jewell PW, Stallard RF (1991) Geochemistry and paleooceanographic setting of central Nevada bedded barites. J Geol 99:151-170
Kadko D, Moore WS (1988) Radiochemical constraints on the crustal residence time of submarine hydrothermal fluids: Endeavor ridge. Geochim Cosmochim Acta 52: 659-668
Kaiser CJ, Kelly WC, Wagner RJ, Shanks WCI (1987) Geologic and geochemical controls of mineralization in the Southeast Missouri barite district. Econ Geol 82:719-734
Kajiwara Y, Honma H (1976) Lead content of barite coexisting with galena—an indicator of oxygen fugacity. Mining Geol (Japan) 25:397-400
Kasting JF (1993) Earth's early atmosphere. Science 259:920-926
Kesler SE (1996) Appalachian Mississippi Valley Type deposits: Paleoaquifers and brine provinces. *In* Carbonate-Hosted Lead-Zinc Deposits. DF Sangster (Ed) Soc Econ Geol Spec Pub 4:29-57
Kesler SE, Jones LM (1981) Sulphur- and strontium-isotopic geochemistry of celestite, barite and gypsum from the Mesozoic Basins of north eastern Mexico. Chem Geol 31:211-24
Kesler, SE, Appold MS, Walter LM, Martini A, Huston TS (1995) Na-Cl-Br systematics of fluid inclusions from MVT deposits. Geology 23:642-644
Kesler TL, Kesler SE (1971) Amphibolites of the Cartersville district, Georgia. Geol Soc Am Bull 82:3163-3168
Khalaf FI, El-Sayed MI (1989) Occurrence of barite-bearing mud balls within the Mio-Pleistocene terrestrial sand (Kuwait Group) in southern Kuwait, Arabian Gulf. Sed Geol 64:197-202
Kinsman D (1969) Reinterpretation of Sr^{2+} concentrations in carbonate minerals and rocks. J Sed Pet 39:512-517
Klein L (1959) River Pollution: 1. Chemical Analyses. Butterworths, London, 206 p
Kornicker WA, Presta PA, Paige CR, Johnson DM, Hileman OE, Snodgrass WJ (1991) The aqueous dissolution kinetics of the barium/lead sulfate solid solution series at 25 degrees Celsius and 60 degrees Celsius. Geochim Cosmochim Acta 55:3531-3541
Koczy FF (1958) Natural radium as a tracer in the ocean. Proc 2nd Int'l Conf on the Peaceful Uses of Atomic Energy 18:351
Krebs W (1981) Geology of the Meggen ore deposit. *In* Handbook of Strata-Bound and Stratiform ore Deposits. K Wolf (Ed) Elsevier, Amsterdam 9:509- 549
Kribek B, Hladikova J, Zak K, Bendl J, Pudilova M, Uhlik Z (1996) Barite-hylophane sulfide ores at Rozna, Bohemian Massif, Czech Republic: Metamorphosed black shale-hosted submarine exhaltive mineralization. Econ Geol 91:14-35
Kritsotakis K, von Platen H (1980) Reduktive Barytmobilisation. Neues Jahrb Mineral Abh 137:282-306
Kusakabe M, Robinson BW (1977) Oxygen and sulfur isotope equilibria in the $BaSO_4$-H_2SO_4-H_2O system from 110 to 350 degrees C and applications. Geochim Cosmochim Acta 41:1033-1040
Kushnir SV (1986) The epigenetic celestine formation mechanism for rocks containing $CaSO_4$. Geochem Int'l 23:1-9
Kyle JR (1994) The barite industry and resources of Texas. Texas Bur Econ Geol, Mineral Res Circ 85, 86 p
Lambert IB, Donelly TH, Dunlop JSR, Groves DI (1978) Stable isotopic compositions of early Archean sulphate deposits of probable evaporitic and volcanogenic origins. Nature 276:808-811
Lambert IB, Sato T (1974) The Kuroko and associated ore deposits of Japan: A review of their features and metallogenesis. Econ Geol 69:1215-1236
Leach DL (1980) Nature of mineralizing fluids in the barite deposits of central and southeast Missouri. Econ Geol 75:1168-1180
Lippmann F (1962) Benstonite, $Ca_7Ba_6(CO_3)_{13}$, and new mineral from the barite deposit in Hot Springs County, Arkansas. Am Mineral 47:585-598
Lonsdale P (1979) A deep-sea hydrothermal site on a strike-slip fault. Nature 282:531-534.

Lottermoser BG, Ashley PM (1996) Geochemistry and explanation of the significance of ironstones and barite-rich rocks in the Proterozoic Willyama Supergroup, Olary Block, South Australia. J Geochem Expl 57:57-73

Lydon JW (1995) Sedimentary exhalative sulfides. *In* Geology of Canadian Mineral Deposit Types. OR Eckstrand, WD Sinclair, RI Thrope (Eds) Geol Soc Am, The Geology of North America P-1:130-152

Macpherson GL (1989) Sources of lithium and barium in Gulf of Mexico formation waters, USA. *In* Water-Rock Interaction (WRI-6). DL Miles (Ed) Balkema, Rotterdam, p 453-456

Malinin SD, Urusov VS (1983) The experimental and theoretical data on isomorphism in the $(Ba,Sr)SO_4$ system in relation to barite formation. Geochem Int'l 20:70-80

Marchev P (1991) Primary barite in high-K dacite from the eastern Rhodope, Bulgaria. Eur J Mineral 3:1005-1008

Margaritz M, Brenner IB, Ronen D (1990) Ba and Sr distribution at the water table: Implications for monitoring ground-water at nuclear waste repository sites. Appl Geochem 5:555-562

Martin EE, McDougall JD, Herbert TD, Paytan A, Kastner M (1995) Strontium and neodymium isotopic analyses of marine barite separates. Geochim Cosmochim Acta 59:1353-1361

Martin JH, Knauer GA (1973) The elemental composition of plankton. Geochim Cosmochim Acta 37:1639-1653

May F, Peacock JD, Smith DL, Barber AJ (1963) Geology of the Kintail district. British Geol Surv Memoir for sheet 72W and part of 71E (Scotland), 77 p

Maynard JB, Okita PM (1991) Bedded barite deposits in the United States. Econ Geol 86:364-376

Maynard JB, Morton J, Valdes-Nodarse EL, Diaz-Carmona, A (1995) Sr isotopes of bedded barites: guide to distinguishing basins with Pb-Zn mineralization. Econ Geol 90:2058-2064

McKibben MA, Hardie, LA (1997) Ore-forming brines in active continental rifts. *In* Geochemistry of Hydrothermal Ore Deposits, 3rd edn. HL Barnes (Ed) Wiley, New York, p 877-936

McLemore VT, Leuth VW (1996) Lead-zinc deposits in carbonate rocks in New Mexico. *In* Carbonate-Hosted Lead-Zinc Deposits. DF Sangster (Ed) Soc Econ Geol Spec Pub 4:264-276

McManus J, Berelson WM, Klinkhammer GP, Kilgore TE, Hammond DE (1998) Geochemistry of barium in marine sediments: Implications for its use as a paleoproxy. Geochim Cosmochim Acta 62:3453-3473

McManus KM, Hanor JS (1988) Calcite and iron sulfide cementation of Miocene sediments flanking the West Hackberry salt dome, southwest Louisiana, U.S.A. Chem Geol 74, 99-112

McManus KM, Hanor JS (1993) Diagenetic evidence for massive evaporite dissolution, fluid flow, and mass transfer in the Louisiana Gulf Coast. Geology 21:727-730.

Mills JW, Carlson CL, Fewkes RH, Handlen LW, Jaypakash GP, Johns MA, Margati JM, Neitzel TW, Ream LR, Sanford SS, Todd SG (1971) Bedded barite deposits of Stevens County, Washington. Econ Geol 66:1157-1163

Misra KC, Gratz JF, Lu C (1996) Carbonate-hosted Mississippi Valley-type mineralization in the Elmwood-Gordonsville deposits, Central Tennessee zinc district: A synthesis. Econ Geol Spec Pub 4:58-73

Mitchell RS, Pharr RF (1961) Celestite and calciostrontianite from Wise County, Virginia. Am Mineral 46:189-185

Mohazzabi P, Searcy AW (1976) Kinetics and the thermodynamics of decomposition of barium sulphate. J Chem Soc Farad Trans 72:290-295

Monnin C (1999) A thermodynamic model for the solubility of barite and celestite in electrolyte solutions and seawater to 200°C and to 1 kbar. Chem Geol 153, 187-209

Monnin C, Galinier C (1988) The solubility of celestite and the barite in electrolyte solutions and natural waters at 25 degrees C: A thermodynamic study. Chem Geol 71:283-296

Monnin C, Jeandel C, Cattaldo T, Dehairs F (1999) The marine barite saturation state of the world ocean. Marine Chem 65:253-261

Moore W, Stakes D (1990) Ages of barite-sulfide chimneys from the Mariana Trough. Earth Planet Sci Lett 100:265-274

Morgan JW, Wandles GA (1980) Rare earth element distribution in some hydrothermal minerals: Evidence for crystallographic control. Geochim Cosmochim Acta 44:973-980

Moro MC, Arribas A (1981) Los yacimientos espanoles de barita estratiforme y su significado metalogenico en el contexto mundial. Tecniterrae 42:18-45

Mossman DJ, Brown MJ (1986) Stratiform barite in sabkha sediments, Walton-Cheverie, Nova Scotia. Econ Geol 81:2016-2021

Müller G (1962) Zur Geochemie des Strontiums in ozeanen Evaporiten unter besonderer Berucksichtigumg der sedimentaren Celestin-Lagerstatten von Hemmelte West. Geologie, Beiheft 35, 90 p

Murchey BL, Madrid RJ, Poole FG (1987) Paleozoic bedded barite associated with chert in western North America. *In* Siliceous Sedimentary Rock-Hosted Ores and Petroleum. JR Hein (Ed) Van Nostrand, p 269-283

Naehr TH, Bohrmann G (1999), Barium-rich authigenic clinoptilolite in sediments from the Japan Sea: a sink for dissolved barium? Chem Geol 158:227-244

Nickless EFP, Booth SJ, Mosley PN (1975) Celestite deposits of the Bristol area. Trans Inst Mining Metall B84:62-64

Nijman W, de Bruijne KH, Valkering ME (1998) Growth fault control of Early Archaean cherts, barite mounds and chert-barite veins, North Pole Dome, Eastern Pilbara, Western Australia. Precamb Res 88:25-52

Nordstrom DK, Munoz JL (1994) Geochemical Thermodynamics. Blackwell, Boston, 493 p

Nuelle LM, Shelton KL (1986) Geologic and geochemical evidence of possible bedded barite deposits in Devonian rocks of the Valley and Ridge Province, Appalachian Mountains. Econ Geol 81:1408-1430

Ober JA (1997) Strontium. US Geol Survey Minerals Inf Circ, 6 p

Oftedahl C (1958) On exhalative-sedimentary ores. Geol Foren Stockholm Forh 80:1-19

Ohmoto H, Lasaga AC (1982) Kinetics of reactions between aqueous sulfates and sulfides in hydrothermal systems. Geochim Cosmochim Acta 46:1727-1745

Okita PM (1983) Petrography of the Fancy Hill (Henderson) stratiform barite deposit, Montgomery County, Arkansas. MS Thesis, Louisiana State University, Baton Rouge, 208 p

Orange DL, Greene HG, Reed D, Martin JB, McHugh CM, Ryan WBF, Maher N, Stakes D, Barry J (1999) Widespread fluid expulsion on a translational continental margin: mud volcanoes, fault zones, headless canyons, and organic-rich substrate in Monterey Bay, California. Geol Soc Am Bull 111:992-1009

Orris GJ (1986) Descriptive model of bedded barite. US Geol Survey Bull 216:112-113

Ostlund H, Craig H, Broecker W, Spencer D (1987) GEOSECS Atlantic, Pacific and Indian ocean expeditions, vol. 7, Shore-based data and graphics, Nat'l Sci Fdn, Washington DC, 200 p

Paige CR, Kornicker WA, Hileman OE, Snodgrass WJ (1998) Solution equilibria for unranium ore processing: the $BaSO_4$-H_2SO_4-H_2O system and the $RaSO_4$-H_2SO_4-H_2O system. Geochim Cosmochim Acta 62:15-23

Papke KG (1984) Barite in Nevada. Nevada Bur Mines Geol Bull 98, 125 p

Paradis S, Lavoie D (1996) Multiple-stage diagenetic alteration and fluid history of Ordovician carbonate-hosted barite mineralization, southern Quebec Appalachians. Sed Geol 107:121-139

Pardue JH, Guo TZ (1998) Biochemistry of Ra-226 in contaminated bottom sediments and oilfield waste pits. J Environ Radioactivity 39:239-253

Park B, Branner JA (1932) A barite deposit in Hot Spring County, Arkansas. Arkansas Geol Surv Inf Circ 1, 52 p

Paytan A, Kastner M, Martin EE, McDougald JD, Herbert T (1993) Marine barite as a monitor of seawater strontium isotope composition. Nature 366:445-449

Paytan A, Moore WS, Kastner M (1996) Sedimentation rate as determined by Ra-226 activity in marine barite. Geochim Cosmochim Acta 60:4313-4319

Perry EC, Monster J, Reimer T (1971) Sulfur isotopes in Swaziland System barites and the evolution of the Earth's atmosphere. Science 171:1015-1016

Peter JM, Scott SD (1988) Mineralogy, composition and fluid-inclusion microthermometry of seafloor hydrothermal deposits in the southern trough of Guymas Basin, Gulf of California. Can Mineral 26:567-587

Pitzer KS (1987) A thermodynamic model for aqueous solutions of liquid-like density. Rev Mineral 17:97-142

Poulsen KH, Hannington MD (1995) Volcanic-associated massive sulfide gold. *In* Geology of Canadian Mineral Deposit Types. OR Eckstrand, W D Sinclair, RI Thorpe (Eds) Geol Soc Am, The Geology of North America P-1:183-196

Prieto M, Putnis A, Fernandez-Diaz L (1990) Factors controlling the kinetics of crystallization; supersaturation evolution in a porous medium: Application to barite crystallization. Geol Mag 127:485-495

Prieto M, Putnis A, Fernandez-Diaz L (1993) Crystallization of solid solutions from aqueous solutions in a porous medium: Zoning in $(Ba,Sr)SO_4$. Geol Mag 130:289-299

Prieto, M, Fernandez Gonzalez A, Putnis A, Fernandez Diaz L (1997) Nucleation, growth, and zoning phenomena in crystallizing $(Ba,Sr)CO_3$, $Ba(SO_4,CrO_4)$, $(Ba,Sr)SO_4$, and $(Cd,Ca)CO_3$ solid solutions from aqueous solutions. Geochim Cosmochim Acta 61: 3383-3397

Puchelt H (1967) Zur Geochemie des Bariums im exogenen Zyklus. Springer-Verlag, Heidelberg, 287 p

Puchelt H (1972) Barium. *In* Handbook of Geochemistry. KH Wedepohl (Ed) Springer-Velag, New York, p 56B1-56O22

Putnis A, Fernandez-Diaz L, Prieto M (1992) Experimentally produced oscillatory zoning in the (Ba,Sr)SO_4 solid solution. Nature 358:743-745

Putnis A, Juntarosso JL, Hochella MF (1995) Dissolution of barite by a chelating ligand - an atomic-force microscopy study. Geochim Cosmochim Acta 59:4623-4632

Ramboz C, Charef A (1988) Temperature, pressure, burial history, and paleohydrogeology of the Les Malines Pb-Zn deposit: Reconstruction from aqueous inclusions in barite. Econ Geol 83:784-800

Ramos VA, Brodtkorb de MK (1989) Celestite, barite, magnesite and fluorspar: Stratabound settings through time and space. *In* Nonmetalliferous Stratabound Ore Fields. MK de Brodtkorb (Ed) Van Nostrand Reinhold, New York, p 297-321

Ramos VA, Brodtkorb de MK (1990) The barite and celestine metalotects of the Neuquen retroarc basin, central Argentina. *In* Stratabound Ore Deposits in the Andes. L Fonbote, GC Amstutz, M Cardozo, E Cedillo, J Frutos (Eds) Springer-Verlag, Berlin, p 599-613

Rankin AH, Sheppard TJ (1978) H_2O-bearing fluid inclusions in baryte from the North Pole deposit, Western Australia. Mineral Mag 42:408-410

Reardon EJ, Armstrong DK (1987) Celestine ($SrSO_4$) solubilty in water, seawater and NaCl solutions. Geochim Cosmochim Acta 51:63-72

Reesman RH (1968) Strontium isotopic composition of gangue minerals from hydrothermal veins. Econ Geol 63:731-736

Reimer TO (1980) Archean sedimentary baryte deposits of the Swaziland Supergroup (Barberton Mountain Land, South Africa). Precamb Res 12:393-410

Revelle RR (1944) Marine bottom samples collected in the Pacific ocean by the Carnegie on its seventh cruise. Publ Carneige Inst Washington 556, 2(1), 133 p

Rhein M, Chan LH, Roether W, Schlosser P (1987) ^{226}Ra and Ba in northeast Atlantic Deep Water. Deep-Sea Res 34:1541-1564

Rhein M, Schlitzer R (1988) Radium-226 and barium sources in the deep East Atlantic. Deep-Sea Res 35:1499-1510

Rietmejer FJM (1990) Salts in two chondritic porous interplanetary dust particles. Meteoritics 25:209-213

Robinson GRJ, Woodruff LG (1988) Characteristics of base-metal and barite vein deposits associated with rift basins, with examples from some early Mesozoic basins of eastern North America. US Geol Survey Bull 1776:377-390

Roedder E, Bodnar RJ (1997) Fluid inclusion studies of hydrothermal ore deposits. *In* Geochemistry of Hydrothermal Ore Deposits, 3rd edn. HL Barnes (Ed) Wiley, New York, Wiley, p 657-698

Ruiz J, Richardson CK, Patchett PJ (1988) Strontium isotope geochemistry of fluorite, calcite, and barite of the Cave-in-Rock fluorite district, Illionois. Econ Geol 83:203-210

Rye RO, Shawe DR, Poole FG (1978) Stable isotope studies of bedded barite at East Northumberland Canyon in Toquima Range, central Nevada. Res US Geol Survey 6:221-229

Sabine PA, Young BR (1954) Cell size and composition of the baryte-celestine isomorphous series. Acta Crystallogr 7:630 (abstract)

Samuelson SF (1992) Anatomy of an elephant: Boling dome. *In* Native Sulfur: Developments in Geology and Exploration. GR Wessel BH Wimberly (Eds) Soc Mining Metall Explor, Littleton, Colorado, p 59-71

Sangster DF (Ed) (1996) Carbonate-hosted lead-zinc deposits. Soc Econ Geol Spec Pub 4, 664 p

Sangster DF, Savard MM, Kontak DJ (1998) A genetic model for mineralization of Lower Windsor (Visean) carbonate rocks of Nova Scotia, Canada: Econ Geol 93:932-952

Saunders JA, Prikryl JD, Posey HH (1988) Mineralogic and isotopic constraints on the origin of the strontium-rich cap rock, Tatum Dome, Mississippi, U.S.A. Mineral Mag 32:63-86

Sawkins FJ and Burke K (1980) Extensional tectonics and mid-Paleozoic massive sulfide occurrences in Europe. Geol Rundschau 69:349-360

Sayles FL, Manheim F (1975) Interstitial solutions and diagenesis in deeply buried marine sediments, results from the deep sea drilling project. Geochim Cosmochim Acta 39:103-127

Schmitz B (1987) Barium, equatorial high productivity, and the northward wandering of the Indian continent. Paleooceanography 2:63-67

Scholle PA, Stemmerik L, Harpoth O (1990) Origin of major karst-associated celestine mineralization in Karstrynggen, Central East Greenland. J Sed Pet 60:397-410.

Schrijver K, Zartman RE, Williams-Jones AE (1994) Lead and barium sources in Cambrian siliciclastics and sediment provenance of a sector of the Taconic orogen: A mixing scenario based on Pb-isotopic evidence. Appl Geochem 9:455-476

Schroeder JO, Murray RW, Leinen M, Pflum RC, Janecek TR (1997) Barium and equatorial Pacific carbonate sediment: Terrigenous, oxide and biogenic associations. Paleooceanography 12:125-146

Scott SD (1997) Submarine hydrothermal systems and deposits. *In* Geochemistry of Hydrothermal Ore Deposits, 3rd edn. HL Barnes (Ed) Wiley, New York, p 797-875

Scull BJ (1958) Origin and occurrence of barite in Arkansas. Ark Geol Conserv Comm Info Circ 18, 101 p
Searls JP (1997) Barite. US Geol Survey Minerals Inf Circ, 7 p
Shaw TJ, Moore WS, Kloepper J, Sochaski K (1998) The flux of barium to the coastal waters of the southeastern USA: the importance of submarine groundwater discharge. Geochim Cosmochim Acta 62:3047-3054
Shawe DR, Poole FG, Brobst DA (1969) Newly discovered barite deposits in East Northumberland Canyon, Nye County, Nevada. Econ Geol 64:245-254
Shelton KL (1989) Mineral deposits and resources of the Ouachita Mountains. *In* The Appalachian-Ouachita Orogen in the United States. RD Hatcher, WA Thomas, GW Viele (Eds) Geol Soc Am, The Geology of North America F-2:729-737
Shikazono N (1994) Precipitation mechanisms of barite in sulfate-sulfide deposits in back-arc basins. Geochim Cosmochim Acta 58:2203-2213
Srinivasin B (1976) Barites: Anomalous xenon from spallation and neutron-induced reactions. Earth Planet Sci Let 31:129-141
Stamatakis MG, Hein JR (1993) Sedimentary rocks from Lefkas island, Greece. Econ Geol 88:91-103
Starke R (1964) Die strontiumgehälte der baryte. Freiberger Forschungsh C150, 123 p
Stecher HA, Kogut MB (1999) Rapid barium removal in the Delaware estuary. Geochim Cosmochim Acta 63:1003-1012
Stokinger HE, Woodward RL (1958) Toxicological methods for establishing drinking water standards. J Am Water Works Assoc 50:515-530
Stoops GJ, Zavaleta A (1978) Micromorphological evidence of barite neoformation in soils. Geoderma 20:63-70
Strizhov VP, Sval VN, Nokolayev SD, Zhabina NV (1988) Isotope composition of sulfur in barite crusts of the Red Sea. Oceanology 28:83-85
Stroobants N, Dehairs F, Goeyens L, Van Der Heijden N, Van Grieken R (1991) Barite formation in the southern-ocean water column. Mar Chem 35:411-421
Strübel G (1966) Die hydrothermale löslichkeit von colestin im system $SrSO_4$-NaCl-H_2O. Neues Jahrb Mineral 99-108
Strübel G (1967) Zur kentniss und genetischen bedetung des systems $BaSO_4$-NaCl-H_2O. Neues Jahrb Mineral 233-338
Takano B, Watanuki K (1974) Geochemical implications of the lead content of barite from different origins. Geochem J 8:87-95
Takano B, Yanagisawa M, Watanuki K (1970) Structure gap in $BaSO_4$-$PbSO_4$ solid solution series. Mineral J (Japan) 6:159-171
Tendal OS (1972) A monograph on the Xenophyophoria. *In* Galathea Report, Scientific Results of the Danish Deep-Sea Expedition Round the World 1950-52. W Torben (Ed) Danish Science Press, Copenhagen, p 6- 90
Tendal OS, Gooday AJ (1981) Xenophoria (Rhizopoda, Protozoa) in the bathyal and abyssal NE Atlantic. Oceanol Acta 4:415-422
Thomas WA (1976) Evolution of the Ouachita–Appalachian continental margin. J Geol 84:323-342
Tischendorf G (1963) Über $SrSO_4$-gehälte im Baryt als ein Kriteium für dessen Bildungs bedingungen. Problems of postmagmatic ore deposition, vol 1, Prague
Tooker EW (1991) Copper and molybdenum deposits in the United States. *In* Economic Geology, U.S. HJ Gluskoter, DD Rice, RB Taylor (Eds) Geol Soc Am, The Geology of North America P-2:23-42
Torres ME, Bohrmann G, Suess E (1996a) Authigenic barites and fluxes of barium associated with fluid seeps in the Peru subduction zone. Earth Planet Sci Lett 144:469-481
Torres ME, Brumsack HJ, Bohrmann G, Emeis KC (1996b) Barite fronts in continental margin sediments: A new look at barium remobilization in the zone of sulfate reduction and formation of heavy barites in diagenetic fronts. Chem Geol 127:125-139
Turner RJW (1992) Bedded barite deposits in the United States, Canada, Germany, and China: two major types based on tectonic setting: A discussion. Econ Geol 87:198-201
Turner RJW, Madrid RJ, Miller EL (1989) Roberts Mountains allochthon: Stratigraphic comparison with lower Paleozoic outer continental margin strata of the northern Canadian Cordillera. Geology 17:341-344
Ulrich MR, Bodnar RJ (1988) Systematics in stretching of fluids inclusions: II. Barite at 1 atm confining pressure. Econ Geol 83:1037-1046
Urabe T, Kusakabe M (1990) Barite silica chimneys from the Simisu Rift, Izu-Bonin Arc: possible analog to hematitic chert associated with kuruko deposits. Earth Planet Sci Lett 100:283-290
Varnavas SP (1987) Marine barite in sediments from deep sea drilling projects sites 424 and 242A (Galapagos hyrothermal mounds field). Mar Chem 20:245-253

Vinogradov VI, Kheraskova TN, Petrova SN (1978) Formation of stratiform barite deposits in the siliceous units of Kazakhstan. Lith Mineral Res 13:238-247

Von Damm KL (1995) Controls on the chemistry and temporal variability of seafloor hydrothermal fluids. Am Geophys Union Geophys Monogr 91:222-247

von Gehlen K, Nielsen H, Chunnett I, Rosendaal A (1983) Sulphur isotopes in metamorphosed Precambrian Fe-Pb-Zn-Cu sulphides and baryte at Aggeneys and Gamsberg, South Africa. Mineral Mag 47:481-486

von Gehlen K, Nielsen H, Ricke W (1962) S-isotopen-verhaltnisse in baryt und sulfiden aus hydrothermalen gangen im Schwarzwald und jungeren barytgangen in Suddeutschland und ihre genetische bedeutung. Geochim Cosmochim Acta 26:1189-1207

Wang ZC, Li GZ (1991) Barite and witherite deposits in the lower cambrian shales of south China: Stratigraphic distribution and geochemical characterization. Econ Geol 86:354-363

Warren JK (1997) Evaporites, brines and base metals: Fluids, flow and 'the evaporite that was.' Australian J Earth Sci 44:149-183

Weast RC (Ed) (1974) Handbook of Chemistry and Physics, 55th edn. CRC Press, Cleveland, Ohio

Weber, FH (1963) Barite in California. Calif Div Mines Geol Mineral Inf Service 16:1-10

Weinritt DJ, Cowan JC (1967) Unique characteristics of barium sulfate scale deposition. J Petroleum Tech 30:1381-1394

Whitford DJ, Kursch MJ, Solomon M (1992) Strontium isotope studies of barites, implications for the origin of base metal mineralization in Tasmania. Econ Geol 87:953-959

Wilcock JR, Perry CC, Williams RPJ, Brook AJ (1989) Biological minerals formed from strontium and barium sulphates. II. Crystallography and control of mineral morphology in desmids. Proc Roy Soc London B238:203-221

Wilcock JR, Perry CC, Williams RPJ, Mantoura RFC (1988) Crystallographic and morphological studies of the celestite skeleton of the acantharian species *Phyllostaurus siculus*. Proc Roy Soc London B233:393-405

Williams-Jones AE, Schrijver K, Doig R, Sangster DF (1992) A model for epigenetic Ba-Pb-Zn mineralization in the Appalachian thrust belt, Quebec: Evidence from fluid inclusions and isotopes. Econ Geol 87:154-174

Wood MW, Shaw HF (1976) The geochemistry of celestites from the Yate area near Bristol (U.K.). Chem Geol 17:179-193

Worl W (1991) The other metals. *In* Economic Geology, U.S. HJ Gluskoter, DD Rice, RB Taylor (Eds) Geol Soc Am, The Geology of North America P-2:125-151.

Zielinski RA, Bloch S, Walker TR (1983) The mobility and distribution of heavy metals during the formation of first cycle red beds. Econ Geol 78:1574-1589

Zimmerman RA (1970) Sedimentary features in the Meggen barite-pyrite-sphelerite deposit and a comparison with Arkansas barite deposits. Neues Jharb Mineral Abh 113:179-214

Zimmerman RA, Amstutz GC (1964) Die Arkansas-schwerspätzone, neue sedimentpetrographisch Beobach-tung und genetische Umdeutung. Z Erz u Metall 7:365-371